Quantum critical behavior in itinerant electron systems: Eliashberg theory and instability of a ferromagnetic quantum critical point

Jérôme Rech,[1,2] Catherine Pépin,[1] and Andrey V. Chubukov[3]
[1]*SPhT, L'Orme des Merisiers, CEA-Saclay, 91191 Gif-sur-Yvette, France*
[2]*Center for Materials Theory, Rutgers University, Piscataway, New Jersey 08855, USA*
[3]*Department of Physics, University of Wisconsin-Madison, 1150 University Avenue, Madison, Wisconsin 53706-1390, USA*
(Received 1 May 2006; published 29 November 2006)

We consider the problem of fermions interacting with gapless long-wavelength collective bosonic modes. The theory describes, among other cases, a ferromagnetic quantum-critical point (QCP) and a QCP towards nematic ordering. We construct a controllable expansion at the QCP in two steps: we first create a non-Fermi-liquid "zero-order" Eliashberg-type theory, and then demonstrate that the residual interaction effects are small. We prove that this approach is justified under two conditions: the interaction should be smaller than the fermionic bandwidth, and either the band mass m_B should be much smaller than $m=k_F/v_F$, or the number of fermionic flavors N should be large. For an SU(2) symmetric ferromagnetic QCP, we find that the Eliashberg theory itself includes a set of singular renormalizations which can be understood as a consequence of an effective long-range dynamic interaction between quasiparticles, generated by the Landau damping term. These singular renormalizations give rise to a negative nonanalytic $q^{3/2}$ correction to the static spin susceptibility, and destroy a ferromagnetic QCP. We demonstrate that this effect can be understood in the framework of the ϕ^4 theory of quantum criticality. We also show that the nonanalytic $q^{3/2}$ correction to the bosonic propagator is specific to the SU(2) symmetric case. For systems with a scalar order parameter, the $q^{3/2}$ contributions from individual diagrams cancel out in the full expression of the susceptibility, and the QCP remains stable.

DOI: 10.1103/PhysRevB.74.195126 PACS number(s): 71.10.Hf, 75.40.−s

I. INTRODUCTION

Quantum-critical behavior in two-dimensional (2D) systems with continuous symmetry continues to attract substantial interest from the condensed-matter community. Near criticality, bosonic collective modes in either the spin or the charge channel (depending on the problem) are soft, and mutual feedback effects between bosonic and fermionic degrees of freedom lead to a rather peculiar behavior of both the fermionic and bosonic propagators. In this paper, we study in detail this behavior for two-dimensional (2D) systems.

For systems with continuous symmetry, the dynamics of low-energy bosons is dominated by Landau damping, and the collective-mode propagator dressed by a particle-hole bubble behaves as

$$\chi(q,\Omega_m)=\frac{\chi_0}{\xi^{-2}+q^2+\gamma(|\Omega_m|/q)}. \tag{1.1}$$

At $\xi=\infty$, the bosonic propagator becomes massless, signaling an instability towards a particular ordering. The dynamical exponent z, which measures how the frequency scales with momentum at criticality ($\omega\sim q^z$), is $z=3$.

Physically, the complexity of the problem resides in the presence of gapless fermions at the quantum critical point (QCP). In ordinary QCP in localized electron systems, one deals with only one type of massless modes, namely a bosonic mode associated with the fluctuations of the order parameter. In itinerant electron QCP, massless bosonic modes interact with conduction electrons, which are gapless at the Fermi surface, and this interaction affects both electrons and bosons. One can still reduce the problem to interacting bosons by formally integrating the fermions out of the partition function. It was originally conjectured[1] that this leads to a conventional ϕ^4 field theory with the bare propagator given by Eq. (1.1), i.e., to a ϕ^4 theory in an effective dimension $d+z$. Since $z=3$, the bosonic sector is above its upper critical dimension for $d>1$, and the critical exponents have mean-field values.

However, this description turns out to be oversimplified by two reasons. First, it does not address the issue of what happens to the fermions at the QCP. It turns out that for fermions, the upper critical dimension is $d_c^+=3$, such that in $d=2$ the fermionic self-energy is singular and critically affects the behavior of low-energy fermions. Second, the ϕ^4 theory for bosons is actually rather peculiar as the prefactors for the ϕ^4 and higher-order terms are determined by low-energy fermions, and are sensitive to the behavior of these fermions near the QCP.

These two arguments imply that at the QCP in itinerant electron systems, fermions and bosons should be considered self-consistently and on equal footing. The key theoretical challenge in this context is to develop a controlled computational scheme to describe the correct behavior of electrons interacting with gapless bosonic collective degrees of freedom.

The problem of fermions interacting with bosons with the propagator (1.1) at $\xi=\infty$ was previously analyzed in the context of 2D fermions interacting with a singular gauge field,[2–6] and was also applied to a gauge theory of high-T_c superconductors,[7] and compressible quantum Hall effect.[8] Later, this problem was studied in the context of 2D fermions near a ferromagnetic instability,[9–12] and, very recently, in the context of fermions near an instability towards a nematic-type ordering with angular momentum $l=2$.[13–16] That last transition was argued by some studies[17] to be relevant to the cuprates. Similar problems have been studied in the context

of finite momentum spin[18] and charge[19] ordering transitions in itinerant fermionic systems.

An analytic treatment of the problem was originally carried out by Lee,[5] and later on by Blok and Monien,[6] and Altshuler, Ioffe, and Millis[2] for the interaction with the gauge field. They showed that the fermionic self-energy scales as $\Sigma(\omega_m)=|\omega_m|^{2/3}\omega_0^{1/3}$ sgn (ω_m) to second-order in perturbation, pointing to a breakdown of the Fermi-liquid behavior. They estimated higher-order terms and argued that the $\omega^{2/3}$ form of the self-energy survives to all orders in perturbation. On the other hand, nonperturbative eikonal expansion[3] and closely related approaches based on 2D bosonization[20,21] yielded a different behavior, in which the fermionic Green's function decays exponentially with coordinate and time. This would be consistent with a divergent perturbative expansion for the self-energy. Altshuler and collaborators argued that this last result only survives in the artificial limit of a vanishing number of fermionic flavors $N\to 0$: at any finite N (including the physical case $N=1$), the finite curvature of the fermionic dispersion prevents the perturbation series for the self-energy to become singular (see also Ref. 22).

The discussion on the interplay between perturbative calculations and 2D bosonization re-emerged recently in the context of the quantum critical point for a Pomeranchuk instability towards nematic ordering. Metzner and collaborators[15] and, very recently, Khveshchenko and one of us[23] argued that $\Sigma(\omega)\propto\omega^{2/3}$ is the correct result at criticality, while Lawler *et al.*[14] argued, based on 2D bosonization, that nonperturbative effects change this behavior. Adding to the controversy, Kopietz[24] argued that higher-order corrections to the self-energy hold in powers of $\omega^{2/3}|\ln\omega|^n$, where the geometrical series of logarithms gives rise to an extra power of frequency, such that $\Sigma\propto\omega^{2/3-a}$.

In this paper, we re-analyze the problem. We consider a ferromagnetic QCP [$z=3$ with spin SU(2) symmetry], and a QCP towards nematic ordering, towards Ising-type ferromagnetism, and a gauge-field problem—these three last problems are mathematically equivalent and correspond to $z=3$ and U(1) symmetry of the order parameter. We construct a controllable expansion at the QCP by creating a non-Fermi-liquid "zero-order" theory by solving the set of coupled equations for the fermionic and bosonic propagators, while neglecting the vertex corrections as well as the momentum dependence of the fermionic self-energy. This procedure is often called the Eliashberg theory because of its resemblance to the Eliashberg theory for the electron-phonon interaction.[25] We analyze the residual interaction effects using our zero-order propagator instead of free fermions. We confirm an earlier result of Ref. 2 that the residual interaction does not change the functional behavior of the self-energy. We perform a careful analysis of the structure of the infrared divergences in the theory. We analyze in detail the vertex corrections at various momenta and frequencies, the interplay between the Migdal approximation and Ward identities, the role of the curvature of the fermionic dispersion, and the interplay between a direct perturbation theory for free fermions and an effective perturbation theory in which one expands around the Eliashberg solution. We also obtain the leading correction to the fermionic density of states (DOS).

A generic condition for the validity of the Eliashberg theory is that bosons should be slow modes compared to fermions (i.e., for a fixed frequency, the bosonic momentum should be larger than the fermionic one). Then fermions, forced by the interaction to vibrate at frequencies near the bosonic pole, are far from their own resonance and thus have a small spectral weight, giving rise to only a small correction to the electron-boson vertex (this is also known as the Migdal theorem). Typical bosonic momenta in Eq. (1.1) scale as $\omega^{1/3}$ and are obviously slower than free fermions whose momenta scale as ω. The situation becomes less clear once the fermionic self-energy is included. We show that the correction to the static fermion-boson vertex is determined by frequencies at which the fermionic self-energy is of order of a bare ω, and the static vertex correction is small, for a fermion-boson coupling smaller than the fermionic bandwidth. This coincides with the generic condition for the validity of the low-energy description since otherwise the physics is not restricted to the vicinity of the Fermi surface.

This generic condition, however, is not a sufficient one at the QCP of spatially isotropic systems—we show that there are corrections to the Eliashberg theory which come from the scattering process in which one component of the bosonic momentum is near the bosonic mass shell, while the other is near the fermionic mass shell. We find that such corrections are dangerous as the expansion around the Eliashberg solution then holds in powers of terms of order 1. The same expansion around free fermions yields terms which formally diverge as powers of $\omega^{-1/3}$ if one neglects the curvature of the Fermi surface.[14,23] We show, in agreement with Ref. 2, that in this situation, the way to construct a fully controllable perturbation expansion around the Eliashberg theory at the QCP is to either assume that the curvature of the Fermi surface is large, or extend the theory to a large number of fermionic flavors N. In this case, the self-energy diagrams with vertex insertions are all small, and the theory is under control.

We emphasize that this smallness does not imply that the theory is in the weak-coupling limit—the Eliashberg self-energy (given by the one-loop diagram) does not "feel" the curvature and diverges as $\omega^{2/3}$ leading to non-Fermi-liquid physics at the QCP. Another exception is the pairing vertex, which does not feel the curvature as well, and is of order 1.

In the second part of the paper we show that there exists a third singular scattering process in which both fermionic and bosonic momenta vibrate near the fermionic mass shell. This third process is qualitatively different from the first two scattering processes in which at least one component of the bosonic momentum is near the bosonic mass shell.

We show that this process (which by virtue of scattering near the fermionic mass shell is within the Eliashberg theory) gives rise to a nonanalytic momentum expansion of the static vertex. We show that for a ferromagnetic SU(2) symmetric QCP, this nonanalyticity eventually gives rise to a nonanalytic and negative correction to the static spin susceptibility. This correction exceeds the q^2 term in Eq. (1.1) and makes a ferromagnetic QCP unstable.

The issue of whether the QCP is internally stable has been the subject of numerous discussions in the recent literature. This work was pioneered by Belitz, Kirkpatrick, and Vojta[26] who found that in a generic 3D Fermi liquid far from the QCP, the static spin susceptibility $\chi_s(q)$ has a negative

nonanalytic momentum dependence, leading to a minimum of $\chi_s^{-1}(q)$ located at some incommensurate momentum, rather than at $q=0$. The same result was later obtained for 2D systems.[27] If one were to formally extend the Fermi-liquid results to the quantum critical region, one would obtain that the continuous QCP becomes unstable.[28] It was *a priori* unclear, however, whether this extension procedure is justified, since the Fermi-liquid behavior does not seem to survive as one approaches the QCP.

To address this issue we explicitly compute the static spin susceptibility at criticality, and show that it is negative and nonanalytic at the smallest momenta. This implies that a ferromagnetic QCP is indeed unstable, as the Fermi-liquid analysis suggests. We argue that the nonanalyticity in $\chi_s(q)$ is associated with the Landau damping term, which gives rise to an effective long-range dynamic interaction between quasiparticles both away from and at the QCP. The singular fermionic self-energy at criticality only modifies, in not a very essential way, the functional form of the nonanalyticity compared to that in a Fermi liquid.

We also discuss the emergence of the nonanalytic term in the static spin susceptibility in the framework of the Hertz-Millis-Moriya (HMM) ϕ^4 theory of quantum criticality.[1] As we said above, this theory assumes that there exists a regular expansion of the effective action in powers of the order-parameter field ϕ. We show that this is actually not the case, and the prefactor of the ϕ^4 term is nonanalytic and depends on the ratio between typical momenta and frequencies. We show that this nonanalyticity feeds back as a nonanalytic $|q|^{3/2}$ correction of the quadratic term in ϕ. We study how the nonanalyticity in $\chi_s(q)$ affects the fermionic self-energy and show that it gives rise to self-energy terms larger than $\omega^{2/3}$ (beginning at the three-loop order). The series of such terms eventually leads to a breakdown of the Eliashberg theory for the fermionic self-energy at the energy scale related to the typical momentum scale at which $\chi_s(q)$ becomes negative.

We show that the nonanalytic corrections to the bosonic propagator and the divergent corrections to the fermionic self-energy are specific to the SU(2) spin-symmetric case. For a nematic instability, as well as for a ferromagnetic instability in systems with Ising symmetry, the dangerous terms in the bosonic propagator and the fermionic self-energy cancel out, and the QCP is stable.

The paper is organized as follows. In Sec. II we discuss the model. In Sec. III we present a quick analysis of the self-energies, justifying all at once the Eliashberg-like treatment and the need to include the curvature of the fermionic dispersion. In Sec. IV, we discuss the Eliashberg theory near quantum criticality. In Sec. V, we analyze in detail the conditions one has to impose in order for the Eliashberg theory to be valid. This includes the computation of all vertex corrections, as well as the momentum-dependent self-energy at the two-loop level. We also compare the results obtained by strict perturbative expansion using free fermions, and the Eliashberg-type calculations.

In Sec. VI we address the issue of the stability of a ferromagnetic QCP. We revisit the scaling arguments that a ferromagnetic QCP must be stable in dimension $D>1$ and show that the prefactor for the ϕ^4 term is actually a nonanalytic function of the ratio of frequency and momentum. We show that this nonanalyticity feeds back as a nonanalytic correction to the static spin susceptibility. We explicitly compute the momentum-dependent term in $\chi_s(q)$ at the two-loop order, both in the Fermi-liquid regime away from a ferromagnetic QCP and at criticality. In both cases, we find that the dominant term at small q is negative and nonanalytic. We also show that the instability of a ferromagnetic QCP can be also detected by computing the fermionic self-energy which at the three-loop order acquires extra singular terms because of the singularity in the static susceptibility. In Sec. VII, we evaluate the charge susceptibility at two-loop and three-loop orders and show that it remains analytic—all nonanalytic contributions from individual diagrams cancel out. Finally, in Sec. VIII, we present our conclusions and discuss the consequences of the instability of a continuous QCP towards ferromagnetic ordering. Technical details are presented in Appendixes A–F. A short version addressing part of the results of Sec. VI has been presented in Ref. 29. For convenience, all the physical parameters used throughout the text are presented in Table I.

II. MODEL

The model we consider describes low-energy fermions interacting with Landau-overdamped collective bosonic excitations which are either gapless by symmetry reasons (as is the case for the interaction with a gauge field), or become gapless at the quantum critical point (for the nematic and the ferromagnetic problems).

The underlying lattice models may be quite different for these three cases, but the low-energy models are very similar, the only difference being that in the case of the ferromagnetic QCP the gapless bosonic excitations are in the spin channel, whereas in the nematic case and the gauge field problem they are in the charge channel.

The general strategy to derive the low-energy model is to start with a model with fermion-fermion interaction, assume that there is only one low-energy collective degree of freedom near the QCP, decouple the four-fermion interaction term using the critical bosonic field as an Hubbard-Stratonovich field, and integrate out of the partition function all high-energy degrees of freedom, with energies between the fermionic bandwidth W and some cutoff Λ.[18,30]

If this procedure was performed completely we would obtain a full renormalization group treatment of the problem. Unfortunately, there is no controllable way of doing so. It is widely believed though that although the propagators of the remaining low-energy modes possess some memory of the physics at high energies, the integration of high-energy fermions does not give rise to anomalous dimensions for the bare fermionic and bosonic propagators in the low-energy model. In practical terms, this assumption implies that the bare propagator of the relevant collective mode is an analytic function of momentum and frequency, and the fermionic propagator has the Fermi-liquid form

$$G(k,\omega) = \frac{Z_0}{i\omega - \epsilon_k}, \tag{2.1}$$

where $Z_0<1$ is a constant, and ϵ_k is the renormalized band dispersion. Near the Fermi surface,

TABLE I. List of the various parameters used in the text, their expression before the rescaling in N, and the reference equation where it is defined in the text.

Expression	Definition	Eq.
v_F	Fermi velocity	(2.2)
m	bare quasiparticle mass, $m=k_F/v_F$	(2.2)
m^*	effective (renormalized) quasiparticle mass	(4.8)
m_B	band mass, determines the curvature of the Fermi surface	(2.2)
g	spin-fermion coupling constant	(2.4)
ξ	ferromagnetic correlation length	(2.3)
$\chi_0\xi^2$	value of the spin susceptibility at $q=0$	(2.3)
N	number of fermionic flavors	
$\bar{g}=g^2\chi_0$	effective four-fermion interaction	(4.6)
$\gamma=\frac{Nm\bar{g}}{\pi v_F}$	Landau damping coefficient	(4.5)
$\lambda=\frac{3\bar{g}\xi}{4\pi v_F}$	dimensionless coupling constant, it measures the mass enhancement: $\lambda=\frac{m^*}{m}-1$	(4.6)
$\omega_0=\frac{3\sqrt{3}\bar{g}^3}{8\pi^3\gamma v_F^3}\sim\frac{\bar{g}^2}{NE_F}$	frequency up to which $\Sigma(\omega)$ dominates over ω in the fermionic propagator	(4.9)
$\omega_{\mathrm{Max}}=\sqrt{\gamma v_F^3}\sim\sqrt{N\bar{g}E_F}$	frequency up to which the fermionic and the bosonic mass shells are well separated	(5.3)
$\alpha=\frac{\bar{g}^2}{\gamma v_F^3}\sim\frac{\bar{g}}{NE_F}$	small parameter, measuring the slowness of the bosonic modes compared to the fermionic ones; the same small parameter justifies the low-energy description	(5.1)
$\beta=\frac{m_B}{mN}$	small parameter related to the curvature of the fermionic dispersion	(5.13)

$$\epsilon_k = v_F k_\perp + \frac{k_\parallel^2}{2m_B}. \tag{2.2}$$

Here $\mathbf{k}$ is the momentum deviation from $\mathbf{k_F}$, the parallel and perpendicular components are with respect to the direction along the Fermi surface at $\mathbf{k_F}$, m_B is the band mass, the Fermi velocity $v_F=k_F/m$, and for a circular Fermi surface one has $m=m_B$.

One can then re-cast the original model of fermion-fermion interaction into an effective low-energy fermion-boson model. Consider for definiteness that the system is close to a ferromagnetic QCP. Then the low-energy degrees of freedom are fermions [with the propagator given by Eq. (2.1)] and long-wavelength collective spin excitations whose propagator (the spin susceptibility) is *analytic* near $q=0$ and $\Omega=0$:

$$\chi_{s,0}(q,\Omega) = \frac{\chi_0}{\xi^{-2}+q^2+A\Omega^2+O(q^4,\Omega^4)}. \tag{2.3}$$

Here A is a constant, and ξ is the correlation length, which becomes infinite at the QCP. We prove in the next section that the Ω^2 term does not play any role in our analysis, and we therefore neglect it for now and approximate the above bare propagator by the static one $\chi_{s,0}(q)$. The model can then be described by the phenomenological spin-fermion Hamiltonian:

$$H_{sf} = \sum_{k,\alpha} \epsilon_k c_{k,\alpha}^\dagger c_{k,\alpha} + \sum_q \chi_{s,0}^{-1}(q)\mathbf{S}_q\mathbf{S}_{-q} + g\sum_{k,q,\alpha,\beta} c_{k,\alpha}^\dagger \boldsymbol{\sigma}_{\alpha\beta} c_{k+q,\beta}\cdot\mathbf{S}_q, \tag{2.4}$$

where $\boldsymbol{\sigma}=(\sigma^x,\sigma^y,\sigma^z)$ are Pauli matrices. Here $\mathbf{S}_q$ with $q<\Lambda/v_F$ are vector bosonic variables, and g is the effective fermion-boson interaction. For convenience, we incorporated the fermionic residue Z_0 into g.

To illustrate how this effective Hamiltonian can, in principle, be derived from the microscopic model of interacting conduction electrons, we consider a model in which the electrons interact with a short-range four-fermion interaction $U(q)$ and assume that only the forward scattering is relevant $[U(0)=U]$:

$$H = \sum_{k,\alpha} \epsilon_k c_{k,\alpha}^\dagger c_{k,\alpha} + \frac{1}{2}\sum_q U \sum_{k,k',\alpha,\beta} c_{k,\alpha}^\dagger c_{k+q,\alpha} c_{k'\beta}^\dagger c_{k'-q,\beta}. \tag{2.5}$$

In this situation, the interaction is renormalized independently in the spin and in the charge channels.[31] Using the identity for the Pauli matrices $\boldsymbol{\sigma}_{\alpha\beta}\cdot\boldsymbol{\sigma}_{\gamma\delta}=-\delta_{\alpha\beta}\delta_{\gamma\delta}+2\delta_{\alpha\delta}\delta_{\beta\gamma}$, one can demonstrate[31] that in each of the channels, the random-phase approximation (RPA) summation is exact, and the fully renormalized four-fermion interaction $U^{full}_{\alpha\beta,\gamma\epsilon}(q)$ is given by

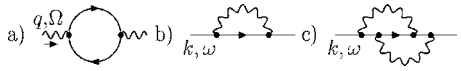

FIG. 1. (a) Polarization bubble. (b) One-loop fermionic self-energy. (c) Two-loop fermionic self-energy.

$$U^{full}_{\alpha\beta,\gamma\varepsilon}(q) = U\left[\delta_{\alpha\gamma}\delta_{\beta\varepsilon}\left(\frac{1}{2}+\mathcal{G}_\rho\right)+\sigma^i_{\alpha\gamma}\sigma^i_{\beta\varepsilon}\left(\frac{1}{2}+\mathcal{G}_\sigma\right)\right], \tag{2.6}$$

where $i=(x,y,z)$, and

$$\mathcal{G}_\rho \equiv \frac{1}{2}\frac{1}{1-U\Pi(q)}; \quad \mathcal{G}_\sigma \equiv -\frac{1}{2}\frac{1}{1+U\Pi(q)}, \tag{2.7}$$

with $\Pi(q)=-\frac{m}{2\pi}[1-a^2(q/k_F)^2]$, $a>0$.

For positive values of U satisfying $mU/2\pi \approx 1$, the interaction in the spin channel is much larger than the one in the charge channel. Neglecting then the latter, we can simplify the Hamiltonian (2.5):

$$H = \sum_{k,\alpha}\epsilon_k c^\dagger_{k,\alpha}c_{k,\alpha} + \frac{1}{2}\sum_q U_{\text{eff}}(q) \times \sum_{k,k',\alpha,\beta,\gamma,\delta} c^\dagger_{k,\alpha}\boldsymbol{\sigma}_{\alpha\beta}c_{k+q,\beta}\cdot c^\dagger_{k'\gamma}\boldsymbol{\sigma}_{\gamma\delta}c_{k'-q,\delta}, \tag{2.8}$$

where $U_{\text{eff}}(q)=(1/2)U^2\Pi(q)/[1+U\Pi(q)]$. Performing a Hubbard-Stratonovich decomposition in the three fields $\mathbf{S}_q$, one recasts Eq. (2.8) into Eq. (2.4) with

$$\begin{cases} g &= U\dfrac{a}{2} \\ \chi_0 &= 2\dfrac{k_F^2}{Ua^2} \\ \bar{g} &= g^2\chi_0 = (U/2)k_F^2 \\ \xi^{-2} &= \dfrac{k_F^2}{a^2}\left(\dfrac{2\pi}{mU}-1\right) \end{cases}. \tag{2.9}$$

The QCP is reached when $mU/2\pi=1$, i.e., $\xi^{-2}=0$. This coincides with the Stoner criterion for a ferromagnetic instability.[32]

We emphasize that the bosonic propagator in Eq. (2.3) does not contain the Landau damping term. This is because we only integrated out the high-energy fermions, whereas the Landau damping of a collective mode of energy Ω comes from fermions of energy $\omega<\Omega$, and can only be generated within the low-energy theory. The dynamics of both the bosonic fields $\mathbf{S}_q$ and the fermionic c and $c^\dagger$ is determined self-consistently by treating both fluctuations on equal footing.

To put under control the computations carried out later in the paper, it is necessary to extend the model by introducing N identical fermion species, while keeping the SU(2) spin symmetry. The Hamiltonian (2.4) can then be rewritten as

$$H_{sf} = H_f + H_b + H_{int},$$

where

$$H_f = \sum_{k,j,\alpha}\epsilon_k c^\dagger_{k,j,\alpha}c_{k,j,\alpha}$$

$$H_b = \sum_q \chi^{-1}_{s,0}(q)\mathbf{S}_q\cdot\mathbf{S}_{-q}$$

$$H_{int} = g\sum_{k,q,j,\alpha,\beta} c^\dagger_{k,j,\alpha}\boldsymbol{\sigma}_{\alpha\beta}c_{k+q,j,\beta}\cdot\mathbf{S}_q, \tag{2.10}$$

where the index $j=1\ldots N$ labels the fermionic species.

We use the spin-fermion Hamiltonian of Eq. (2.10) as the starting point of our analysis. In the case of a QCP in the charge channel, or a ferromagnetic instability with Ising symmetry, the bosonic vector field $\mathbf{S}$ becomes a scalar field designated as ϕ. The interacting term is also modified, the Pauli matrices being replaced by $\delta_{\alpha\beta}$ for the interaction with charge fluctuations, and by $\sigma^Z_{\alpha\beta}$ in the Ising case. The corresponding interaction Hamiltonians are

$$\begin{cases} H^{Charge}_{int} &= g\sum_{k,q,j,\alpha,\beta} c^\dagger_{k,j,\alpha}\delta_{\alpha\beta}c_{k+q,j,\beta}\phi_q \\ H^{Ising}_{int} &= g\sum_{k,q,j,\alpha,\beta} c^\dagger_{k,j,\alpha}\sigma^Z_{\alpha\beta}c_{k+q,j,\beta}\phi_q \end{cases}. \tag{2.11}$$

III. DIRECT PERTURBATION THEORY

In this section we compute the fermionic and bosonic self-energies for the model presented in Eq. (2.4) using a perturbation expansion around noninteracting fermions. Our goal here is threefold: to relate the Landau damping coefficient to the fermion-boson coupling constant g, to distinguish between $\Sigma(\omega)$ and $\Sigma(k)$, and to demonstrate the importance of the curvature of the Fermi surface.

We evaluate the self-energy in this section up to two-loop order. We verified that to this order, there is no qualitative difference between the quantum critical point in the spin or in the charge channel. We then restrict our presentation to the spin-fermion model near a ferromagnetic QCP.

A. Bosonic self-energy: Landau damping term

The full bosonic propagator depends on the self-energy $\Pi(q,\Omega)$ according to

$$\chi_s(q,\Omega) = \frac{\chi_0}{\xi^{-2}+q^2+\Pi(q,\Omega)}. \tag{3.1}$$

At the lowest order in the spin-fermion interaction, the bosonic self-energy is given by the first diagram in Fig. 1, and reads

$$\Pi(\mathbf{q},\Omega) = 2N\bar{g}\int\frac{d^2k d\omega}{(2\pi)^3}G(\mathbf{k},\omega)G(\mathbf{k}+\mathbf{q},\omega+\Omega), \tag{3.2}$$

where $\bar{g}=g^2\chi_0$.

The curvature of the fermionic dispersion does not affect much the result of this computation as it only leads to small corrections in $q/m_B v_F$. Neglecting the quadratic term in the

fermionic propagators, we introduce the angle θ defined as $\epsilon_{\mathbf{k}+\mathbf{q}}=\epsilon_{\mathbf{k}}+v_F q\cos\theta$ and perform the integration over $\epsilon_{\mathbf{k}}$, which gives us

$$\Pi(\mathbf{q},\Omega)=i\frac{N\bar{g}m}{2\pi^2}\int_{-\infty}^{+\infty}d\omega[\theta(\omega+\Omega)-\theta(\omega)]\times\int_0^{2\pi}d\theta\frac{1}{i\Omega-v_F q\cos\theta}=\frac{Nm\bar{g}}{\pi}\frac{|\Omega|}{\sqrt{(v_F q)^2+\Omega^2}}. \tag{3.3}$$

At the QCP, the bosonic mass shell corresponds to the region of momentum and frequency space for which the terms in the inverse propagator are of the same order, i.e., near a mass shell q and Ω satisfies $\Pi(q,\Omega)\sim q^2$. It follows that, at the QCP, near the bosonic mass shell, $v_F q/\Omega\sim v_F(m\bar{g}v_F^2/\Omega^2)^{1/3}\gg 1$ at small enough frequency, so that $v_F q$ is the largest term in the denominator of $\Pi(q,\Omega)$. The expression of the bosonic self-energy then reduces to

$$\Pi(\mathbf{q},\Omega)=\gamma\frac{|\Omega|}{q}, \tag{3.4}$$

where $\gamma=\frac{Nm\bar{g}}{\pi v_F}$.

This expression describes the Landau damping with a prefactor depending on the fermion-boson coupling constant. This term is larger than a regular $O(\Omega^2)$ term, and fully determines the dynamics of the collective bosonic mode.

B. One-loop fermionic self-energy

We now turn to the fermionic self-energy, right at the QCP, where $\xi^{-1}=0$. To the lowest order in the interaction, the fermionic self-energy contains one bosonic line, as represented in Fig. 1(b), and its analytic form writes

$$\Sigma_1^{\text{free}}(\mathbf{k},\omega)=3ig^2\int\frac{d^2q d\Omega}{(2\pi)^3}G_0(\mathbf{k}+\mathbf{q},\omega+\Omega)\chi(\mathbf{q},\Omega). \tag{3.5}$$

The superscript "free" implies that we use the free fermionic $G_0(k,\omega)$ in the integral for the self-energy.

In a direct perturbation theory in g, one would have to use the bare form of the bosonic propagator, Eq. (2.3), which leads to $\Sigma(\omega)\propto\ln\omega$. However, this result is useless, as we already know that the Landau damping term completely overshadows a regular frequency dependence in Eq. (2.3). It makes more sense then to estimate the perturbative self-energy using the full bosonic propagator Eq. (3.1). This is *not* a fully self-consistent procedure, but we use it here to estimate the functional forms of the self-energy at various orders in perturbation around free fermions.

It is instructive to distinguish between $\Sigma(\mathbf{k_F},\omega)=\Sigma(\omega)$ and $\Sigma(\mathbf{k},0)=\Sigma(\mathbf{k})$. Substituting the renormalized bosonic propagator with the Landau damping term into Eq. (3.5), the frequency-dependent self-energy reads

$$\Sigma_1^{\text{free}}(\omega)=\frac{3i\bar{g}}{(2\pi)^3}\int d\Omega\, q dq\, d\theta\frac{1}{q^2+\gamma\dfrac{|\Omega|}{q}}\times\frac{1}{i(\omega+\Omega)-v_F q\cos\theta}. \tag{3.6}$$

Here θ is the angle between $\mathbf{k_F}$ and $\mathbf{q}$, and we linearized the fermionic dispersion. Evaluating the integral over the angle, and using that the typical internal bosonic momentum $q\sim\Omega^{1/3}$ is much larger than $\Omega\sim\omega$, we obtain

$$\Sigma_1^{\text{free}}(\omega)=\frac{3\bar{g}}{2\pi^2 v_F}\int_0^{\omega}d\Omega\int\frac{dqq}{q^3+\gamma|\Omega|}=\omega_0^{1/3}\omega^{2/3}, \tag{3.7}$$

where

$$\omega_0=\frac{3\sqrt{3}\bar{g}^3}{8\pi^3 v_F^3\gamma}=\frac{3\sqrt{3}\bar{g}^2}{8\pi^2 Nmv_F^2}. \tag{3.8}$$

This result has been obtained in Ref. 5. It shows that in $D=2$, the interaction between bare fermions and critical bosons leads to a breakdown of the Fermi-liquid behavior: at low energies, the $\omega^{2/3}$ term in Eq. (3.7) is larger than the bare ω in the fermionic propagator. This obviously makes one wonder if higher-order insertions lead to even more singular contributions.

We next compute the one-loop self-energy $\Sigma(\mathbf{k})$, given by

$$\Sigma_1^{\text{free}}(\mathbf{k})=\frac{3i\bar{g}}{(2\pi)^3}\int d\Omega\, q dq\, d\theta\frac{1}{q^2+\gamma(|\Omega|/q)}\times\frac{1}{i\Omega-\epsilon_k-v_F q\cos\theta}=\frac{3\bar{g}}{(2\pi)^2}\epsilon_k\int\frac{d\Omega\, dq}{q^2+\gamma(|\Omega|/q)}\frac{q|\Omega|}{[\Omega^2+(v_F q)^2]^{3/2}}. \tag{3.9}$$

One can make sure that the integral is infrared convergent, i.e., $\Sigma^{\text{free}}(\epsilon_k)\propto\epsilon_k$, with an interaction dependent prefactor, which also depends on the upper cutoff of the theory, Λ. This suggests that the momentum dependent part of the fermionic self-energy is regular at the QCP and only leads to a finite mass renormalization.

C. Two-loop fermionic self-energy

We next calculate the contribution to the fermionic self-energy $\Sigma(\omega)$ from diagrams at the two-loop level. For illustrative purposes, we consider the diagram presented in Fig. 1(c), which writes

$$\Sigma_2^{\text{free}}(\omega)\sim g^4\int d\omega_1 d^2q_1\int d\omega_2 d^2q_2 G(\mathbf{k_F}+\mathbf{q_1},\omega+\omega_1)\times G(\mathbf{k_F}+\mathbf{q_1}+\mathbf{q_2},\omega+\omega_1+\omega_2)G(\mathbf{k_F}+\mathbf{q_2},\omega+\omega_2)\times\chi(\mathbf{q_1},\omega_1)\chi(\mathbf{q_2},\omega_2), \tag{3.10}$$

where we use the full bosonic propagator, the free fermionic one, and we restrict ourselves to the frequency dependence.

We first compute this integral expanding the dispersion of the internal fermions to linear order, since the quadratic term was not significant in the computation of the one-loop bosonic and fermionic self-energy. Choosing the x axis along the external $\mathbf{k}=\mathbf{k_F}$ and integrating over q_1^x and q_2^x, we are left with

$$\Sigma_2^{\text{free}}(\omega) \sim \frac{\bar{g}^2}{v_F^2\omega}\int_0^\omega \frac{d\omega_1 dq_{1y}}{q_{1y}^2+\gamma|\omega_1|/q_{1y}}\int_{\omega-\omega_1}^\omega \frac{d\omega_2 dq_{2y}}{q_{2y}^2+\gamma|\omega_2|/q_{2y}} \sim \omega_0^{2/3}\omega^{1/3}, \tag{3.11}$$

where ω_0 is defined in Eq. (3.8). At low energy, this two-loop self-energy diverges faster than the one-loop self-energy obtained in Eq. (3.7). Estimating higher-order diagrams, we find that they form a series in powers of $(\omega_0/\omega)^{1/3}$, such that the perturbative expansion around free fermions breaks up at $\omega\sim\omega_0$. This result is in line with the one obtained by Lawler *et al.*[14] using a two-dimensional bosonization scheme. The scale ω_0 is related by $\omega_0=v_F/x_0$ to the spatial scale at which the equal-time fermionic Green's function $G(x)$, obtained from bosonization, begins decaying exponentially $[G(x)\propto e^{-(x/x_0)^{1/3}}]$.

However, the divergence of the perturbation theory can be cured once the curvature of the fermionic dispersion is included, as we now show. We re-evaluate the two-loop self-energy (3.10), using now the full fermionic dispersion, Eq. (2.2). After integrating over the momentum component q_1^x and q_2^x, one has

$$\Sigma_2^{\text{free}}(\omega) \sim \frac{\bar{g}^2}{v_F^2}\int_0^\omega \frac{d\omega_1 dq_{1y}}{q_{1y}^2+(\gamma|\omega_1|/q_{1y})}\int_{\omega-\omega_1}^\omega \frac{d\omega_2 dq_{2y}}{q_{2y}^2+\gamma|\omega_2|/q_{2y}} \times \frac{1}{i\omega-q_{1y}q_{2y}/m_B} \sim \frac{m_B^2\bar{g}^2}{\gamma^2 v_F^2}\omega\ln^2\omega. \tag{3.12}$$

This result agrees with Ref. 2. We see that, when the curvature of the fermionic dispersion is included, the two-loop self-energy turns out to be small compared to its one-loop counterpart, at low energy. In a separate study,[23] one of us (A.C.) and D. Khveshchenko reconsidered the bosonization procedure in the presence of the curvature and obtained the same results as in Eq. (3.12).

D. Summary

As a conclusion, this first approach suggests that both the fermionic and the bosonic self-energies are important at the QCP. The bosonic self-energy sets the dynamics of the bosons, while the fermionic self-energy is nonanalytic and parametrically larger than the bare ω term at low energy, which implies a breakdown of the Fermi-liquid behavior at criticality.

We also found that only the frequency-dependent part of the self-energy matters, the momentum-dependent one only leads to a regular renormalization of the effective mass. Finally, we found that the curvature of the Fermi surface plays an important role in regularizing the perturbation expansion.

The full account of these effects cannot be obtained from this simple analysis and one has to develop a controllable way to treat the bosonic and fermionic self-energies on equal footing. Since we found that only the frequency-dependent $\Sigma(\omega)$ is relevant, a way to proceed is to verify whether an Eliashberg-like theory, similar to the one developed in the context of phonon superconductivity,[25] may be such a controllable approximation.

IV. ELIASHBERG THEORY

The Eliashberg procedure allows us to compute the fermionic self-energy $\Sigma(\omega)$ and the bosonic polarization $\Pi(q,\Omega)$, by solving the self-consistent set of coupled Dyson's equations, neglecting all contributions coming from the vertex corrections and the momentum-dependent fermionic self-energy.

Specifically the Eliashberg theory follows three steps:

(i) neglect both the vertex corrections and the momentum dependent part of the fermionic self-energy, i.e., approximate

$$\Sigma(\mathbf{k},\omega_n)=\Sigma(\omega_n),$$

$$g_{\text{Tot}}=g+\Delta g=g; \tag{4.1}$$

(ii) construct the set of self-consistent Dyson's equations:

$$G^{-1}(k,\omega_n)=i\omega_n-v_F(k-k_F)+i\Sigma(\omega_n)$$

$$\chi(q,\Omega_m)=\frac{\chi_0}{\xi^{-2}+q^2+\Pi(q,\Omega_m)}, \tag{4.2}$$

with the following fermionic and bosonic self-energies:

$$i\Sigma(\omega_n) = \quad k,\omega_n$$

$$\chi_0^{-1}\Pi(q,\Omega_m) = \quad q,\nu_m \tag{4.3}$$

The fermionic Green's functions in Eq. (4.3) are full (they are represented diagrammatically by a straight line) and $\chi(q,\Omega_m)$ is the full bosonic propagator (represented by a wavy line);

(iii) check *a posteriori* that the neglected terms Δg and $\Sigma(\mathbf{k})$, are all parametrically small.

The evaluation of the momentum integral for the fermionic self-energy in the Eliashberg theory has to be carried out with care. Since fermions are faster than bosons, the leading contribution to $\Sigma(\omega)$ is obtained if one integrates over the momentum component transverse to the Fermi surface only in the fermionic propagator and sets this component to zero in the bosonic propagator (this implies that the momentum integral is factorized). One can show that the corrections that arise from keeping the transverse component of momentum in the bosonic propagator are small to the same parameter as $\Delta g/g$ and should therefore be neglected, as keeping them would be beyond the accuracy of the theory. The factorization of the momentum integration is what distinguishes the Eliashberg theory from the fluctuation exchange (FLEX) approximation. In the FLEX approximation, one also neglects vertex corrections, but does not factorize the momentum integral in Eq. (4.3).

The evaluation of the bosonic and fermionic self-energies within the Eliashberg theory is presented in Appendix A and B. We list here the main results.

At large but finite correlation length ξ and for a bosonic momentum and frequency satisfying $v_F q \gg \Sigma(\Omega)$ we obtain:

$$\begin{cases} \Pi(q,\Omega) = \gamma \dfrac{|\Omega|}{q} \quad \text{and} \\ \Sigma(\omega) = \lambda \omega F(\gamma \omega \xi^3), \end{cases} \tag{4.4}$$

where $F(x \ll 1) = 1 + O(x)$, and $F(x \gg 1) = \frac{2}{\sqrt{3}} x^{-1/3}$. The parameter γ is the same as for free fermions,

$$\gamma = \frac{N m \bar{g}}{\pi v_F}, \tag{4.5}$$

and λ is the dimensionless coupling

$$\lambda = \frac{3\bar{g}}{4\pi v_F \xi^{-1}}, \tag{4.6}$$

where $\bar{g} = g^2 \chi_0$. At finite ξ^{-1} and vanishing ω, the self-energy has a Fermi-liquid form:

$$\Sigma(\omega) = \lambda \omega. \tag{4.7}$$

The Fermi-liquid theory is stable, and the low-energy quasiparticles have a finite effective mass:

$$m^* = m(1 + \lambda). \tag{4.8}$$

The effective mass diverges proportionally to ξ in the vicinity of the QCP.

At $\omega \gg (\gamma \xi^3)^{-1}$, however, the system is in the quantum-critical regime. Here the Fermi-liquid theory breaks down in the sense that the quasiparticle damping becomes comparable to its energy. We have

$$\Sigma(\omega) = \omega_0^{1/3} |\omega|^{2/3} \mathrm{sgn}(\omega), \tag{4.9}$$

where $\omega_0 = 3\sqrt{3}\bar{g}^2/(8\pi^2 N m v_F^2)$ is the same as in Eq. (3.8).

At the QCP, $\xi^{-1} = 0$, the region of Fermi-liquid behavior collapses, and the $\omega^{2/3}$ dependence of the self-energy extends down to the lowest frequencies. The expression for $\Sigma(\omega)$ is valid for all frequencies below the cutoff Λ. However, only frequencies $\omega \leq \omega_0$ are actually relevant as at higher frequencies the system behaves as a nearly ideal Fermi gas. Note that the curvature of the fermionic dispersion is unimportant here and only accounts for small corrections containing higher powers of frequencies.

Comparing Eqs. (4.4) and (4.9) with Eqs. (3.4) and (3.7), we see that the self-energies in the Eliashberg theory coincide with the one-loop perturbative results around free fermions. This arises from the fact that the momentum integration is factorized in the Eliashberg theory, and the full fermionic propagator appears in both self-energies only via the fermionic density of states (DOS):

$$N(\omega) = \frac{i}{\pi} \int d\epsilon_k \frac{1}{\omega + \Sigma(\omega) - \epsilon_k}. \tag{4.10}$$

This DOS reduces to $N(\omega) = \mathrm{sgn}(\omega)$, independently on the self-energy: it remains the same as for free fermions. Note that Eq. (4.4) for the bosonic self-energy is only valid as long as the interplay between the external momentum and frequency is such that $v_F q \gg \Sigma(\Omega)$. In the opposite limit, the vertex corrections cannot be neglected as we argue in the next section.

We also argue in the next section that the extension of the model to N fermionic flavors is essential for the validity of the current approach. The large-N Eliashberg theory is, however, somewhat tricky, as it can be readily seen from Eqs. (4.5) and (4.9) that both self-energies contain factors of N through their prefactors. These factors can be rescaled out of the Eliashberg theory by rescaling k_F,

$$k_F \to k_F/N, \tag{4.11}$$

and leaving v_F intact. This change of k_F also rescales both masses: $m \to m/N$ and $m_B \to m_B/N$.

In terms of the rescaled variables, both the fermionic self-energy and the Landau damping term become independent on N:

$$\begin{cases} \chi(q,\Omega) = \dfrac{\chi_0}{\xi^{-2} + q^2 + \gamma|\Omega|/q} \\ G(k,\omega) = \dfrac{1}{i[\omega + \Sigma(\omega)] - v_F k_\perp - N(k_\parallel^2/2m_B)}. \end{cases} \tag{4.12}$$

However, after the rescaling, the "zero-order" Eliashberg theory does not become completely free from N—the factor N now appears in front of the $k_\parallel^2$ term, which, we recall, is present in the dispersion because of the curvature of the Fermi surface.

As a consequence, we do not formally take the $N \to \infty$ limit of our model [otherwise, the fermionic Green's function in Eq. (4.12) would just vanish]. Instead, we carry out an expansion where we keep N large, yet finite, allowing us to use $1/N$ as a small parameter.

Furthermore, one can verify, using our expression for the effective Lagrangian below, that once we rescale the fermionic and bosonic fields to compensate for the rescaling of k_F and eliminate N from the quadratic part of the effective action, we do not obtain a factor $1/N$ in the interaction term. In other words, the curvature term in the fermionic propagator is the only place where the factor N is present. This already suggests (as we confirm in the next section) that the curvature plays a major role in our $1/N$ expansion.

From this perspective, our large-N expansion is different from the "conventional" large-N expansion, in which the zero-order theory is independent on N, but the interaction is small in $1/N$. For that class of theories, the $N = \infty$ limit is well defined as the bare, noninteracting theory. In our case, like we said, only large, but finite N values make sense.

For the SU(2) ferromagnetic case, we show below that Eq. (4.12) is incomplete. There are extra contributions to both $\chi(q,\Omega)$ and $\Sigma(\omega)$ which also belong to the Eliashberg theory, showing up at the three-loop level and higher for the fermionic self-energy. These terms, however, appear due to rather specific reasons related to the presence of an effective dynamic long-range interaction in the theory and all cancel out for the gauge field problem, at a nematic QCP and for an Ising ferromagnetic QCP. We consider these extra terms in

the next section and proceed here without taking them into consideration.

We can reformulate the Eliashberg theory by introducing the following effective Lagrangian describing the fermion-boson interaction:

$$L = L_F + L_B + L_{int},$$

with

$$L_B = T\sum_{q,n} \mathbf{S}_{q,n}\chi^{-1}(q,\Omega_n)\mathbf{S}_{-q,-n},$$

$$L_F = T\sum_{k,n,\alpha,j} c^{\dagger}_{k,j,n,\alpha}G^{-1}(k,\omega_n)c_{k,j,n,\alpha},$$

$$L_{int} = gT^2\sum_{n,m,k,q} \mathbf{S}_{q,m}c^{\dagger}_{k,j,n\alpha}\boldsymbol{\sigma}_{\alpha\beta}c_{k-q,j,n-m,\beta}, \qquad (4.13)$$

where n, m number Matsubara frequencies, α, β are spin indices, and j is a flavor index. The upper limit of the frequency summation is the cutoff Λ.

We emphasize that there is no double counting in the bosonic propagator (4.13). The integration of high-energy fermions above the cutoff Λ leads to the momentum dependence of the static bosonic propagator, whereas the interaction at frequencies below Λ gives rise to the Landau damping, without affecting the static part.

To summarize, the Eliashberg-type theory at the QCP contains a nonanalytic fermionic self-energy which scales as $\omega^{2/3}$ and breaks down the Fermi-liquid description of fermions. At the same time, the bosonic propagator is regular—the only effect of the interaction with low-energy fermions is the appearance of a Landau damping.

We will see below that for a charge QCP (and for a spin QCP with a scalar order parameter) this Eliashberg theory is entirely stable. For a ferromagnetic SU(2) symmetric QCP, the Eliashberg theory has to be extended, as we will see in Sec. VI, to incorporate extra singular terms associated with the existence of long-range dynamic interaction between quasiparticles.

We emphasize that even for a charge QCP the fully renormalized *bosonic* susceptibility does not necessary coincide with the one in Eq. (4.12) and may, in particular, acquire an anomalous dimension[33] if d is low enough. However, this can only be due to infrared divergent corrections to the Eliashberg theory, which are fully captured by the effective low-energy model of Eq. (4.13). Such an anomalous dimension emerges at the antiferromagnetic QCP in $d=2$ (Refs. 20 and 33), but not in our case.

V. VALIDITY OF THE ELIASHBERG THEORY

The essential part of the Eliashberg procedure is an *a posteriori* verification that the neglected terms in the self-energies are small. Quite generally, the validity of this procedure is based on the idea that the fermions are fast excitations compared to the bosons, and hence the fermionic and bosonic mass shells are well separated in energy.

When scattering off physical mass-shell bosons, the fermions are forced to vibrate on the bosonic mass shell, which is far away from their own. The electronic spectral function near the bosonic mass shell is then small and this reduces the self-energy that arises from true fermion-boson scattering. In the case of the electron-phonon interaction, this is known as the Migdal theorem.

The computation of the fermionic self-energy $\Sigma(\omega)$ gives us an idea of what the typical intermediate momenta and frequencies are in the problem. One can make sure that at criticality the typical fermionic momenta $k-k_F$ are of order $\Sigma(\omega)/v_F=\omega_0^{1/3}\omega^{2/3}/v_F$. On the other hand, the typical bosonic momenta $q_\perp$ along the direction of $\mathbf{k}_F$ (i.e., transverse to the Fermi surface) are of the same order as the typical fermionic momenta, while the momenta $q_\parallel$ transverse to $\mathbf{k}_F$ (i.e., along the Fermi surface) are of order $(\gamma\omega)^{1/3} \gg \omega_0^{1/3}\omega^{2/3}/v_F$. We see that for a given frequency ω, the typical $|q|=\sqrt{q_\perp^2+q_\parallel^2}$ are much larger than $k-k_F$, i.e., the effective boson velocity is much smaller than v_F. One then expects that the Migdal theorem holds.

The ratio of the typical fermionic $k-k_F$ and bosonic $|q|$ at the same frequency ω is $(\omega_0\omega/\gamma v_F^2)^{1/3}$. At $\omega\sim\omega_0$, this ratio then becomes

$$\alpha = \left(\frac{\omega_0^2}{\gamma v_F^3}\right)^{1/3} \sim \frac{\bar{g}}{E_F}, \qquad (5.1)$$

and the slowness of the bosonic mode is then ensured in the quantum critical regime provided that $\alpha \ll 1$. This condition coincides, in our case, with the condition that the interaction should be smaller than the bandwidth. This is a necessary condition for the effective low-energy model to be valid, for if it is not satisfied, one cannot distinguish between contributions coming from low and from high energies.

However, the smallness of α is not sufficient. In the integral for the fermionic self-energy, only one component of the bosonic momentum, namely $q_\parallel$, is much larger than $k-k_F$, the other one is comparable: $q_\perp \sim k-k_F$. One needs to check whether the corrections to the Eliashberg theory scale as the ratio of $k-k_F$ to the modulus of $|q|$ or one of its components.

To address these issues, we explicitly compute the vertex corrections and the fermionic self-energy at the two-loop level.

A. Vertex corrections

We consider the vertex corrections due to the insertion of one bosonic propagator (three-leg vertex) and two bosonic propagators (four-leg vertex). The behavior of these vertex corrections strongly depends on the interplay between the internal and external momenta and frequencies. We present the results below and discuss all the technical details of these calculations in Appendix C.

1. Three-leg vertex with zero external momentum and frequency

We begin with the simplest three-leg vertex, with strictly zero incoming frequency Ω and momentum q. The one-loop vertex renormalization diagram contains one bosonic line and is presented in Fig. 2(a). In analytic form, it writes

$$\left.\frac{\Delta g}{g}\right|_{q=\Omega=0} \sim g^2 \int d\omega d^2p G(\mathbf{k_F},\omega)^2 \chi(\mathbf{p},\omega)$$
$$\sim \bar{g} \int \frac{d\omega d^2p}{\gamma|\omega|/p+p^2} \frac{1}{[i\tilde{\Sigma}(\omega)-v_F p_x - N(p_y^2/2m_B)]^2},$$

where we defined $\tilde{\Sigma}(\omega)=\omega+\Sigma(\omega)$ and we have chosen $\mathbf{k_F}$ along the x axis, so that $p_x=p_\perp$ and $p_y=p_\parallel$.

Since the poles coming from the fermionic Green's functions are in the same half plane, the integral over q_x is only nonzero because of the branch cut in the bosonic propagator. At the branch cut $p_x \sim p_y$, so that we can safely drop the quadratic term in the fermionic propagators. Introducing polar coordinates, and integrating successively over the angle between $\mathbf{k_F}$ and $\mathbf{p}$, then over the modulus p, we obtain

$$\left.\frac{\Delta g}{g}\right|_{q=\Omega=0} \sim \frac{\bar{g}}{\gamma v_F^3} \int_0^{\omega_{\mathrm{Max}}} d\omega \frac{\tilde{\Sigma}(\omega)}{\omega}, \tag{5.2}$$

where ω_{Max} is the frequency up to which bosons are slow modes compared to fermions, i.e., up to which $\tilde{\Sigma}(\omega)/v_F < (\gamma\omega)^{1/3}$. This frequency exceeds ω_0, so to find it we have to use $\tilde{\Sigma}(\omega) \approx \omega$. We then obtain

$$\omega_{\mathrm{Max}} = \sqrt{\gamma v_F^3} \sim \sqrt{\bar{g} E_F}. \tag{5.3}$$

Note that for small values of α, $\omega_{\mathrm{Max}} \gg \omega_0$, and the maximum frequency up to which the bosons can be treated as slow modes well exceeds the upper limit of the quantum critical behavior.

Substituting $\tilde{\Sigma}$ and ω_{Max} into Eq. (5.2), we obtain

$$\left.\frac{\Delta g}{g}\right|_{q=\Omega=0} \sim \sqrt{\alpha}. \tag{5.4}$$

This correction to the vertex can then be neglected provided that α is small.

2. Three-leg vertex with finite external momentum

We now turn to the three-leg vertex with zero external frequency but a finite bosonic momentum $\mathbf{q}$. The one-loop renormalization is given in Fig. 2, and its analytic form writes

$$\left.\frac{\Delta g}{g}\right|_{q,\Omega=0}$$
$$\sim g^2 \int d\omega d^2p G(\mathbf{k_F}+\mathbf{p}+\mathbf{q},\omega) G(\mathbf{k_F}+\mathbf{p},\omega) \chi(\mathbf{p},\omega)$$
$$\sim \bar{g} \int \frac{d\omega d^2p}{\gamma|\omega|/p+p^2} \frac{1}{i\tilde{\Sigma}(\omega)-v_F p_x - N(p_y^2/2m_B)}$$
$$\times \frac{1}{i\tilde{\Sigma}(\omega)-v_F q_x - v_F p_x - N(p_y^2/2m_B) - N(q_y p_y/m_B)},$$

where p_x is the projection of $\mathbf{p}$ along $\mathbf{k_F}$.

As before, the integral over p_x reduces to the contribution from only the branch cut in the bosonic propagator. At the branch cut, $p_x \sim p_y$, hence we can neglect the quadratic term in the fermionic Green's function, which then allows us to integrate over p_y. Expanding in q_x, and subtracting the constant term at zero momentum calculated in Eq. (5.2), we obtain (see Appendix C for details)

$$\left.\frac{\Delta g}{g}\right|_{q,\Omega=0} - \left.\frac{\Delta g}{g}\right|_{q=\Omega=0} \sim i\frac{q_x}{k_F} \int_{|v_F q_x|} \frac{d\omega}{|\omega|} \ln[i\tilde{\Sigma}(\omega)]$$
$$\sim \frac{q_x}{k_F} \ln|q_x|. \tag{5.5}$$

When not only the bosonic momentum q is finite but also the external fermionic momentum for the static three-leg vertex is away from k_F, the $q \times \ln q$ dependence of the static $\Delta g/g$ survives, but the argument of the logarithm is the maximum of bosonic q and fermionic $k-k_F$ (we directed both along x).

In general, the typical value of q_x is much smaller than k_F, hence the momentum dependent part of this vertex correction is small. However, we argue in the next sections that because of the logarithmic term in Eq. (5.5), the insertion of this vertex correction into the SU(2) static susceptibility gives rise to a nonanalytic $q^{3/2}$ term.

We also emphasize that although the calculations of $\frac{\Delta g}{g}|_{q=\Omega=0}$ and $\frac{\Delta g}{g}|_{q,\Omega=0}$ look similar, the characteristic bosonic momenta are different for the two cases. At $q=\Omega=0$, typical bosonic momenta in Eq. (5.2) are of order $(\gamma\omega)^{1/3}$, i.e., near the bosonic mass shell. On the other hand, typical bosonic momenta in Eq. (5.5) are of order $\tilde{\Sigma}(\omega)/v_F$, i.e., near the fermionic mass shell.

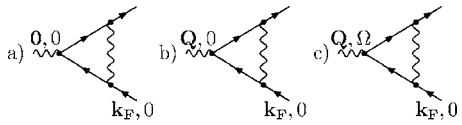

FIG. 2. Three-leg vertices: (a) zero external momentum and frequency; (b) finite momentum; (c) generic vertex.

3. Generic three-leg vertex

We next consider the same vertex with small but finite external momentum q and frequency Ω. This diagram, presented in Fig. 2(b), reads

$$\left.\frac{\Delta g}{g}\right|_{q,\Omega}$$
$$\sim g^2 \int d\omega d^2p G(\mathbf{k_F}+\mathbf{p}+\mathbf{q},\omega+\Omega) G(\mathbf{k_F}+\mathbf{p},\omega) \chi(\mathbf{p},\omega)$$
$$\sim \bar{g} \int \frac{d\omega d^2p}{\gamma|\omega|/p+p^2} \frac{1}{i\tilde{\Sigma}(\omega)-v_F p_x - N(p_y^2/2m_B)}$$
$$\times \frac{1}{i\tilde{\Sigma}(\omega+\Omega)-v_F q_x - v_F p_x - N(p_y^2/2m_B) - N(q_y p_y/m_B)}, \tag{5.6}$$

where we have chosen $\mathbf{k}_F$ along the x axis, so that $q_x=q_\perp$ and $q_y=q_\parallel$.

Integrating over p_x first, one obtains two contributions: one arising from the poles in the fermionic Green's functions (which now can be in different half planes since Ω is finite), and the other from the branch cut in the bosonic propagator. The latter leads to the same result as Eq. (5.2), up to small corrections due to the finiteness of the external q and Ω. Focusing on the other contribution, one has

$$\left.\frac{\Delta g}{g}\right|_{q,\Omega} \sim i\frac{\bar{g}}{v_F}\int_0^\Omega d\omega \int dp_y \frac{|p_y|}{\gamma|\omega|+|p_y|^3} \times \frac{1}{i\tilde{\Sigma}(\Omega-\omega)+i\tilde{\Sigma}(\omega)-v_F q_x - N(q_y p_y/m_B)}, \tag{5.7}$$

where the simplification of the frequency integral comes from the pole structure in p_x.

This generic correction to the vertex strongly depends on the interplay between the external q_x, q_y, and Ω.

When $q=0$, but Ω is finite, the integration over p_y gives

$$\left.\frac{\Delta g}{g}\right|_{q=0,\Omega} \sim \frac{\bar{g}}{v_F\gamma^{1/3}}\int_0^\Omega \frac{d\omega}{\omega^{1/3}}\frac{1}{\tilde{\Sigma}(\Omega-\omega)+\tilde{\Sigma}(\omega)} \sim \frac{\bar{g}}{v_F\gamma^{1/3}\omega_0^{1/3}} = O(1). \tag{5.8}$$

We see that the finite external frequency leads to a vertex correction that is not small, and one can make sure that higher-order corrections are of the same order. The series of vertex corrections have been summed up in Ref. 34 (for a charge vertex), where $\Delta g/g$ was proved to diverge like $(\omega_0/\Omega)^{1/3}$ at low frequency, as expected from the Ward identity.

When q and Ω are both finite,

$$\left.\frac{\Delta g}{g}\right|_{q,\Omega} = \mathcal{F}\left(\frac{\Sigma(\Omega)}{v_F q_x}\right), \tag{5.9}$$

where

$$\mathcal{F}(x) = \int_0^1 \frac{dz}{z^{1/3}}\frac{1}{(1-z)^{2/3}+z^{2/3}+i/x} \tag{5.10}$$

has the following asymptotic behavior:

$$\begin{cases} \mathcal{F}(x \gg 1) = O(1) \\ \mathcal{F}(x \ll 1) = O(x) \end{cases}. \tag{5.11}$$

If the typical external momentum q is on the bosonic mass shell, then $q_x \sim q_y \sim (\gamma\Omega)^{1/3}$, and one has

$$\left.\frac{\Delta g}{g}\right|_{q,\Omega} \sim \frac{\Sigma(\Omega)}{v_F q_x} \sim \sqrt{\alpha}\left(\frac{\Omega}{\omega_{\mathrm{Max}}}\right)^{1/3}. \tag{5.12}$$

This is obviously small in α.

It turns out that the behavior of the vertex correction is more complex and the result for $\Delta g/g$ strongly depends on the direction of q compared to the direction of fermionic momentum $\mathbf{k}=\mathbf{k}_F$. This directional dependence is important for our purposes as we know from previous self-energy calculations that in the integral for the self-energy only the y component of the bosonic momentum is near a bosonic mass shell and scales as $(\gamma\Omega)^{1/3}$, the x component is actually of the order of $\tilde{\Sigma}(\omega)/v_F$, i.e., is near a fermionic mass shell and is much smaller. We therefore take a more careful look at the vertex correction.

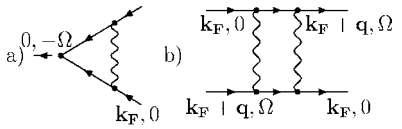

FIG. 3. (a) Cooper pairing vertex. (b) Four-leg vertex.

For the case where $q_x \sim \tilde{\Sigma}(\Omega)/v_F$ and $q_y \sim (\gamma\Omega)^{1/3}$, one would argue from Eq. (5.12) that the vertex correction now becomes of order $O(1)$ and is no longer parametrically small. However, the computation that led to Eq. (5.12) cannot be extended so easily to the strongly anisotropic case, as for an external $q_x \sim \tilde{\Sigma}(\Omega)/v_F$ and $q_y \sim (\gamma\Omega)^{1/3}$, the curvature of the fermionic dispersion becomes relevant and changes the result. The full dependence on q_x and q_y is rather complex and we restrict ourselves to the case when

$$\beta = \frac{1}{N}\frac{m_B}{m} \ll 1. \tag{5.13}$$

In this situation, $q_y^2/m_B \sim (v_F q_x)/\beta \gg v_F q_x$, i.e., the quadratic term in the fermionic propagator dominates. Performing the integration, we then find that

$$\left.\frac{\Delta g}{g}\right|_{q,\Omega} \sim \beta^2\left(\frac{\gamma\Omega}{q_y^3}\right)^{2/3}\ln^2\left[\beta\frac{(\gamma\Omega)^{1/3}}{q_y}\right] \sim \beta^2\ln^2\beta. \tag{5.14}$$

It follows that even when only one component of the bosonic momentum is near a bosonic mass shell, the vertex correction is small if β is small. This is the second condition for the Eliashberg theory to be controllable at criticality.

The smallness of β can be ensured by either extending the theory to large values of N, or by considering a very strong curvature of the Fermi surface which implies that $m_B \ll m$. Even though the latter can hardly be satisfied for realistic Fermi surfaces, we emphasize that the curvature of the dispersion plays a crucial role in the theory, for even in the case of $N \gg 1$, the vertex correction is of order $O(1)$ without this curvature.

4. Four-leg vertex

We consider now higher-order corrections to the vertex through the example of a four-leg vertex correction with two crossed bosonic lines, also called a Cooperon insertion. Analytically, the expression for this renormalized vertex, presented diagrammatically in Fig. 3, writes

$$\Gamma_2(q,\Omega) \sim g^4\int d\omega d^2p\,\chi\left(\frac{\Omega+\omega}{2},\frac{\mathbf{p}+\mathbf{q}}{2}\right) \times \chi\left(\frac{\Omega-\omega}{2},\frac{\mathbf{q}-\mathbf{p}}{2}\right)G\left(\frac{\Omega+\omega}{2},\mathbf{k_F}+\frac{\mathbf{p}+\mathbf{q}}{2}\right) \times G\left(\frac{\Omega-\omega}{2},\mathbf{k_F}+\frac{\mathbf{q}-\mathbf{p}}{2}\right). \tag{5.15}$$

After integrating over p_x (projection of $\mathbf{p}$ along $\mathbf{k_F}$) and ω, were are left with

$$\Gamma_2(q,\Omega) \sim \frac{\bar{g}^2}{v_F}\frac{\Omega}{|q_y|^3}\int dz \frac{\sqrt{(z^2+q^2/q_y^2)^2-4z^2}}{2i\Sigma(\Omega/2)-v_F q_x - N(q_y^2/4m)(1+z^2)} \times \frac{1}{(z^2+2z+q^2/q_y^2)^{3/2}+(\gamma|\Omega|/|q_y|^3)} \times \frac{1}{(z^2-2z+q^2/q_y^2)^{3/2}-(\gamma|\Omega|/|q_y|^3)}, \quad (5.16)$$

where we have changed p_y into $z=p_y/|q_y|$.

This renormalized four-leg vertex $\Gamma_2(q,\Omega)$ has to be compared with the bare four-leg vertex, whose analytic form is given by the bosonic propagator multiplied by g^2:

$$\Gamma_1(q,\Omega) \sim \frac{\bar{g}}{q^2+\gamma|\Omega|/q}. \quad (5.17)$$

In the case of a typical external momentum $q_x \sim q_y \sim (\gamma\Omega)^{1/3}$, the ratio Γ_2/Γ_1 is of order α. For a typical $q_x \sim \tilde{\Sigma}(\omega)/v_F$ and $q_y \sim (\gamma\omega)^{1/3}$, we obtain, to logarithmic accuracy,

$$\frac{\Gamma_2}{\Gamma_1} \sim \beta \ll 1. \quad (5.18)$$

This last result again critically depends on the curvature of the Fermi surface: neglecting the quadratic terms in the fermionic propagators, one would obtain $\Gamma_2/\Gamma_1=O(1)$. We see that likewise to the three-loop vertices, the smallness of the crossed vertex $\Gamma_2(q,\Omega)$ requires both α and β to be small.

5. Interplay between the Landau damping and the fermionic self-energy

The system behavior at strongly anisotropic external momenta $q_x \sim \tilde{\Sigma}(\Omega)/v_F$ and $q_y \sim (\gamma\Omega)^{1/3}$ (as encountered in the three-leg vertex for finite q and Ω, and the four-leg vertex) allows us to underline a few important points related to the role of the curvature.

We have found above that for these momenta, some vertex corrections are $O(1)$ for *any* N, if one does not take into account the curvature of the fermionic dispersion, and are small, and inversely proportional to both the curvature and N, if $\beta=m_B/(mN)$ is small.

The reason for this behavior is a peculiar interplay between the Landau damping and the fermionic self-energy, specific to the ferromagnetic case. Namely, the characteristic values of both the linear and the quadratic term in the fermionic dispersion scale with the frequency in exactly the same way. This is related to the fact that the mismatch between the momenta near the fermionic and the bosonic mass shell at a given frequency is the same as the mismatch between the longitudinal and transverse components of the fermionic dispersion.

Indeed, the typical x component of the external momentum is of order $\tilde{\Sigma}(\Omega)/v_F$, and scales as the square of the y component, whose typical value $q_y \sim \Omega^{1/3}$ is the same as near a bosonic mass shell. The x component enters the fermionic dispersion as a single power while the y component comes with a power of 2, meaning that in the dispersion one has to compare q_x to q_y^2. Ultimately, the two terms entering the fermionic dispersion behave like

$$v_F q_x \sim \tilde{\Sigma}(\Omega) \sim \omega_0^{1/3}\Omega^{2/3}, \quad (5.19)$$

$$\frac{q_y^2}{2m_B} \sim \frac{(\gamma\Omega)^{1/3}}{m_B} \sim \frac{m}{m_B}\omega_0^{1/3}\Omega^{2/3} \quad (5.20)$$

and thus differ precisely by m/m_B. Besides, the $q_y^2/(2m)$ term comes with an overall extra factor of N as we argued in Eq. (4.12). This is the only place where N appears in the theory. The relative factor between the q_y^2 and q_x terms is then $Nm/m_B=1/\beta$. When β is large, the q_y^2 term is subleading compared to the q_x term, the curvature is irrelevant, and the correction to the spin-fermion vertex does not depend on N. When β is small, the q_y^2 term dominates over q_x, and the fermionic dispersion contains N. In this situation, the vertex correction becomes small in $1/N$.

6. Pairing vertex

By contrast to the previous vertices we studied, the pairing vertex in the Cooper channel is not sensitive to the curvature of the Fermi surface. This leads to a vertex of order $O(1)$ even in the large-N limit and the pairing problem then has to be carried out exactly within the Eliashberg theory.

This vertex renormalization is presented in Fig. 3 and its analytic form is given by

$$\left.\frac{\Delta g}{g}\right|_{\text{Cooper}} \sim g^2 \int d\omega d^2q \chi(\mathbf{q},\omega) G(\mathbf{k_F}+\mathbf{q},\omega) \times G(-\mathbf{k_F}-\mathbf{q},-\omega-\Omega) \sim \bar{g}\int \frac{d\omega d^2q}{\gamma|\omega|/q+q^2}\frac{1}{i\tilde{\Sigma}(\omega)-v_F q_x - N(q_y^2/2m_B)} \times \frac{1}{-i\tilde{\Sigma}(\omega+\Omega)-v_F q_x - N(q_y^2/2m_B)}. \quad (5.21)$$

Integrating over q_x, restricting ourselves to the contribution from the fermionic poles (the one from the branch cut can be proved to be smaller), we find that the quadratic terms cancel out, leaving us with

$$\left.\frac{\Delta g}{g}\right|_{\text{Cooper}} \sim \frac{\bar{g}}{v_F}\int_{|\Omega|}^{D}\frac{d\omega}{\tilde{\Sigma}(\omega+\Omega)+\tilde{\Sigma}(\omega)}\int_0^\infty \frac{dq_y q_y}{\gamma\omega+q_y^3}. \quad (5.22)$$

Performing the remaining integral, the prefactor simplifies and we obtain

$$\left.\frac{\Delta g}{g}\right|_{\text{Cooper}} \sim \frac{\bar{g}}{\gamma^{1/3}\omega_0^{1/3}v_F}\ln\left|\frac{\Omega}{D}\right| \sim \ln\left|\frac{\Omega}{D}\right|, \quad (5.23)$$

where we assumed that we were in the quantum critical regime, i.e., $|\Omega|<\omega_0$.

We emphasize that the prefactor of the ln in Eq. (5.23) is $O(1)$, even when one takes into account the curvature of the

fermionic dispersion. The result of Eq. (5.23) confirms previous studies[10] advocating that the system at a ferromagnetic QCP is unstable towards pairing.

B. Self-energy corrections

1. Corrections to the self-energy at the two-loop level

We found in our analysis of the vertex corrections that the result depends on the interplay between the typical momentum and frequency. In our estimates, we considered two regions of external q and Ω, namely $q_x \sim q_y \sim (\gamma\Omega)^{1/3}$ and $q_x \sim \tilde{\Sigma}(\omega)/v_F$, $q_y \sim (\gamma\Omega)^{1/3}$. In both cases, we found that vertex corrections are small. We verify here that the two-loop self-energy, obtained by inserting vertex corrections into the one-loop self-energy diagram, is also small.

The two-loop self-energy diagram is presented in Fig. 1(c). We have

$$\Sigma_2(\omega) \sim g^4 \int d\omega_1 d^2q_1 \int d\omega_2 d^2q_2 \chi(\mathbf{q}_1,\omega_1)\chi(\mathbf{q}_2,\omega_2) \times G(\mathbf{k_F}+\mathbf{q_1},\omega+\omega_1)G(\mathbf{k_F}+\mathbf{q_2},\omega+\omega_2) \times G(\mathbf{k_F}+\mathbf{q_1}+\mathbf{q_2},\omega+\omega_1+\omega_2) \tag{5.24}$$

$$\sim \bar{g}^2 \int d\omega_1 d^2q_1 \int d\omega_2 d^2q_2 \frac{q_1}{\gamma|\omega_1|+q_1^3}\frac{q_2}{\gamma|\omega_2|+q_2^3} \times \frac{1}{i\tilde{\Sigma}(\omega+\omega_1)-v_F q_{1x}-N(q_{1y}^2/2m_B)} \times \frac{1}{i\tilde{\Sigma}(\omega+\omega_2)-v_F q_{2x}-N(q_{2y}^2/2m_B)} \times \frac{1}{i\tilde{\Sigma}(\omega+\omega_1+\omega_2)-v_F(q_{1x}+q_{2x})-N(q_{1y}+q_{2y})^2/2m_B}, \tag{5.25}$$

where we recall $\tilde{\Sigma}(\omega)=\omega+\Sigma(\omega)$.

Integrating successively over q_{1x} and q_{2x}, and rescaling the remaining momentum components by introducing $x=q_{1y}/(\gamma|\omega_1|)^{1/3}$ and $y=q_{2y}/(\gamma|\omega_2|)^{1/3}$, we obtain

$$\Sigma_2(\omega) \sim \frac{m_B\bar{g}^2}{Nv_F^2}\int_0^\omega d\omega_2 \int_{\omega-\omega_2}^{\omega} d\omega_1 \frac{1}{(\gamma^2\omega_1\omega_2)^{2/3}} \times \int_{-\infty}^{\infty}\frac{dxdy}{xy+i\zeta}\frac{|xy|}{(1+|x|^3)(1+|y|^3)}, \tag{5.26}$$

where $\zeta = m_B \frac{\tilde{\Sigma}(\omega+\omega_1)+\tilde{\Sigma}(\omega+\omega_2)-\tilde{\Sigma}(\omega+\omega_1+\omega_2)}{N(\gamma^2\omega_1\omega_2)^{1/3}}$.

As the typical frequencies ω_1 and ω_2 are of order ω, the typical value of ζ is of order $\beta \ll 1$. Expanding then in Eq. (5.26) to first order in ζ and performing the remaining integrals, we obtain in the quantum critical regime

$$\Sigma_2(\omega) \sim \frac{m_B\bar{g}^2}{Nv_F^2}\int_0^\omega d\omega_2 \int_{\omega-\omega_2}^{\omega} d\omega_1 \frac{\zeta \ln^2\zeta}{(\gamma^2\omega_1\omega_2)^{2/3}} \sim \Sigma(\omega)\beta^2\ln^2\beta, \tag{5.27}$$

where $\Sigma(\omega)=\Sigma_1(\omega)=\omega_0^{1/3}\omega^{2/3}$ is the self-energy in the Eliashberg theory.

This result agrees with the one obtained in Ref. 2, and shows that $\Sigma_2(\omega)\sim\Sigma_1(\omega)\times\frac{\Delta g}{g}|_{q,\Omega}$ where $\frac{\Delta g}{g}|_{q,\Omega}$ is given by Eq. (5.14). This last result implies that the typical internal q and Ω for the Eliashberg self-energy and for $\Sigma_2(\omega)$ are the same.

It is also instructive to compare these two-loop results, obtained as an expansion around the Eliashberg solution, to the perturbation expansion around free fermions. In the latter, we found in Eq. (3.12) that $\Sigma_2(\omega)\sim\omega\ln^2\omega$ whereas in the former we have $\Sigma_2(\omega)\propto\beta(\omega_0^{1/3}\omega^{2/3})\ln^2\beta$, Eq. (5.27). The free-fermion result can be reproduced if we neglect the self-energy in Eq. (5.26). We see that the expansion around free fermions does not reproduce the correct frequency dependence of $\Sigma_2(\omega)$. This obviously implies that if one expands around free fermions, there exist higher-order terms associated with insertions of the self-energy $\Sigma(\omega)$ into the internal fermionic lines, which may overshadow the two-loop result around free fermions. Accordingly, near the QCP, the expansion around free fermions does not converge, even if the curvature of the fermionic dispersion is included. On the other hand, the expansion around the Eliashberg solution is regular and holds in powers of the small parameters α and β.

2. Momentum dependence of the self-energy and the density of states

Along with the vertex corrections, we also neglected the momentum dependence of the fermionic self-energy in order to proceed with the Eliashberg scheme. We now verify whether the momentum dependent part of the self-energy $\Sigma(\mathbf{k},\omega=0)=\Sigma(\mathbf{k})$ remains small when evaluated with the full fermionic propagator. The k-dependent self-energy is given by

$$\Sigma(\mathbf{k},0) = 3ig^2\int\frac{d^2qd\Omega}{(2\pi)^3}G(\mathbf{k}+\mathbf{q},\Omega)\chi(\mathbf{q},\Omega) = \frac{3i\bar{g}}{(2\pi)^3}\int\frac{d\Omega d^2q}{i\tilde{\Sigma}(\Omega)-\epsilon_{k+q}}\frac{q}{\gamma|\Omega|+q^3}. \tag{5.28}$$

Defining the angular variable θ as $\epsilon_{k+q}=\epsilon_k+v_Fq\cos\theta$, integrating over it, and expanding to linear order in ϵ_k we obtain

$$\Sigma(\mathbf{k},0) = -3i\epsilon_k \times \frac{\bar{g}}{2\pi^2}\int_0^\infty d\Omega\tilde{\Sigma}(\Omega) \times \int\frac{q^2dq}{[q^3+(\gamma|\Omega|)][(v_Fq)^2+\tilde{\Sigma}(\Omega)^2]^{3/2}}. \tag{5.29}$$

A simple experimentation with the integrals shows that the integration over momentum is confined to $q\sim\tilde{\Sigma}(\Omega)/v_F$, while the frequency integral is confined to $\Omega<\omega_{\mathrm{Max}}$, where

ω_{Max}, defined in Eq. (5.3), is the scale where $(\gamma\Omega)^{1/3} = \tilde{\Sigma}(\Omega)/v_F$. The computation of $\Sigma(\mathbf{k})$ is given in Appendix B, and the result is

$$\Sigma(\mathbf{k},0) = -i\epsilon_k \frac{3\times 1.3308}{2\sqrt{2}\pi^{3/2}}\sqrt{\alpha} = -i\epsilon_k 0.253\sqrt{\alpha}. \quad (5.30)$$

Using our definition of Σ, we then obtain that $\Sigma(\mathbf{k},0)$ gives rise to a small, regular correction to the quasiparticle mass $\epsilon_k - i\Sigma(\mathbf{k},0) = \epsilon_k^* = v_F^*(k-k_F)$, where

$$v_F^* = v_F(1-0.253\sqrt{\alpha}). \quad (5.31)$$

Like the vertex correction at zero external bosonic momentum and frequency, this small correction is of order $O(\sqrt{\alpha})$ and comes from frequencies of order ω_{Max}.

The momentum dependent self-energy, unlike the frequency dependent part, generally gives rise to corrections to the fermionic density of states (DOS),

$$N(\omega) = -N_0 \int \frac{d\epsilon_k}{\pi} \mathrm{Im}G(\epsilon_k,\omega), \quad (5.32)$$

where N_0 is the DOS of free fermions.

Assuming that $\Sigma(k)$ is small and expanding in it in the fermionic propagator, we obtain, in real frequencies,

$$\frac{N(\omega)}{N_0} = 1 - \mathrm{Im}\left(\frac{\Sigma(\mathbf{k})}{\epsilon_k}\bigg|_{\epsilon_k = i\tilde{\Sigma}(-i\omega)} \right). \quad (5.33)$$

Substituting Eq. (5.30) into Eq. (5.33), we find that the density of states just shifts by a constant. In order to extract the frequency dependence of the density of states, one has to evaluate the momentum dependent self-energy to the next order in ϵ_k and on the mass shell, where $\epsilon_k = i\tilde{\Sigma}(\omega)$.

The evaluation of the self-energy near a mass shell generally requires extra caution as the self-energy may possess mass-shell singularities.[31] We, however, have checked in Appendix F that in our case the self-energy does not possess any mass-shell singularity, and the self-energy remains finite on the mass shell.

The calculation of the self-energy up to the second order in ϵ_k is displayed in Appendix B, and the result is

$$\Sigma(\mathbf{k},\omega) = i\epsilon_k \times \frac{0.45}{8\pi}\frac{|\Sigma(\omega)|}{E_F}\ln\frac{\omega_1}{|\omega|}. \quad (5.34)$$

Substituting this self-energy into the expression for the DOS and converting to real frequencies, we find at small ω

$$N(\omega) \sim N_0\left[1 - \left(\frac{\omega}{\omega_1}\right)^{2/3}\ln\frac{\omega_{\mathrm{Max}}}{\omega}\right], \quad (5.35)$$

where we explicitly defined

$$\omega_1 = \frac{128\pi^{5/2}}{(0.45)^{3/2}3^{3/4}}\frac{E_F^2}{\bar{g}}. \quad (5.36)$$

The correction to the fermionic DOS was earlier computed by Lawler *et al.*[14] using the bosonization technique. They obtained the same $\omega^{2/3}\ln\omega$ dependence as in Eq. (5.35). The agreement with Ref. 14 is, however, likely accidental as they evaluated $N(\omega)$ in the expansion around free fermions, while we obtained $N(\omega)$ by evaluating the k-dependent self-energy at $\epsilon_k = i\tilde{\Sigma}(-i\omega)$. If we neglected the Eliashberg self-energy (i.e., expanded around free fermions), we would obtain an $\omega\ln\omega$ correction to the DOS. This last result agrees with the one obtained by Ref. 23 using the same technique as in Ref. 14.

C. Summary

We have shown in this section that there are two conditions for the validity of the Eliashberg theory that one can recast as the smallness of two parameters:

$$\alpha \sim \frac{\bar{g}^2}{\gamma v_F^3} \sim \frac{\bar{g}}{E_F} \ll 1, \quad \beta \sim \frac{m_B\bar{g}}{\gamma v_F} \sim \frac{m_B}{Nm} \ll 1. \quad (5.37)$$

The first condition is quite generic for a low-energy theory since it requires that the fermion-fermion interaction mediated by the exchange of a boson should be smaller than the Fermi energy. Otherwise, the physics is not restricted to the vicinity of the Fermi surface anymore. The parameter α plays the same role as the Migdal parameter for the electron-phonon interaction: it sets the condition that fermions are fast excitations compared to bosons. In the scattering processes that are small in α, fermions are forced by the interaction to vibrate at frequencies near the bosonic mass shell. They are then far from their own resonance and thus have a small spectral weight.

However, the condition $\alpha \ll 1$ is not sufficient to construct a fully controllable perturbation expansion around the non-Fermi-liquid state at the QCP. In spatially isotropic systems there exist vertex corrections for which the external momentum has a component on the fermionic mass shell. These corrections do not contain α. However, they are sensitive to the curvature of the Fermi surface, and are small if β is small which can be achieved either by imposing $m_B \ll m$ or by extending the theory to a large number N of fermionic flavors.

A word of caution is due here. In evaluating the renormalization of the static vertex, we silently assumed that $\sqrt{\alpha} \ll \beta$, i.e., $\bar{g}/E_F < (m_B/Nm)^2$. At very large N, this is no longer valid. For this situation, i.e., when $\beta \ll \sqrt{\alpha}$, our estimates show that the static vertex is even smaller than $\sqrt{\alpha}$.

Finally, the pairing vertex in the Cooper channel stays of order $O(1)$, signaling the possibility of a pairing instability close to the quantum critical point. Nevertheless, we assume, based on explicit calculations worked out in Ref. 10, that the quantum critical behavior extends in the parameter space to a region where the superconductivity is not present.

VI. INSTABILITY OF THE FERROMAGNETIC QUANTUM CRITICAL POINT

We found that the Eliashberg theory for fermions interacting with gapless long-wavelength bosons is stable and controlled by two small parameters. We verified this by calculating the fermionic self-energy in a two-loop expansion around the Eliashberg solution.

One may wonder whether the same conclusions hold for the bosonic self-energy as well. In particular, what are the corrections to the static susceptibility $\chi_s(q,0)$? Naively one could assume that they are unimportant and do not change the bare q^2 behavior of the inverse bosonic propagator at the QCP.

For a ferromagnetic SU(2) QCP, for which the massless bosons are spin fluctuations, we show in this section that the corrections to the static spin susceptibility are nonanalytic: they scale like $q^{3/2}$, and *do not* contain any prefactor except for a proper power of k_F. Such terms obviously overshadow the regular q^2 of the bare susceptibility at small enough momenta. These terms therefore belong to the Eliashberg theory, which has to be extended to incorporate them.

The physics behind the $q^{3/2}$ term in $\chi(q,0)$ at a ferromagnetic QCP is, by itself, not directly related to criticality: far away from the QCP, the spin susceptibility also contains negative, nonanalytic $|q|$ term.[26,27,35–38] This term gradually evolves as the correlation length ξ increases, and transforms into the $q^{3/2}$ term at the QCP. Both these nonanalyticities, at and away from the QCP, emerge because the boson-mediated interaction between fermions contain a long-range dynamic component, generated from the Landau damping.

For charge fluctuations, the $q^{3/2}$ terms appear in the individual diagrams for the susceptibility but cancel out in the full formula for $\chi(q,\Omega)$. We discuss the physical origin of the difference between spin and charge susceptibilities in the next section.

One of the reasons why the nonanalyticity of the static spin susceptibility at the QCP has not been analyzed much earlier is because it was widely believed that an itinerant fermionic system near a ferromagnetic QCP is adequately described by a phenomenological 2+1D ϕ^4 bosonic theory (in our case, the role of ϕ is played by the vector field $\mathbf{S}$) with the dynamic exponent $z=3$ and a constant prefactor for the ϕ^4 term.[1] In dimensions $d \geq 4-z=1$, the model lies above its upper critical dimension and the ϕ^4 term is simply irrelevant.

In this section, we derive the effective ϕ^4 theory from the spin-fermion model Hamiltonian, and show that it contains two elements absent from the phenomenological approach. First, the prefactor of the ϕ^4 term strongly depends on the ratio between the external momenta and frequencies, and contains a nonanalytic term in addition to the constant one. Second, there also exists a cubic ϕ^3 term whose prefactor, although vanishing in the static limit, also strongly depends on the interplay between the external momenta and frequencies. We can recast the nonanalytic $q^{3/2}$ term in the static spin susceptibility as arising from these cubic and quartic terms in ϕ.

We also prove that the nonanalyticity appears in the temperature-dependent uniform static susceptibility $\chi_s(T)$. We show below that $\chi_s^{-1}(T) \propto T|\ln T|$, again with a negative prefactor.

Finally, we show that the instability of the ferromagnetic QCP can also be seen from the fermionic self-energy, which acquires singular terms beginning at the three-loop order in the case of spin fluctuations.

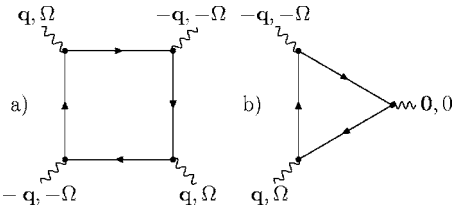

FIG. 4. "ϕ^4" and "ϕ^3" type diagram.

A. Hertz-Millis-Moriya theory revisited

In order to derive a quantum critical ϕ^4 model, one has to integrate the fermions out of the partition function, noticing that the Lagrangian of the spin-fermion model is quadratic in the fermions.

Expanding then in the number of bosonic fields $\mathbf{S}$, the quartic term in the effective action reads

$$\int \frac{d^2q d^2p d^2p' d\Omega d\nu d\nu'}{(2\pi)^9} A(\mathbf{p},\mathbf{p}',\mathbf{q},\nu,\nu',\Omega) \times [\mathbf{S}_{p+q/2}\cdot\mathbf{S}_{q/2-p}\mathbf{S}_{p'-q/2}\cdot\mathbf{S}_{-p'-q/2} + \mathbf{S}_{p+q/2}\cdot\mathbf{S}_{-p'-q/2}\mathbf{S}_{q/2-p}\cdot\mathbf{S}_{p'-q/2} - \mathbf{S}_{p+q/2}\cdot\mathbf{S}_{p'-q/2}\mathbf{S}_{-q/2-p'}\cdot\mathbf{S}_{q/2-p}], \tag{6.1}$$

where p, p', q are bosonic momenta, and ν, ν', Ω are bosonic frequencies.

Our goal here is to prove that the prefactor A is not a regular function of momenta and frequencies. To simplify the presentation, we choose to study only the dependence of A on q and Ω and set $\mathbf{p}$, $\mathbf{p}'$, ν, ν' to zero (see Fig. 4).

The analytic form of this prefactor then writes

$$A(q,\Omega) \sim Ng^4 \int d\omega \int d^2k G(\mathbf{k},\omega)^2 \times G(\mathbf{k}+\mathbf{q},\omega+\Omega)^2. \tag{6.2}$$

Defining θ as the angle between $\mathbf{k}$ and $\mathbf{q}$, and performing the integration over ϵ_k and the angular variable, we find

$$A(q,\Omega) \sim \frac{mg^4}{\omega_0\Omega}\int_0^1 dz \frac{\{[v_F q/\Sigma(\Omega)]^2 - 2[z^{2/3}+(1-z)^{2/3}]^2\}}{\{[v_F q/\Sigma(\Omega)]^2 + [z^{2/3}+(1-z)^{2/3}]^2\}^{5/2}}, \tag{6.3}$$

where we defined $z=\omega/\Omega$, and neglected at this stage a regular part that comes from large values of ϵ_k and for which the curvature is relevant.

We see that $A(q,\Omega)$ depends on the interplay between the momentum and frequency. We can identify two regimes.

(i) If $|q| \sim (\gamma|\Omega|)^{1/3}$, i.e., if the bosonic momenta are near the bosonic mass shell, the self-energy in the denominator can be neglected, the frequency factors in the numerator and the denominator are canceled out, and we obtain

$$A(\Omega) \sim \frac{mg^4}{\gamma v_F^3} \sim \frac{1}{\chi_0^2}\alpha m. \tag{6.4}$$

We see that A can be safely replaced by a constant $O(\alpha)$. This is consistent with the previous works.[1] The agreement is not surprising as the relation $q \sim (\gamma|\Omega|)^{1/3}$ is assumed in

power counting based on $z=3$ scaling. Note that the condition $|q| \sim (\gamma|\Omega|)^{1/3}$ only specifies the magnitude of q, one of its components (e.g., q_x) can be much smaller.

(ii) If $q \sim \tilde{\Sigma}(\omega)/v_F \sim \omega_0^{1/3}\Omega^{2/3}/v_F$ (at $\omega < \omega_0$), i.e., when a boson resonates near a fermionic mass shell, the $z=3$ scaling arguments are not applicable. We have in this regime

$$A(q,\Omega) \sim \frac{mg^4}{\omega_0 \Omega} \sim \frac{m}{\chi_0^2}\frac{1}{\sqrt{\alpha}}\frac{\omega_{\mathrm{Max}}}{\Omega}. \tag{6.5}$$

In this case, $A(\Omega)$ is a singular function of frequency, and cannot be replaced by a constant.

We see therefore that the prefactor of the ϕ^4 term is actually singular outside the scaling regime of a $z=3$ theory.

In the similar spirit, one can construct a cubic term in the bosonic fields:

$$\int \frac{d^2q d^2p d\Omega d\nu}{(2\pi)^9} B(\mathbf{p},\mathbf{q},\nu,\Omega)\mathbf{S}_p \cdot (\mathbf{S}_{q-p/2} \times \mathbf{S}_{-q-p/2}), \tag{6.6}$$

where the prefactor B is a convolution of three fermionic Green's functions as presented in Fig. 4, and is given by

$$B(\mathbf{q},\mathbf{p},\Omega,\nu) \sim Ng^3 \int d\omega \int d^2k G(\mathbf{k}-\mathbf{p},\omega-\nu) \times G(\mathbf{k}-\mathbf{p/2}-\mathbf{q},\omega-\nu/2-\Omega)G(\mathbf{k},\omega). \tag{6.7}$$

Proceeding as for the quartic term, we set for simplicity $\mathbf{p}=\mathbf{0}$, $\nu=0$, and integrate over ϵ_k and the angular variable, leading to

$$B(q,\Omega) \sim \frac{mg^3}{\omega_0^{2/3}\Omega^{1/3}} \int_0^1 dz \times \frac{[z^{2/3}+(1-z)^{2/3}]}{\{[v_F q/\Sigma(\Omega)]^2 + [z^{2/3}+(1-z)^{2/3}]^2\}^{3/2}}, \tag{6.8}$$

where we again introduced the rescaled frequency $z=\omega/\Omega$.

We can again identify two regimes.

(i) In the $z=3$ regime where $q \sim (\gamma\Omega)^{1/3}$, one can expand for large $\frac{v_F q}{\Sigma(\Omega)}$, which leads to

$$B(q,\Omega) \sim \frac{mg}{\chi_0}\alpha\left(\frac{\Omega}{\omega_{\mathrm{Max}}}\right)^{2/3}, \tag{6.9}$$

where ω_{Max} is given by Eq. (5.3). This term is small in the quantum critical regime where $\Omega < \omega_0 \sim \omega_{\mathrm{Max}}\alpha^{3/2}$, and can be safely neglected.

(ii) For $q \sim \Sigma(\Omega)$, the remaining integral is of order $O(1)$ and the result writes

$$B(q,\Omega) \sim \frac{mg}{\chi_0}\frac{1}{\sqrt{\alpha}}\left(\frac{\omega_{\mathrm{Max}}}{\Omega}\right)^{1/3}, \tag{6.10}$$

which is large and cannot be neglected.

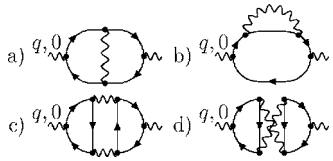

FIG. 5. Corrections to the polarization bubble from diagrams with one and two extra bosonic lines.

We demonstrate in the next section how the singular behavior of the ϕ^3 and ϕ^4 terms leads to a nonanalytic contribution to the static spin susceptibility.

B. Nonanalyticity in the static spin susceptibility

We now estimate the effect of these singularities on physical quantities. Both the ϕ^3 and ϕ^4 terms in the effective action give rise to corrections to the ϕ^2 term, i.e., to the spin susceptibility. These corrections are obtained diagrammatically by contracting the external legs of the ϕ^3 and ϕ^4 terms, as shown in Fig. 5. The computations are described in detail in Appendix D.

The contributions from the ϕ^4 terms have been considered in our short publication.[29] The contributions from cubic terms were missed, and were first considered in Ref. 39 in the analysis of the spin susceptibility in the paramagnetic phase, away from a QCP.

In analytic form, we have, using $\chi(q,0)=\chi_0/[\xi^{-2}+q^2+\Pi(q,0)]$, and $\Pi=\Pi_1(q,0)+\Pi_2(q,0)+\Pi_3(q,0)+\Pi_4(q,0)$:

$$\Pi_1(q,0) = \Gamma_1^S \frac{N\bar{g}^2}{(2\pi)^6\chi_0}\int d^2k d\omega d^2l d\Omega \chi(l+q,\Omega)G(\omega,k) \times G(\omega+\Omega,k+l)G(\omega+\Omega,k+q+l)G(\omega,k+q),$$

$$\Pi_2(q,0) = \Gamma_2^S \frac{N\bar{g}^2}{(2\pi)^6\chi_0}\int d^2k d\omega d^2l d\Omega \chi(l,\Omega)G(\omega,k)^2 \times G(\omega+\Omega,k+l)G(\omega,k+q),$$

$$\Pi_3(q,0) = \Gamma_3^S \frac{N^2\bar{g}^3}{(2\pi)^9\chi_0^2}\int d^2k d\omega d^2k' d\omega' dl d\Omega \chi(l,\Omega) \times \chi(q+l,\Omega)G(\omega,k)G(\omega,k+q) \times G(\omega+\Omega,k+l+q)G(\omega',k')G(\omega',k'+q) \times G(\omega'+\Omega,k'+l+q),$$

$$\Pi_4(q,0) = \Gamma_4^S \frac{N^2\bar{g}^3}{(2\pi)^9\chi_0^2}\int d^2k d\omega d^2k' d\omega' dl d\Omega \chi(l,\Omega)\chi(l+q,\Omega) \times G(\omega,k)G(\omega,k+q)G(\omega+\Omega,k+l+q) \times G(\omega',k')G(\omega'+\Omega,k'+l)G(\omega'+\Omega,k'+l+q). \tag{6.11}$$

The factors of N come from the fermionic loops and the numerical prefactors from the following spin summations:

$$\begin{cases} \Gamma_1^S = \sum_{\alpha,\beta,\gamma,\delta} \sigma^Z_{\alpha\beta}\boldsymbol{\sigma}_{\beta\gamma}\sigma^Z_{\gamma\delta}\boldsymbol{\sigma}_{\delta\alpha} = -2 \\ \Gamma_2^S = \sum_{\alpha,\beta,\gamma,\delta} \sigma^Z_{\alpha\beta}\boldsymbol{\sigma}_{\beta\gamma}\cdot\boldsymbol{\sigma}_{\gamma\delta}\sigma^Z_{\delta\alpha} = 6 \\ \Gamma_3^S = \sum_{\alpha,\beta,\gamma,\delta,\epsilon,\zeta} \sigma^Z_{\alpha\beta}(\boldsymbol{\sigma}_{\beta\gamma}\cdot\boldsymbol{\sigma}_{\delta\epsilon})(\boldsymbol{\sigma}_{\gamma\alpha}\cdot\boldsymbol{\sigma}_{\zeta\delta})\sigma^Z_{\epsilon\zeta} = 8 \\ \Gamma_4^S = \sum_{\alpha,\beta,\gamma,\delta,\epsilon,\zeta} \sigma^Z_{\alpha\beta}(\boldsymbol{\sigma}_{\beta\gamma}\cdot\boldsymbol{\sigma}_{\epsilon\delta})(\boldsymbol{\sigma}_{\gamma\alpha}\cdot\boldsymbol{\sigma}_{\delta\zeta})\sigma^Z_{\zeta\epsilon} = -8. \end{cases} \tag{6.12}$$

These four diagrams are related by pairs. To verify this, it is useful to expand the products of Green's functions according to

$$G(\omega_1,k_1)G(\omega_2,k_2) = \frac{G(\omega_1,k_1) - G(\omega_2,k_2)}{G^{-1}(\omega_2,k_2) - G^{-1}(\omega_1,k_1)}. \tag{6.13}$$

Applying this to $\Pi_2(q,0)$, we find that it splits into two parts. In one part, the poles in ϵ_k are located in the same half plane, leading to a vanishing contribution. The remaining term in $\Pi_2(q,0)$ is related to $\Pi_1(q,0)$ in such a way that

$$\Pi_1(q,0) = -\frac{2\Gamma_1}{\Gamma_2}\Pi_2(q,0) \tag{6.14}$$

(see Appendix D for details).

Similarly, $\Pi_3(q,0)$ and $\Pi_4(q,0)$ are related as

$$\Pi_3(q,0) = -\frac{\Gamma_3}{\Gamma_4}\Pi_4(q,0). \tag{6.15}$$

Collecting all four contributions and using the relations between prefactors, we obtain

$$\Pi(q,0) = \Pi_A(q,0) + \Pi_B(q,0),$$

$$\begin{aligned} \Pi_A(q,0) &= \Pi_1(q,0) + 2\Pi_2(q,0) \\ &= 16\frac{N\bar{g}^2}{(2\pi)^6\chi_0}\int d^2K d\omega d^2l d\Omega \chi(l,\Omega)G(\omega,k)^2 \\ &\quad \times G(\omega+\Omega,k+l)G(\omega,k+q), \end{aligned} \tag{6.16}$$

$$\begin{aligned} \Pi_B(q,0) &= \Pi_3(q,0) + \Pi_4(q,0) \\ &= 16\frac{N^2\bar{g}^3}{(2\pi)^9\chi_0^2}\int d^2k d\omega d^2k' d\omega' dl d\Omega \chi(l,\Omega) \\ &\quad \times \chi(q+l,\Omega)G(\omega,k)G(\omega,k+q) \\ &\quad \times G(\omega+\Omega,k+l+q)G(\omega',k'+q) \\ &\quad \times G(\omega',k')G(\omega'+\Omega,k'+l+q). \end{aligned} \tag{6.17}$$

1. Fermi-liquid regime

Away from criticality, the correlation length ξ is finite, and at low frequency, the system is in the Fermi-liquid regime. The fermionic self-energy is $\Sigma(\omega)=\lambda\omega$, Eq. (4.7).

The spin susceptibility in this regime has been analyzed in Refs. 27 and 35–39. It was shown there that to the lowest order in the interaction, $\Pi_B(q,0)=\Pi_A(q,0)$, i.e., $\Pi(q,0)=2\Pi_A(q,0)$. Beyond leading order, $\Pi_B(q,0)$ and $\Pi_A(q,0)$ are not equivalent but are of the same sign and of comparable magnitude. For simplicity, we assume that the relation $\Pi_B(q,0)=\Pi_A(q,0)$ holds in the whole Fermi-liquid regime. We show below that even at the QCP, $\Pi_B(q,0)$ and $\Pi_A(q,0)$ are quite similar [at criticality $\Pi_B(q,0)\approx 1.3\Pi_A(q,0)$].

Introducing $\cos\theta=\frac{\mathbf{k}\cdot\mathbf{l}}{|\mathbf{k}||\mathbf{l}|}$ and $\cos\theta'=\frac{\mathbf{k}\cdot\mathbf{q}}{|\mathbf{k}||\mathbf{q}|}$, and successively integrating over $|\mathbf{k}|$, ω and θ', Eq. (6.16) can be rewritten as

$$\begin{aligned} \Pi(q,0) &= \frac{8\bar{g}|q|}{\pi^3(1+\lambda)v_F}\int_0^\infty dz \int_0^{\pi/2} d\phi \int_0^\pi d\theta \frac{1}{1/\tilde{\gamma}\xi^2 + \tan\phi} \\ &\quad \times \frac{\cos\phi\sin\phi}{(i\sin\phi - \cos\theta\cos\phi)^2} \\ &\quad \times \frac{z}{\sqrt{1+z^2(\sin\phi + i\cos\phi\cos\theta)^2}}, \end{aligned} \tag{6.18}$$

where we defined $\tilde{\gamma}=\frac{\gamma v_F}{1+\lambda}$, and introduced the new variables z and ϕ, which satisfy $z\cos\phi=\frac{l}{q}$ and $z\sin\phi=\frac{(1+\lambda)\Omega}{v_F q}$.

The universal part of $\Pi(q,0)$ can be isolated by subtracting from it the constant part $\Pi(0,0)$. The integral over z then becomes convergent. Integrating successively over z, ϕ, and θ, we obtain

$$\Pi(q,0) = -\frac{4}{\pi^2}\frac{\bar{g}}{v_F(1+\lambda)}|q|\mathcal{H}\left(\frac{1+\lambda}{\tilde{\gamma}\xi^2}\right), \tag{6.19}$$

where $\mathcal{H}(0)=\frac{1}{3}$, and $\mathcal{H}(x\gg 1)\approx 2/(3x^2)$. We do recover the nonanalytic $|q|$ correction to the static spin susceptibility in $D=2$, as obtained in earlier studies.[26,27,35,36]

Note that Eq. (6.20) does not contradict the Fermi-liquid relation $\chi_s(q\to 0,\omega=0)\propto(1+F_{1,s})/(1+F_{0,a})$, where $F_{1,s}$ and $F_{0,a}$ are Landau parameters. The Fermi-liquid theory only implies that the static spin susceptibility saturates to a constant value as $q\to 0$, but does not impose any formal constraint on the q dependence of $\chi_s(q,\omega)$.

As one gets closer to the QCP, $\lambda=3\bar{g}/(4\pi v_F\xi^{-1})$ diverges and the prefactor of the $|q|$ term vanishes as

$$\Pi(q,0) = -\frac{16}{9\pi}\xi^{-1}|q|. \tag{6.20}$$

This is not surprising since the Fermi-liquid regime extends on a region of the phase diagram that shrinks and ultimately vanishes as one approaches the QCP.

Now, two different scenarios are possible:

(i) the divergence of ξ at the QCP completely eliminates the nonanalyticity and the expansion of $\Pi(q,0)$ begins as q^2, like in a bare spin susceptibility;

(ii) the self-energy $\Sigma(\omega)\propto\omega^{2/3}$ at the QCP still leads to a nonanalytic term $\Pi(q,0)\propto|q|^\delta$, with $1<\delta<2$, which dominates over the bare q^2 term.

We show in the next subsection that the second scenario is realized, and at the QCP, one has $\Pi(q,0)\propto|q|^{3/2}$.

2. At criticality

At the QCP, we have to take into account two new elements: the bosonic propagator is massless ($\xi^{-1}=0$) and the

fermionic self-energy is no longer Fermi-liquid-like, it is given by Eq. (4.9).

The full calculation of $\Pi_A(q,0)$ and $\Pi_B(q,0)$ is presented in Appendix D. We just outline here the main steps of the computation and show where the $q^{3/2}$ term comes from.

Consider first $\Pi_A(q,0)$. Using Eq. (6.16) as a starting point, and substituting the full form of the spin susceptibility, Eq. (A8), we then expand $\epsilon_{\mathbf{k+l}}$ and $\epsilon_{\mathbf{k+q}}$, and integrate successively over l_y (projection of $\mathbf{l}$ perpendicular to $\mathbf{k_F}$) and ϵ_k, leading to

$$\Pi_A(q,0) = 16i\frac{m\bar{g}^2}{(2\pi)^5}\int_0^{2\pi} d\theta \int_{-\infty}^{+\infty} dl_x \int_{-\infty}^{+\infty} d\Omega \int_{-\Omega}^{0} d\omega \times \frac{1}{[i\Sigma(\omega+\Omega)-i\Sigma(\omega)-v_F l_x]^2} h\left(\frac{\sqrt{l_x^2+c^2\Sigma^2(\Omega)}}{(\gamma|\Omega|)^{1/3}}\right) \times \frac{1}{(\gamma|\Omega|)^{1/3}} \frac{1}{i\Sigma(\omega+\Omega)-i\Sigma(\omega)-v_F l_x + v_F q\cos\theta}, \tag{6.21}$$

where $c \simeq 1.198\,78$ [see Eq. (A6)], and $h(x)$ is the bosonic propagator $\chi(l,\Omega)/\chi_0$ integrated over the momentum component l_y. The asymptotic behavior of $h(x)$ is given by

$$\begin{cases} h(x \gg 1) = \dfrac{\pi}{x} \\ h(x \ll 1) = \dfrac{4\pi}{3\sqrt{3}} + (\ln 2 - 1)x^2 - \dfrac{x^2 \ln x^2}{2}. \end{cases} \tag{6.22}$$

Since the integrand in Eq. (6.21) has poles in l_x located in the same half plane, the only nonvanishing contributions to Π comes from the nonanalyticities in $h(x)$.

There are two nonanalyticities in $h(x)$. The first one comes from the $1/x$ behavior at large x, which extends to $x \sim 1$. This is a conventional nonanalyticity associated with bosons vibrating near their own mass shell, since at $x \sim 1$, $l_x \sim l_y \sim (\gamma|\Omega|)^{1/3}$.

Subtracting the constant $\Pi_A(0,0)$, expanding in q in Eq. (6.21) and substituting $l_x \sim (\gamma|\Omega|)^{1/3}$, we find for this contribution to Π

$$\delta\Pi_A^{(1)} \propto q^2 \frac{m\bar{g}^2}{v_F^3 \gamma^{5/3}} \int_0^{\omega_{\mathrm{Max}}} \frac{d\Omega}{\Omega^{2/3}} \propto \sqrt{\alpha} q^2, \tag{6.23}$$

where $\omega_{\mathrm{Max}} \sim \sqrt{\gamma v_F^3}$.

We see that the integration over the momentum range relevant to the $z=3$ scaling regime yields a regular q^2 contribution to the static susceptibility. Not only is this contribution regular in q, but it is also small in α. This result is similar to the one we obtained in Eq. (5.2) for the static vertex at a vanishing momentum.

However, Eq. (6.22) shows that $h(x)$ has a nonanalytic $x^2 \ln x$ term already at small x, i.e., far from the bosonic mass shell: the branch cut associated with the logarithmic term emerges at $v_F l_x \sim \Sigma(\omega)$. The typical value of l_y in the integral that leads to this $x^2 \ln x$ term is also of the same order, although larger in the logarithmic sense. This implies that this second nonanalyticity comes from a process in which the bosons are vibrating near a fermionic mass shell and far from their own.

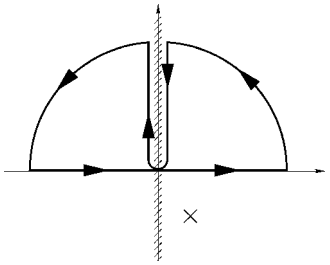

FIG. 6. Integration contour: the hatched region stands for a branch cut, and the cross for a pole.

Furthermore, this logarithmic term in Eq. (6.22) comes exclusively from the Landau damping term in the bosonic propagator—the q^2 term in $\chi(l,\Omega)$ can be safely omitted. Indeed, one has

$$\int_{-\Lambda}^{\Lambda} dl_y \frac{1}{\gamma|\Omega|/\sqrt{l_x^2+l_y^2}} = f(\Lambda) - \frac{l_x^2 \ln l_x^2}{2\gamma\Omega}. \tag{6.24}$$

Substituting the logarithmic term from Eq. (6.22) into the formula (6.21) for $\Pi_A(q)$ and again subtracting the nonuniversal constant term $\Pi_A(0,0)$, we find that the integral over l_x is convergent. Introducing $z=l_x/[c\Sigma(\Omega)]$, one can perform the integral over z over the contour of Fig. 6, which leads to the following contribution to Π, which we label as $\Pi_A^{(2)}(q,0)$:

$$\Pi_A^{(2)}(q,0) - \Pi_A(0,0) = \frac{4m\bar{g}^2}{c^2\pi^4\gamma v_F} q^2 \int_0^{\pi/2} d\theta \int_1^{+\infty} dy \int_0^{+\infty} \frac{d\omega}{\Sigma(\Omega)^2} \times \int_0^1 dw \frac{\cos^2\theta}{\{c^{-1}[(1-w)^{2/3}+w^{2/3}]+y\}^3} \times \frac{1-y^2}{\{y+c^{-1}[(1-w)^{2/3}+w^{2/3}]\}^2 + (v_F q\cos\theta/c\Sigma(\Omega))^2}, \tag{6.25}$$

where we defined $w=\omega/\Omega$.

Introducing the new variables $t=\left(\frac{c\Sigma(\Omega)}{v_F q\cos\theta}\right)^{3/2}$ and $v=t\{y+c^{-1}[(1-w)^{2/3}+w^{2/3}]\}$, it becomes possible to separate the integrals, leading to the following final result:

$$\begin{aligned} \Pi_A(q,0) - \Pi_A(0,0) &\approx \Pi_A^{(2)}(q,0) - \Pi_A(0,0) \\ &= -0.8377 q^{3/2} \frac{m\bar{g}^2}{\pi^4 \gamma v_F^{3/2} \omega_0^{1/2}} \\ &= -0.1053\sqrt{k_F} q^{3/2}. \end{aligned} \tag{6.26}$$

We emphasize that this dependence comes from bosonic modes vibrating at the fermionic mass shell. This explains why the result of Eq. (6.26) is not small in α, as this small parameter measures the softness of the mass-shell bosons compared to the mass-shell fermions.

The integrals for $\Pi_B(q,0)$ cannot be exactly evaluated analytically, but an approximate calculation (presented in Appendix D) yields

$$\Pi_B(q,0) - \Pi_B(0,0) = -0.14 q^{3/2}\sqrt{k_F}, \tag{6.27}$$

such that the total

$$\Pi(q,0) - \Pi(0,0) = -0.25 q^{3/2}\sqrt{k_F}. \tag{6.28}$$

We see that $\Pi(q,0)$ is still nonanalytic in q and the prefactor is negative. At small q, the negative $q^{3/2}$ term well exceeds the regular q^2 term. This implies that *the static spin susceptibility is negative at small momenta, i.e., a ferromagnetic QCP is unstable*. We discuss the consequences of this instability in the concluding section. The momentum $q_{\min}$ below which χ_s is negative is determined by

$$\chi^{-1}(q_{\min}) \propto q_{\min}^2 - 0.25 q_{\min}^{3/2}\sqrt{k_F} = 0, \tag{6.29}$$

which gives $q_{\min}=0.06k_F$. Parametrically, $q_{\min}$ is of order k_F, which is the largest momentum scale in our problem. Strictly speaking, this suggests that the whole quantum critical theory for the ferromagnetic case is not valid, for the quantum critical behavior extends up to energies of order ω_0, i.e., up to momenta of order $q \leq \omega_0/v_F \sim \alpha^2 k_F \ll k_F$. Numerically, however, $q_{\min}$ is much smaller than k_F. This implies that for reasonable values of α, there exists an intermediate momentum and energy range $q_{\min} < q < \omega_0/v_F$ where the system is in the quantum critical regime, but the static spin susceptibility is still positive.

The $q^{3/2}$ nonanalyticity can also be viewed as emerging from the $q \ln q$ momentum dependence of the static vertex. Using Eq. (5.5), one can rewrite

$$\Pi(q,0) \sim N\bar{g} \int d^2k d\omega \frac{1}{i\Sigma(\omega) - \epsilon_k} \frac{(\Delta g/g)|_{q,\Omega=0}}{i\Sigma(\omega) - \epsilon_{k+q}}. \tag{6.30}$$

Performing the contour integration over ϵ_k, and changing variables into $y=\epsilon_k/\Sigma(\omega)$ and $t=\sqrt{\omega_0}\omega/(v_F q)^{3/2}$, we obtain

$$\Pi(q,0) \sim \sqrt{k_F} q^{3/2}. \tag{6.31}$$

We note in this regard that the nonanalytic momentum dependence of the fermion-boson static vertex also comes from bosons vibrating near the fermionic mass shell, i.e., it emerges due to the same physics as we outlined above.

C. Temperature dependence of the static uniform spin susceptibility

In this section, we show that the static uniform susceptibility is negative at finite temperature above a ferromagnetic QCP. To demonstrate this, we compute the static uniform $\Pi_A(q=0,\omega=0,T)=\Pi_A(T)$, assuming that $\xi^{-1}=0$. The contribution from $\Pi_B(T)$ is of the same sign and comparable in magnitude. We have

$$\Pi_A(0,T) = 16i \frac{m\bar{g}^2}{(2\pi)^3} T \sum_{p\neq 0} \Omega_p \int d^2q \times \frac{1}{q^2 + \gamma|\Omega_p|/q} \frac{1}{\left[i\Sigma(\Omega_p) - v_F q_x - q_y^2/2m\right]^3}. \tag{6.32}$$

Since the poles in q_x from the fermionic Green's functions are all in the same half plane, one expects that $q_x^{\mathrm{Typ}} \sim (\gamma\Omega)^{1/3}$ and thus dominates over the q_y^2 term, which in turn can be neglected in the fermionic Green's functions. It then becomes possible to perform the integral over q_y, which gives

$$\Pi_A(0,T) = 2i \frac{m\bar{g}^2}{\pi^3 \gamma v_F^3} T \sum_{p\neq 0} \frac{\Omega_p}{|\Omega_p|} \int_0^{(\gamma\Omega_p)^{1/3}} dq_x \frac{q_x^2 \ln|q_x|}{[i\tilde{\Sigma}(\Omega_p) - v_F q_x]^3}. \tag{6.33}$$

Integrating over the half space where there is no triple pole, we find that the integral is determined by the branch cut in $\ln|q_x|$. Evaluating the integral we obtain

$$\int \frac{dq_x q_x^2 \ln|q_x|}{[i\tilde{\Sigma}(\Omega_p) - v_F q_x]^3} = \mathrm{sgn}(\Omega_p) \frac{i\pi}{v_F^3} \ln\left(\frac{E_F}{|\tilde{\Sigma}(\Omega_p)|}\right). \tag{6.34}$$

Thus

$$\Pi_A(0,T) = \frac{2m\bar{g}^2}{3\pi^2 \gamma v_F^3} T \sum_{p\neq 0} \ln \frac{E_F}{|\Omega_p|}. \tag{6.35}$$

To perform the summation over p, we notice that when the summand does not depend on p,

$$T \sum_{-\Lambda/T}^{\Lambda/T} A = 2A\Lambda \tag{6.36}$$

is independent on T. Then the same sum but without the $p=0$ term just gives $2A\Lambda - AT$. Using this, we obtain with logarithmic accuracy

$$T \sum_{p\neq 0} \ln \frac{E_F}{|\Omega_p|} = -T \ln \frac{E_F}{T} + \cdots, \tag{6.37}$$

where dots stand for $O(T)$ terms. Substituting this into Eq. (6.35), we obtain the final result:

$$\Pi_A(0,T) = -\frac{2k_F^2}{3\pi^2} \alpha \frac{T}{E_F} \ln\left(\frac{E_F}{T}\right). \tag{6.38}$$

Although small, because of the prefactor in α, this term dominates at low temperature over any regular T^2 term. The sign of this $T\ln(E_F/T)$ term is opposite to the sign of a conventional correction to scaling HMM theory, which comes from a constant part of the prefactor for the ϕ^4 term. In the HMM theory the temperature dependence of the spin susceptibility is $bT^{d+z-2}z$, $b>0$, which in $d=2$ leads to a linear in T contribution with positive prefactor. The negative sign of nonanalytic temperature correction in Eq. (6.38) implies that the static spin susceptibility is negative right above

the QCP. This is another indication that the ferromagnetic QCP is unstable.

D. Self-energy at the three-loop level

Finally, we show how one can detect the instability of a ferromagnetic QCP from an analysis of higher-order self-energy diagrams. This analysis is complimentary to the calculations that we have already done in the previous subsections. We show that upon inserting the contributions from the diagrams presented in Fig. 5 into the fermionic self-energy, we obtain series of singular corrections in powers of $\omega_{\min}/\omega$, where $(\gamma\omega_{\min})^{1/3}=q_{\min}$, and $q_{\min}$ is the scale at which the static susceptibility $\chi_s(q)$ becomes negative, Eq. (6.29).

To illustrate this, we consider one of the three-loop diagrams, represented in Fig. 7. In the case of a spin interaction, we obtained a finite result after collecting the various diagrams, so we restrict ourselves here with just one of these contributions. The analytic form of the diagram in Fig. 7 writes

$$\Sigma_3(\omega) \sim \bar{g} \int d\omega_1 d^2q_1 \frac{A(q_1,\omega_1)}{i\Sigma(\omega-\omega_1) - v_F q_{1x} - Nq_{1y}^2/2m} \times \left(\frac{1}{q_1^2 + \gamma|\omega_1|/q_1}\right)^2, \tag{6.39}$$

where $A(q_1,\omega_1)$ is the dynamic fermionic bubble given by

$$A(q_1,\omega_1) \sim N\bar{g}^2 \int d^2k d\Omega \int d^2q_2 d\omega_2 \frac{1}{q_2^2 + \gamma|\omega_2|/q_2} \times \frac{1}{i\Sigma(\Omega) - \epsilon_k} \frac{1}{i\Sigma(\Omega+\omega_1+\omega_2) - \epsilon_{k+q_1+q_2}} \times \frac{1}{i\Sigma(\Omega-\omega_1) - \epsilon_{k+q_1}} \frac{1}{i\Sigma(\Omega+\omega_2) - \epsilon_{k+q_2}}.$$

Approximating $A(q_1,\omega_1)$ by its singular static part $q_1^{3/2}\sqrt{k_F}$ and substituting into Eq. (6.39) we obtain

$$\Sigma_3(\omega) \sim \bar{g}\sqrt{k_F} \int d\omega_1 d^2q_1 \left(\frac{q_1}{q_1^3 + \gamma|\omega_1|}\right)^2 \times \frac{q_1^{3/2}}{i\Sigma(\omega-\omega_1) - v_F q_{1x} - Nq_{1y}^2/2m}. \tag{6.40}$$

A simple analysis of this expression shows that the dominant contribution to $\Sigma_3(\omega)$ comes from $q_{1x} \sim q_{1y} \sim (\gamma\omega_1)^{1/3}$ since the integral over q_{1x} is determined by the branch cut in the bosonic propagator. One can then safely drop the quadratic term in the fermionic propagator and integrate over the angle θ between $\mathbf{k_F}$ and $\mathbf{q_1}$. This leads to

$$\Sigma_3(\omega) \sim \bar{g}\sqrt{k_F} \int_0^\omega d\omega_1 \int dq_1 \frac{q_1^{9/2}}{(q_1^3 + \gamma\omega_1)} \times \frac{1}{\sqrt{(v_F q_1)^2 + \Sigma(\omega)^2}} \sim \frac{\bar{g}\sqrt{k_F}}{v_F\sqrt{\gamma}} \int_0^\omega \frac{d\omega_1}{\sqrt{\omega_1}}. \tag{6.41}$$

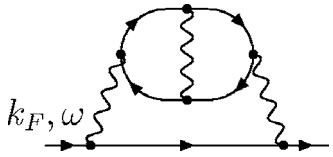

FIG. 7. Three-loop contribution to the fermionic self-energy.

Collecting the prefactors, we find

$$\Sigma_3(\omega) \sim (\bar{g}\omega)^{1/2}. \tag{6.42}$$

We see that the nonanalyticity in the static spin susceptibility feeds back into the fermionic self-energy leading to a contribution from the three loop self-energy whose frequency dependence is more singular than the $\omega^{2/3}$ dependence that we obtained assuming that the static susceptibility is regular. Comparing these two contributions, we see that they become comparable at a frequency

$$\omega_0^{1/3}\omega_{\min}^{2/3} \sim \sqrt{\bar{g}\omega_{\min}} \Rightarrow \omega_{\min} \sim \frac{q_{\min}^3}{\gamma} \sim \frac{E_F^2}{\bar{g}}, \tag{6.43}$$

where $q_{\min}$ is given by Eq. (6.29). Parametrically, $q_{\min}$ is not small since $q_{\min} \sim k_F$, and $\omega_{\min} \sim E_F/\alpha$ is larger than E_F. However, $q_{\min} \sim 0.06k_F$ is small numerically so that $\omega_{\min}$ is four orders of magnitude smaller than E_F/α.

E. Summary

To summarize, we found that the Eliashberg theory for an SU(2) symmetric ferromagnetic QCP has to be extended to include extra singular terms into both the spin susceptibility and the fermionic self-energy. These terms originate from the "anti-Migdal" processes in which slow bosons are vibrating near the fermionic mass shell. Physically, these extra processes originate from the dynamic long-range interaction between fermions, which is still present at the QCP despite the fact that fermions are no longer good quasiparticles.

We demonstrated that these extra nonanalytic terms can be understood in the framework of HMM ϕ^4 theory of quantum criticality. We showed that the prefactor for the ϕ^4 term is nonanalytic and depends on the interplay between momentum and frequency. The nonanalytic bosonic self-energy is the feedback from the nonanalytic ϕ^4 term to the quadratic ϕ^2 term.

We found that these extra terms in the Eliashberg theory make a ferromagnetic QCP unstable below a certain momentum and energy scale. We detected the instability by analyzing the momentum and temperature dependence of the spin susceptibility, and also the fermionic self-energy at three-loop order.

VII. STATIC SUSCEPTIBILITY IN THE NON-SU(2) SYMMETRIC CASE

The problem of fermions interacting with bosonic collective modes with a propagator similar to the one we considered is quite general, and one can wonder to what extent our

analysis for a ferromagnetic case can be extended to the case of an interaction with charge fluctuations, a nematic QCP, or a ferromagnetic instability with Ising symmetry.

The essential difference between these cases and the ferromagnetic one lies in the symmetry of the order parameter. In an SU(2) spin-symmetric ferromagnetic case, the order parameter (magnetization) is a three-dimensional vector, while in the other cases, it is a scalar.

As we already discussed, the Eliashberg theory and the analysis of its validity at the two-loop level can be carried out equally for systems with vector and with scalar order parameter: the only unessential difference is in the numerical prefactors. On the other hand, the evaluation of the corrections to the static susceptibility leads to different results for scalar and vector order parameters, as we now demonstrate.

A. Ising ferromagnet

Consider first the situation of a magnetically mediated interaction, where we change the spin symmetry of the bosons from SU(2) to Ising. The Ising case was argued to be relevant for metamagnetic quantum critical points.[40]

The use of Ising spins does not change the expression for the Green's functions but replaces the Pauli matrix $\boldsymbol{\sigma}$ at the fermion-boson vertex by σ^z. As a consequence, the computations performed for the SU(2) case still hold, but the interplay between different diagrams changes because of a change in the numerical prefactors. In particular, instead of Eq. (6.12) we now have

$$\Gamma_1^{\text{Ising}} = \Gamma_2^{\text{Ising}} = 2,$$

$$\Gamma_3^{\text{Ising}} = \Gamma_4^{\text{Ising}} = 0. \tag{7.1}$$

Under these circumstances, the nonanalytic contributions from the diagrams in Fig. 5 cancel each other out. As a result, the static spin susceptibility remains analytic and scales as $\chi^{-1}(q) \propto q^2$ with a positive prefactor at the QCP.

This result can be extended to the case of a nematic instability, following the same arguments.

B. Charge channel

For a charge vertex, one has to replace the Pauli matrices present at the vertex by Kronecker symbols $\delta_{\alpha\beta}$. We then have

$$\Gamma_1^{\text{Charge}} = \Gamma_2^{\text{Charge}} = \sum_{\alpha,\beta,\gamma,\delta} \delta_{\alpha\beta}\delta_{\beta\gamma}\delta_{\gamma\delta}\delta_{\delta\alpha} = 2,$$

$$\Gamma_3^{\text{Charge}} = \Gamma_4^{\text{Charge}} = \sum_{\alpha,\beta,\gamma,\delta,\epsilon,\zeta} \delta_{\alpha\beta}\delta_{\beta\gamma}\delta_{\delta\epsilon}\delta_{\gamma\alpha}\delta_{\zeta\delta}\delta_{\epsilon\zeta} = 4.$$

Substituting these Γ^{Charge} into the expressions for Π, we find that the diagrams Π_1 and Π_2 as well as Π_3 and Π_4 cancel each other out. This leaves only regular q^2 term in the static charge susceptibility.

C. Physical arguments

The cancellation of the nonanalytic terms in the charge susceptibility is not a direct consequence of the conservation laws. These laws impose constraints (Ward identities) on the behavior of the susceptibilities in the opposite limit $q=0$, $\omega \neq 0$ [$\chi_c(q=0,\omega)$ vanishes as a uniform perturbation cannot affect a time independent, conserved quantity].

Instead, the absence of the nonanalytic terms in the charge channel is related to the fact that this susceptibility measures the response of the system to a change in the chemical potential. We showed that the origin of the singular behavior of the static spin susceptibility lies in the Landau damping term in the bosonic propagator [see Eqs. (6.24) and (6.28)]. The Landau damping does not depend in a singular way on k_F (i.e., on the density of electrons), and therefore there is no singular response of the system to a change in the chemical potential.

Conversely, the effect of a magnetic field on the Landau damping is singular: for a fermionic bubble with opposite spin projections of the two fermions, $\Pi_{\pm} \sim |\Omega| / \sqrt{\Omega^2 + (v_F l)^2}$ is replaced by $|\Omega| / \sqrt{(\Omega + 2i\mu_B H)^2 + (v_F l)^2}$ in the presence of a small magnetic field H. As a consequence, taking the second derivative of $\Pi_{\pm}$ with respect to H, and setting then $H=0$, one obtains, for $v_F l \gg \Omega$, a nonanalytic $d^2\Pi_{\pm}/dH^2 \sim \Omega/l^3$. This nonanalyticity gives rise to a $q^{3/2}$ term in the static spin susceptibility.[38,39] For an Ising ferromagnet, this effect does not exist as there are no bubbles with opposite spin projections in the theory.

The above reasoning shows that the nonanalyticity appears in the spin response but not in the charge one. To further verify this argument, we computed the subleading, three-loop diagrams for the charge susceptibility and found that the nonanalytic contributions from individual diagrams all cancel out. We present the calculations in Appendix E.

The same argument holds for the self-energy at the three-loop and higher orders. The singular $\omega^{1/2}$ term obtained in Eq. (6.42) appears in individual diagrams, but in the case of a QCP in the charge channel (or an Ising QCP in the spin channel) the total singular contribution cancel out.

D. Summary

To summarize, the extra singular additions to the Eliashberg theory are specific to the SU(2) spin case and all cancel out for the charge QCP, the gauge-field problem, the nematic QCP, and the spin QCP for a scalar (Ising) order parameter.

VIII. CONCLUSIONS

We have constructed a fully controllable large-N quantum critical theory describing the interaction of fermions with gapless long-wavelength collective bosonic modes. Our approach, similar but not identical to the Eliashberg theory for the electron-phonon interaction, allows us to perform detailed calculations of the fermionic self-energy and the vertex corrections at the QCP.

We constructed a controllable expansion at the QCP as follows: we first created a non-Fermi-liquid "zero-order" theory by solving a set of coupled equations for the fermi-

onic and the bosonic propagators, neglecting the vertex corrections as well as the momentum dependence of the fermionic self-energy, and then analyzed the residual interaction effects in a perturbative expansion around our zero-order theory.

We have proved that this approach is justified under two conditions: (i) the interaction $\bar{g}$ should be smaller than the fermionic bandwidth (which we assumed for simplicity to be of the same order as E_F), and (ii) either the band mass m_B should be smaller than $m=k_F/v_F$, or the number of fermionic flavors N should be large. When $N=O(1)$ and $m_B \sim m$, the corrections are of order $O(1)$. We found that the corrections that are small in $\bar{g}/E_F$ come from bosons near their resonance, as in the Eliashberg theory for the electron-phonon interaction. The corrections small in $m_B/(Nm)$ come from bosons for which one of the momentum component (the larger one) is near the bosonic resonance, while the other component is close to the fermionic mass shell.

For an SU(2)-symmetric quantum critical point towards ferromagnetic ordering, we found that there exists an extra set of singular renormalizations which come from bosons with both momentum components vibrating near the fermionic mass shell. These processes can be understood as a consequence of an effective long-range dynamic interaction between quasiparticles, generated by the Landau damping term. These singular renormalizations are not small and have to be included into the Eliashberg theory. They give rise to a negative nonanalytic $q^{3/2}$ correction to the static spin susceptibility, signaling that the ferromagnetic QCP is unstable.

We also demonstrated that the nonanalytic $q^{3/2}$ term can be understood in the framework of the ϕ^4 theory of quantum criticality. We showed how the effective long-range dynamic interaction between fermions affects the structure of the ϕ^4 theory, once fermions are integrated out: we found that the prefactors of the ϕ^3 and ϕ^4 terms appearing in the effective action are nonanalytic and depend on the interplay between the typical external momentum and frequency.

We showed that the nonanalytic corrections to the bosonic propagator are specific to the SU(2)-symmetric case when the order parameter is a vector. For systems with a scalar order parameter, like a QCP in the charge channel, a nematic QCP, or a ferromagnetic QCP with Ising symmetry, the $q^{3/2}$ contributions from individual diagrams cancel out in the full expression of the susceptibility.

The consequences of the instability of the ferromagnetic QCP still needs to be fully understood. We only considered the behavior of the spin susceptibility at a finite q, and found that the system is unstable towards an incommensurate state (a similar state has recently been analyzed in detail in Ref. 42). Belitz, Kirkpatrick, and others[28,39,41,43] considered in detail the behavior of the thermodynamic potential as a function of the magnetization, and found a negative, nonanalytic term which favors a first-order transition to ferromagnetism. Our results are not in conflict with these works, but rather point on a different, competing instability near a ferromagnetic QCP. The full analysis of what actually substitutes a continuous second-order transition in itinerant ferromagnets is clearly called on.

ACKNOWLEDGMENTS

This work was supported by NSF-DMR 0240238 (A.V.Ch.). J.R. and C.P. were supported by an ACI grant of the French Ministry of Research. We acknowledge useful discussions with Ar. Abanov, D. Belitz, C. Castellani, A. Castro-Neto, C. DiCastro, E. Fradkin, M. Grilli, D. Khveshchenko, T. Kirkpatrick, S. Kivelson, M. Lawler, D. Maslov, W. Metzner, A. Millis, R. Ramazashvili, J. Schmalian, O. Starykh, and T. Vojta.

APPENDIX A: BOSONIC SELF-ENERGY

In this section, we compute the bosonic self-energy at the one-loop level, in the case of both free and fully renormalized fermions. We prove that for an external bosonic momentum on the bosonic mass shell, this self-energy becomes independent on the actual form of the fermionic self-energy, and reduces to the usual Landau damping term, whereas an extra term has to be included if this same external momentum is on the fermionic mass shell.

After performing the sum over spin matrices, we are left with the following expression:

$$\Pi(\mathbf{q},\Omega) = 2N\bar{g}\int \frac{d^2k d\omega}{(2\pi)^3} G(\mathbf{k},\omega)G(\mathbf{k}+\mathbf{q},\omega+\Omega). \tag{A1}$$

Introducing the angle θ defined by $\epsilon_{k+q}=\epsilon_k+v_F q\cos\theta$, this writes

$$\Pi(\mathbf{q},\Omega) = N\frac{\bar{g}m}{4\pi^3}\int d\omega d\epsilon_k d\theta \frac{1}{i[\omega+\Sigma(\omega)]-\epsilon_k} \times \frac{1}{i[\omega+\Omega+\Sigma(\omega+\Omega)]-\epsilon_k-v_F q\cos\theta}. \tag{A2}$$

Proceeding with a contour integration over ϵ_k, and noticing that ω and $\Sigma(\omega)$ have the same sign, we get

$$\Pi(\mathbf{q},\Omega) = iN\frac{\bar{g}m}{2\pi^2}\int_{-\infty}^{+\infty} d\omega \int_0^{2\pi} d\theta [\theta(\omega+\Omega)-\theta(\omega)] \times \frac{1}{i[\Omega+\Sigma(\Omega+\omega)-\Sigma(\omega)]-v_F q\cos\theta}. \tag{A3}$$

Performing the integration over θ, and rearranging a little bit the integration over Ω, we are left with

$$\Pi(\mathbf{q},\Omega) = N\frac{m\bar{g}}{\pi v_F}\int_0^{\Omega} d\omega\,\mathrm{sgn}(\Omega) \times \frac{1}{\sqrt{(v_F q)^2+[\Omega+\Sigma(\Omega-\omega)+\Sigma(\omega)]^2}}. \tag{A4}$$

We know from direct perturbative calculation that the fermionic self-energy goes like $\Sigma(\omega)=\omega_0^{1/3}\omega^{2/3}$, where ω_0

$\sim \alpha\bar{g}$. It follows that if the external bosonic momentum is on the bosonic mass shell, i.e., if $q \sim \Omega^{1/3}$, it dominates over the frequency-dependent term in the integral, so that

$$\Pi(\mathbf{q},\Omega) = N\frac{m\bar{g}}{\pi}\int_0^{\Omega} d\omega\, \frac{\mathrm{sgn}(\Omega)}{v_F q} = N\frac{m\bar{g}}{\pi v_F}\frac{|\Omega|}{q}. \quad \text{(A5)}$$

We recover here the expression of the Landau damping term with a prefactor depending on the details of the interaction considered in our model. This result is independent on the fermionic self-energy provided that $v_F q \gg [\Omega + \Sigma(\Omega)]$.

However, if the external bosonic momentum is on the fermionic mass shell, i.e., if $v_F q \sim \Sigma(\Omega)$, the frequency-dependent term can no longer be neglected. Defining $z = \frac{\omega}{\Omega}$, one then has

$$\Pi(\mathbf{q},\Omega) = N\frac{m\bar{g}}{\pi}\left|\frac{\Omega}{\Sigma(\Omega)}\right| \times \int_0^1 dz \frac{1}{\sqrt{(v_F q/\Sigma(\Omega))^2 + [z^{2/3} + (1-z)^{2/3}]^2}}. \quad \text{(A6)}$$

This formula is of limited use as it is modified by vertex corrections. For the calculations of the static spin susceptibility, we actually only need the leading $O(1/q)$ and the subleading, $O(1/q^3)$ terms in $\Pi(q,\Omega)$. We show in Appendix C that these two terms still can be evaluated without taking into account the vertex corrections [see Eq. (C20) below]. Expanding Eq. (A6) in $1/q$ up to the third order, we find, at $\Omega < \omega_0$,

$$\Pi(\mathbf{q},\Omega) = \gamma\frac{|\Omega|}{q}\left(1 - \frac{c^2\Sigma^2(\Omega)}{2v_F^2 q^2}\right), \quad \text{(A7)}$$

where $c \sim 1.198\,78$. It is convenient to rewrite this expression in a condensed form, by plugging back the $\Sigma(\Omega)^2$ term into the denominator, leaving only the $|\Omega|$ dependence in the numerator, i.e.,

$$\Pi(\mathbf{q},\Omega) = N\frac{m\bar{g}}{\pi}\frac{|\Omega|}{\sqrt{(v_F q)^2 + c^2\Sigma(\Omega)^2}}. \quad \text{(A8)}$$

Finally, one should keep in mind that we actually only need in our further calculations the $1/q$ and $1/q^3$ terms from the small-q expansion of this last expression.

APPENDIX B: FERMIONIC SELF-ENERGY

In this section, we compute the fermionic self-energy at the one-, two-, and three-loop levels, for an external momentum taken to be on the Fermi surface. We also analyze the momentum dependence of the one-loop fermionic self-energy.

1. One loop

a. At the Fermi level

After summing over the spin matrices, the fermionic self-energy at the one-loop level is given by

$$\Sigma(\omega) = 3ig^2\int \frac{d^2q d\Omega}{(2\pi)^3} G(\mathbf{k_F}+\mathbf{q},\omega+\Omega)\chi(\mathbf{q},\Omega) = \frac{3ig^2}{(2\pi)^3}\int d\Omega dq d\theta \frac{\chi_0}{\xi^{-2} + q^2 + \gamma(|\Omega|/q)} \times \frac{q}{i[\omega + \Omega + \Sigma(\omega+\Omega)] - v_F q\cos\theta}, \quad \text{(B1)}$$

where we defined θ as the angle between $\mathbf{k}$ and $\mathbf{q}$, and considered an external fermionic momentum $k \simeq k_F$. The i prefactor comes from the convention $G^{-1} = G_0^{-1} + i\Sigma$.

Since the pole in q from the fermionic propagator is in a definite half plane, the integral in q is dominated by poles coming from the bosonic Green's function, so that one can perform the integral over the angular variable and simplify the result as follows:

$$\Sigma(\omega) = -\frac{3g^2}{(2\pi)^2}\int d\Omega dq \frac{\chi_0}{q^3 + \gamma|\Omega| + q\xi^{-2}} \times \frac{q^2\mathrm{sgn}(\omega+\Omega)}{\sqrt{(v_F q)^2 + [\omega + \Omega + \Sigma(\omega+\Omega)]^2}} = -\frac{3\bar{g}}{(2\pi)^2}\int_{-\infty}^{+\infty} d\Omega \int_0^{+\infty} dq \frac{q^2\mathrm{sgn}(\omega+\Omega)}{v_F q} \times \frac{1}{q^3 + \gamma|\Omega| + q\xi^{-2}}. \quad \text{(B2)}$$

Defining the new variables $z = \frac{\Omega}{\omega}$ and $u = \frac{v_F q}{\omega}$, this leads to

$$\Sigma(\omega) = \frac{3\bar{g}}{2\pi^2}\frac{\omega^2}{\gamma v_F^3}\int_0^1 dz \int_0^{+\infty} du \frac{u}{z + au + bu^3}, \quad \text{(B3)}$$

where we have used $a = \frac{1}{\gamma v_F \xi^2}$ and $b = \frac{\omega^2}{\gamma v_F^3}$.

Let us denote by $\mathcal{I}$ the last double integral, and define the new variables $y = \sqrt{\frac{b}{a^3}}z = (\omega\gamma\xi^3)z$ and $t = \sqrt{\frac{b}{a}}u = \frac{\xi\omega}{v_F}u$. Now $\mathcal{I}$ reduces to

$$\mathcal{I} = \left(\frac{v_F}{\xi\omega}\right)^2 \int_0^{\gamma\omega\xi^3} dy \int_0^{+\infty} dt \frac{t}{t^3 + t + y} = \left(\frac{v_F}{\xi\omega}\right)^2 h(\gamma\omega\xi^3). \quad \text{(B4)}$$

Substituting this back into our expression for the self-energy:

$$\Sigma(\omega) = \frac{3}{2\pi m\xi^2} h(\gamma\omega\xi^3), \quad \text{(B5)}$$

with the following asymptotic behavior: $h(x \to 0) = \frac{\pi x}{2}$ and $h(x \to \infty) = \frac{\pi x^{2/3}}{\sqrt{3}}$.

In the two regimes we are interested in, this last result can be rewritten as

$$\Sigma(\omega) = \begin{cases} \lambda\omega & \text{for } \xi^{-1} \gg 1, \\ \omega_0^{1/3}\omega^{2/3} & \text{for } \xi^{-1} \to 0, \end{cases} \quad \text{(B6)}$$

where the constant prefactors are defined as

$$\begin{cases} \lambda &= \dfrac{3}{4\pi}\dfrac{\bar{g}\xi}{v_F}, \\ \omega_0 &= \dfrac{3\sqrt{3}}{8\pi^3}\dfrac{\bar{g}^3}{\gamma v_F^3}. \end{cases} \tag{B7}$$

b. Momentum dependence

For definiteness, we set $\xi^{-1}=0$. We first compute the momentum-dependent part of the one-loop fermionic self-energy at zero external frequency:

$$\Sigma(\mathbf{k},\omega=0) = 3ig^2 \int \frac{d^2q d\Omega}{(2\pi)^3} G(\mathbf{k}+\mathbf{q},\Omega)\chi(\mathbf{q},\Omega)$$
$$= \frac{3i\bar{g}}{(2\pi)^3}\int \frac{d\Omega d^2q}{i\tilde{\Sigma}(\Omega)-\epsilon_{k+q}}\frac{q}{\gamma|\Omega|+q^3}. \tag{B8}$$

Expanding $\epsilon_{k+q}=\epsilon_k+v_Fq\cos\theta$ and integrating over θ, we obtain

$$\Sigma(\mathbf{k},0) = \frac{3\bar{g}}{4\pi^2}\int d\Omega\ \mathrm{sgn}(\Omega)\int \frac{q^2dq}{q^3+\gamma|\Omega|} \times \frac{1}{\{(v_Fq)^2+[\tilde{\Sigma}(\Omega)+i\epsilon_k]^2\}^{1/2}}. \tag{B9}$$

At $\epsilon_k=0$, the integral vanishes by parity. Expanding to linear order in ϵ_k we obtain

$$\Sigma(\mathbf{k},0) = -3i\epsilon_k \times \frac{\bar{g}}{2\pi^2}\int_0^\infty d\Omega\tilde{\Sigma}(\Omega) \times \int \frac{q^2dq}{[q^3+(\gamma|\Omega|)][(v_Fq)^2+\tilde{\Sigma}(\Omega)^2]^{3/2}}. \tag{B10}$$

Simple estimates show that the result depends on the interplay between $(\gamma\Omega)^{1/3}$ and $\tilde{\Sigma}(\Omega)/v_F$. Introducing the scale ω_{Max}, defined as the frequency at which $(\gamma\Omega)^{1/3}=\tilde{\Sigma}(\Omega)/v_F$ [see Eq. (5.3)], and rescaling variables as $q=(\gamma\omega_{\mathrm{Max}})^{1/3}y$, $\Omega=\omega_{\mathrm{Max}}x$, we re-write Eq. (B10) as

$$\Sigma(\mathbf{k},0) = -3i\epsilon_k \times \frac{\bar{g}\omega_{\mathrm{Max}}}{2\pi^2 v_F^3\gamma}I, \tag{B11}$$

where

$$I = \int_0^\infty dx\int_0^\infty dy\frac{xy^2}{(x^2+y^2)^{3/2}(x+y^3)} \simeq 1.3308. \tag{B12}$$

Substituting $\omega_{\mathrm{Max}}=(\gamma v_F^3)^{1/2}$, we obtain Eq. (5.30).

To obtain the frequency dependence of the fermionic density of states at small ω, we have to evaluate the second-order term in ϵ_k at the mass shell, where $\epsilon_k=i\tilde{\Sigma}(\omega)$ and convert the result to real frequencies. Therefore we now keep both ω and ϵ_k finite, and use

$$\Sigma(\mathbf{k},\omega) = \frac{3i\bar{g}}{(2\pi)^3}\int d\Omega d^2q\frac{q}{\gamma|\Omega|+q^3}\frac{1}{i\tilde{\Sigma}(\omega+\Omega)-\epsilon_{k+q}}. \tag{B13}$$

Writing, as before, $\epsilon_{k+q}=\epsilon_k+v_Fq\cos\theta$ and integrating over θ, we obtain

$$\Sigma(\mathbf{k},\omega) = \frac{3\bar{g}}{4\pi^2}\int \frac{d\Omega q^2dq}{\gamma|\Omega|+q^3}\frac{\mathrm{sgn}(\omega+\Omega)}{\sqrt{[\tilde{\Sigma}(\omega+\Omega)+i\epsilon_k]^2+(v_Fq)^2}}. \tag{B14}$$

We assume and then verify that the internal v_Fq are still larger than $\tilde{\Sigma}(\omega+\Omega)$ and ϵ_k, and expand

$$\Sigma(\mathbf{k},\omega) = -\frac{3\bar{g}}{8\pi^2v_F^3}\int d\Omega\ \mathrm{sgn}(\omega+\Omega)\int \frac{dq}{q(\gamma|\Omega|+q^3)} \times(\tilde{\Sigma}(\omega+\Omega)+i\epsilon_k)^2. \tag{B15}$$

The lower limit of the momentum integral is $[\tilde{\Sigma}(\omega+\Omega)+i\epsilon_k]/v_F$. At the mass shell, $i\epsilon_k=\tilde{\Sigma}(\omega)$. Substituting, we find

$$\Sigma(\mathbf{k},\omega) = -\frac{3\bar{g}}{8\pi^2v_F^3}\int d\Omega\ \mathrm{sgn}(\omega+\Omega)\int \frac{dq}{q(\gamma|\Omega|+q^3)} \times[\tilde{\Sigma}(\omega+\Omega)-\tilde{\Sigma}(\omega)]^2. \tag{B16}$$

We only need the contribution which is confined to $\Omega\sim\omega$. The contributions from $|\Omega|\gg|\omega|$ diverge in our expansion procedure, and account for the regular $O(\epsilon_k)$ and $O(\omega)$ terms in the self-energy. The last term is even smaller in α than the regular $O(\epsilon_k)$ term and is totally irrelevant. As $\Omega\sim\omega$ is small, $\tilde{\Sigma}(\Omega)\approx\Sigma(\Omega)=\Omega^{2/3}\omega_0^{1/3}$.

Because of the sgn factor in the numerator of Eq. (B14), there are two distinct contributions from $\Omega\sim\omega$. For both of them, the momentum integral is logarithmic (which justifies the expansion) and yields $(1/3)\ln(\omega_1/\omega)$, where $\omega_1\sim N^2E_F^2/\bar{g}$. The first contribution comes from $|\Omega|\leq|\omega|$ and to logarithmic accuracy is

$$\Sigma(\mathbf{k},\omega)_A = -\frac{\bar{g}}{8\pi^2v_F^3\gamma}\mathrm{sgn}(\omega)\int_{-|\omega|}^{|\omega|}\frac{d\Omega}{|\Omega|} \times[\Sigma(|\omega|+\Omega)-\Sigma(|\omega|)]^2\ln\frac{\omega_1}{|\omega|}. \tag{B17}$$

Rescaling the frequency, we obtain from Eq. (B17)

$$\Sigma(\mathbf{k},\omega)_A = -\frac{\bar{g}I_1}{4\pi^2v_F^3\gamma}\Sigma(\omega)|\Sigma(\omega)|\ln\frac{\omega_1}{\omega}, \tag{B18}$$

where

$$I_1 = \frac{1}{2}\int_{-1}^{1}\frac{dx}{|x|}[(1+x)^{3/2}-1]^2 = 0.254. \tag{B19}$$

Another comes from $|\Omega|>|\omega|$, and is

$$\Sigma(\mathbf{k},\omega)_B = \frac{\bar{g}\Sigma(\omega)}{4\pi^2 v_F^3 \gamma} \ln\frac{\omega_1}{|\omega|}\int_{|\omega|}^{\infty}\frac{d\Omega}{\Omega} \times[\Sigma(|\omega|+\Omega)+\Sigma(\Omega-|\omega|)-2\Sigma(\Omega)]. \tag{B20}$$

Rescaling, we obtain

$$\Sigma(\mathbf{k},\omega)_B = \frac{\bar{g}I_2}{4\pi^2 v_F^3\gamma}\Sigma(\omega)|\Sigma(\omega)|\ln\frac{\omega_1}{|\omega|}, \tag{B21}$$

where

$$I_2 = \int_1^{\infty}\frac{dx}{x}[(1+x)^{2/3}+(x-1)^{2/3}-2x^{2/3}] = -0.195. \tag{B22}$$

Combining $\Sigma(\mathbf{k},\omega)_A$ and $\Sigma(\mathbf{k},\omega)_B$, we obtain

$$\Sigma(\mathbf{k},\omega)_{=} -\frac{0.45\bar{g}}{4\pi^2 v_F^3\gamma}\Sigma(\omega)|\Sigma(\omega)|\ln\frac{\omega_1}{|\omega|}. \tag{B23}$$

Substituting the expression for γ in this last expression, we obtain Eq. (5.34).

2. Two loop

We compute here one of the contributions to the two-loop self-energy, given by Fig. 1. This contribution originates from the insertion of the vertex correction into the Eliashberg self-energy.

We have

$$\Sigma_2(\omega) \sim g^4\int d\omega_1 d^2q_1\int d\omega_2 d^2q_2\chi(\mathbf{q_1},\omega_1)\chi(\mathbf{q_2},\omega_2) \times G(\mathbf{k_F}+\mathbf{q_1},\omega+\omega_1)G(\mathbf{k_F}+\mathbf{q_2},\omega+\omega_2) \times G(\mathbf{k_F}+\mathbf{q_1}+\mathbf{q_2},\omega+\omega_1+\omega_2), \tag{B24}$$

which gives, once we replace each propagator by its full expression,

$$\Sigma_2(\omega) \sim \bar{g}^2\int d\omega_1 d^2q_1\int d\omega_2 d^2q_2\frac{q_1}{\gamma|\omega_1|+q_1^3}\frac{q_2}{\gamma|\omega_2|+q_2^3}\frac{1}{i\tilde{\Sigma}(\omega+\omega_1)-v_F q_{1x}-N(q_{1y}^2/2m_B)}\frac{1}{i\tilde{\Sigma}(\omega+\omega_2)-v_F q_{2x}-N(q_{2y}^2/2m_B)} \times\frac{1}{i\tilde{\Sigma}(\omega+\omega_1+\omega_2)-v_F(q_{1x}+q_{2x})-N[(q_{1y}+q_{2y})^2/2m_B]}, \tag{B25}$$

where we use the shorter notation $\tilde{\Sigma}(\omega)=\omega+\Sigma(\omega)$.

Integrating successively over q_{1x} and q_{2x}, closing each contour on the upper half plane, one has

$$\Sigma_2(\omega) \sim \frac{m_B\bar{g}^2}{Nv_F^2}\int d\omega_1\int d\omega_2\Theta(\omega,\omega_1,\omega_2)\int dq_{1y}\int dq_{2y} \times\frac{|q_{1y}|}{|q_{1y}|^3+\gamma|\omega_1|}\frac{|q_{2y}|}{|q_{2y}|^3+\gamma|\omega_2|} \times\frac{1}{(\gamma^2\omega_1\omega_2)^{1/3}}\frac{1}{[q_{1y}q_{2y}/(\gamma^2\omega_1\omega_2)^{1/3}]+i\zeta}, \tag{B26}$$

where $\zeta = m_B\frac{\tilde{\Sigma}(\omega+\omega_1)+\tilde{\Sigma}(\omega+\omega_2)-\tilde{\Sigma}(\omega+\omega_1+\omega_2)}{N(\gamma^2\omega_1\omega_2)^{1/3}}$ and $\Theta(\omega,\omega_1,\omega_2)$ comes from the choice of a contour for the integration and is given in our case by

$$\Theta(\omega,\omega_1,\omega_2) = [\theta(\omega+\omega_1)-\theta(\omega+\omega_1+\omega_2)] \times\{\theta(\omega+\omega_2)-\theta[\tilde{\Sigma}(\omega+\omega_1+\omega_2) -\tilde{\Sigma}(\omega+\omega_1)]\}. \tag{B27}$$

It is convenient at this stage to rescale the perpendicular components of the bosonic momenta. Introducing $x=q_{1y}/(\gamma|\omega_1|)^{1/3}$ and $y=q_{2y}/(\gamma|\omega_2|)^{1/3}$, we obtain

$$\Sigma_2(\omega) \sim \frac{m_B\bar{g}^2}{Nv_F^2}\int d\omega_2\int d\omega_1\int_0^{\infty}dxdy\frac{\Theta(\omega,\omega_1,\omega_2)}{(\gamma^2\omega_1\omega_2)^{2/3}} \times\frac{i\zeta}{x^2y^2+\zeta^2}\frac{xy}{(1+x^3)(1+y^3)}, \tag{B28}$$

where we rearranged the double integral over x and y to make it real.

Since all internal frequencies typically go like ω, the typical value of ζ is given by the small parameter β given in Eq. (5.13). Expanding the double integral for small values of ζ, the leading contribution from the integral over x and y reads

$$\int_0^{\infty}dxdy\frac{1}{x^2y^2+\zeta^2}\frac{xy}{(1+x^3)(1+y^3)} \sim \ln^2\zeta. \tag{B29}$$

If one considers now free fermions, it becomes possible to reduce the expression of the two-loop self-energy to

$$\Sigma_2^{\text{free}}(\omega) \sim \frac{m_B^2\bar{g}^2}{N^2v_F^2}\int_0^{\omega}d\omega_2\int_{\omega-\omega_2}^{\omega}d\omega_1\frac{\ln^2[m_B\omega/N(\gamma^2\omega_1\omega_2)^{2/3}]}{\gamma^2\omega_1\omega_2} \sim \frac{m_B^2\bar{g}^2}{N^2\gamma v_F^2}\omega\int_0^1 dz_2\int_{1-z_2}^1 dz_1\frac{\ln^2(m_B^3\omega/N^3\gamma z_1z_2)}{z_1z_2} \sim \beta^2\omega\ln^2\omega, \tag{B30}$$

where we only kept the leading contribution in the last expression, and $\beta=m_B/mN$ is one of the small parameters defined in the text.

Now, in the case of dressed fermions, we need to take $\tilde{\Sigma}(\omega)=\omega_0^{1/3}\omega^{2/3}$. The procedure is identical to the free fermion case, but the final expression is a bit more complicated:

$$\Sigma_2^{\text{Dressed}}(\omega) \sim \frac{m_B^2\bar{g}^2}{N^2\gamma^2 v_F^2}\omega_0^{1/3}\omega^{2/3}\int_0^1 dz_2\int_{1-z_2}^1 dz_1\frac{1}{z_1 z_2} \times[(1-z_1)^{2/3}+(1-z_2)^{2/3}+(z_1+z_2-1)^{2/3}] \times \ln^2\left(\frac{(1-z_1)^{2/3}+(1-z_2)^{2/3}+(z_1+z_2-1)^{2/3}}{(N\gamma^{2/3}/m_B\omega_0^{1/3})z_1^{1/3}z_2^{1/3}}\right). \tag{B31}$$

Expanding the $\ln^2$, one is left with a double integral that only contributes as a numerical prefactor, and the dominant term is then given by

$$\Sigma_2(\omega) \sim \Sigma_1(\omega)\beta^2\ln^2\beta, \tag{B32}$$

where $\Sigma_1(\omega)=\omega_0^{1/3}\omega^{2/3}$ is the self-energy in the Eliashberg theory.

3. Three loop

We now turn to the computation of the three-loop self energy. We are only interested here in one diagram, given in Fig. 7, where we try to analyze the feedback of the nonanalytic susceptibility into the higher-order diagrams for the fermionic self-energy. For spin interaction, there is no cancellation between different diagrams for the static susceptibility, which justifies that we restrict ourselves to just one contribution.

The analytic expression for this diagram is

$$\Sigma_3(\omega) \sim \bar{g}\int d\omega_1 d^2q_1 \frac{A(q_1,\omega_1)}{i\Sigma(\omega-\omega_1)-v_F q_{1x}-Nq_{1y}^2/2m_B} \times\left(\frac{1}{q_1^2+\gamma|\omega_1|/q_1}\right)^2, \tag{B33}$$

where $A(q_1,\omega_1)$ is the factor from the fermionic bubble:

$$A(q_1,\omega_1) \sim N\bar{g}^2\int d^2k d\Omega\int d^2q_2 d\omega_2 \frac{1}{q_2^2+\gamma|\omega_2|/q_2} \times\frac{1}{i\Sigma(\Omega)-\epsilon_k}\frac{1}{i\Sigma(\Omega+\omega_1+\omega_2)-\epsilon_{k+q_1+q_2}} \times\frac{1}{i\Sigma(\Omega-\omega_1)-\epsilon_{k+q_1}}\frac{1}{i\Sigma(\Omega+\omega_2)-\epsilon_{k+q_2}}.$$

Approximating $A(q_1,\omega_1)$ by its singular static part $q_1^{3/2}\sqrt{k_F}$ and substituting into the expression of Σ_3 we obtain

$$\Sigma_3(\omega) \sim \bar{g}\sqrt{k_F}\int d\omega_1 d^2q_1\left(\frac{q_1}{q_1^3+\gamma|\omega_1|}\right)^2 \times\frac{q_1^{3/2}}{i\Sigma(\omega-\omega_1)-v_F q_{1x}-N(q_{1y}^2/2m_B)}. \tag{B34}$$

The integral over q_{1x} is determined by the branch-cut in the bosonic propagator and one then expects that this very integral is dominated by $q_{1x}\sim(\gamma\omega_1)^{1/3}$. It follows that the term in q_{1x} dominates inside the fermionic propagator allowing us to neglect the curvature term. Defining the angle θ between $\mathbf{k_F}$ and $\mathbf{q_1}$, and integrating over it, this leads to

$$\Sigma_3(\omega) \sim \frac{\bar{g}\sqrt{k_F}}{v_F}\int\frac{d\omega_1 dq_1 \text{sgn}(\omega-\omega_1)}{\sqrt{q_1^2+\Sigma(\omega-\omega_1)^2/v_F^2}}\frac{q_1^{9/2}}{(q_1^3+\gamma|\omega_1|)^2}. \tag{B35}$$

Since the dominant contribution comes from $q_1\sim(\gamma\omega_1)^{1/3}$, one can neglect the fermionic self-energy in the denominator. This in turn allows us to simplify the frequency integral, which then writes

$$\Sigma_3(\omega) \sim \frac{\bar{g}\sqrt{k_F}}{v_F}\int_0^\omega d\omega_1\int dq_1\frac{q_1^{7/2}}{(q_1^3+\gamma\omega_1)^2} \sim \frac{\bar{g}\sqrt{k_F}}{\sqrt{\gamma}v_F}\int_0^\omega\frac{d\omega_1}{\sqrt{\omega_1}}, \tag{B36}$$

where we introduced $z=q_1/(\gamma\omega_1)^{1/3}$, so that the integral over z just contributes to the numerical prefactor.

Collecting prefactors, one finally has

$$\Sigma_3(\omega) \sim \sqrt{\bar{g}\omega}. \tag{B37}$$

APPENDIX C: VERTEX CORRECTIONS

In this section, we compute the various vertex corrections analyzed in the text.

1. $q=\Omega=0$

Consider first the simplest three-leg vertex, with strictly zero incoming frequency Ω and momenta q, as presented in Fig. 2(a). Its analytic expression writes

$$\left.\frac{\Delta g}{g}\right|_{q=\Omega=0} \sim g^2\int d\omega d^2p G(\mathbf{k_F},\omega)^2\chi(\mathbf{p},\omega) \sim\bar{g}\int\frac{d\omega d^2p}{\gamma|\omega|/p+p^2}\frac{1}{[i\tilde{\Sigma}(\omega)-v_F p_x-N(p_y^2/2m_B)]^2},$$

where we defined $\tilde{\Sigma}(\omega)=\omega+\Sigma(\omega)$ and we have chosen $\mathbf{k}_F$ along the x axis.

Since both poles coming from the fermionic Green's functions are in the same half plane, the integral over q_x is finite only because of the branch cut in the bosonic propagator. Since at the branch cut p_x and p_y are of the same order, we can drop the curvature term in the fermionic propagators and introduce polar coordinates for the internal bosonic momen-

tum. Defining θ as the angle between $\mathbf{k_F}$ and $\mathbf{p}$, and integrating over it, one has

$$\left.\frac{\Delta g}{g}\right|_{q=\Omega=0} \sim \bar{g}\int \frac{d\omega dp}{p^3+\gamma|\omega|}\frac{p^2|\tilde{\Sigma}(\omega)|}{[(v_F p)^2+\tilde{\Sigma}(\omega)^2]^{3/2}}. \quad \text{(C1)}$$

Introducing the frequency ω_{Max} up to which bosons are slow modes compared to fermions, i.e., up to which $(\gamma\omega)^{1/3} > \tilde{\Sigma}(\omega)/v_F$, one can split the frequency integral into two parts, and define in each of them the reduced momentum $z=p/\mathrm{Min}((\gamma\omega)^{1/3}, \tilde{\Sigma}(\omega)/v_F)$ so that the integral over z only contributes to the numerical prefactor, leading to

$$\left.\frac{\Delta g}{g}\right|_{q=\Omega=0} \sim \bar{g}\int_0^{\omega_{\mathrm{Max}}} d\omega \frac{\tilde{\Sigma}(\omega)}{\gamma v_F^3 \omega} \sim \frac{\bar{g}}{\gamma v_F^3}\tilde{\Sigma}(\omega_{\mathrm{Max}}). \quad \text{(C2)}$$

One can easily make sure that the frequency ω_{Max} at which $(\gamma\omega)^{1/3}=\tilde{\Sigma}(\omega)/v_F$ exceeds ω_0, such that one should use $\tilde{\Sigma}(\omega)=\omega$ to find ω_{Max}. Substituting, we obtain $\omega_{\mathrm{Max}} \sim (N\bar{g}E_F)^{1/2}$, and

$$\left.\frac{\Delta g}{g}\right|_{q=\Omega=0} \sim \sqrt{\alpha}. \quad \text{(C3)}$$

2. $q=0$, Ω finite

Considering the same vertex, now with a finite external frequency, one has

$$\begin{aligned}\left.\frac{\Delta g}{g}\right|_{q=0,\Omega} &\sim g^2\int d\omega d^2p G(\mathbf{k_F}+p,\omega+\Omega) \\ &\times G(\mathbf{k_F}+p,\omega)\chi(\mathbf{p},\omega) \sim \bar{g}\int \frac{d\omega d^2p}{\gamma|\omega|/p+p^2} \\ &\times \frac{1}{i\tilde{\Sigma}(\omega)-v_F p_x - N(p_y^2/2m_B)} \\ &\times \frac{1}{i\tilde{\Sigma}(\omega+\Omega)-v_F p_x - N(p_y^2/2m_B)}, \end{aligned} \quad \text{(C4)}$$

where we chose the x axis along $\mathbf{k_F}$.

From the pole structure in p_x of this expression, one expects two contributions to this integral. A first term comes from the branch cut in the bosonic propagator, however, this contribution ultimately leads to the same result as the $q=\Omega=0$ vertex, up to small corrections from the finiteness of Ω. The second contribution arises from taking the poles in the fermionic propagators. At zero external frequency, these two poles were in the same half plane of p_x, so we could close the integration contour over a different half plane and only consider the contribution from the branch cut in the bosonic propagator. At a finite Ω, there is a range where ω and $\omega+\Omega$ have different signs, and the two poles are in different half planes of p_x. The result after integration reads

$$\begin{aligned}\left.\frac{\Delta g}{g}\right|_{q=0,\Omega} &\sim \frac{\bar{g}}{v_F}\int_0^{\Omega} d\omega \int dp_y \frac{|p_y|}{\gamma|\omega|+|p_y|^3} \\ &\times \frac{1}{\tilde{\Sigma}(\Omega-\omega)+\tilde{\Sigma}(\omega)}, \end{aligned} \quad \text{(C5)}$$

where we slightly rearranged the frequency integral.

Performing the integration over p_y, we are left with

$$\begin{aligned}\left.\frac{\Delta g}{g}\right|_{q=0,\Omega} &\sim \frac{\bar{g}}{\gamma^{1/3}v_F}\int_0^{\Omega} d\omega \frac{\omega^{-1/3}}{\tilde{\Sigma}(\Omega-\omega)+\tilde{\Sigma}(\omega)} \sim \frac{\bar{g}}{(\omega_0\gamma v_F^3)^{1/3}} \\ &\sim \mathrm{const}, \end{aligned} \quad \text{(C6)}$$

where we assumed that Ω is small, i.e., $\tilde{\Sigma}(\Omega)=\omega_0^{1/3}\Omega^{2/3}$. This vertex thus reduces to a numerical constant, that does not contain any small parameter.

3. q finite, $\Omega=0$

Conversely, the same vertex taken at finite external momentum q, but zero external frequency writes

$$\begin{aligned}&\left.\frac{\Delta g}{g}\right|_{q,\Omega=0} \\ &\sim g^2\int d\omega d^2p G(\mathbf{k_F}+\mathbf{p}+\mathbf{q},\omega)G(\mathbf{k_F}+\mathbf{p},\omega)\chi(\mathbf{p},\omega) \\ &\sim \bar{g}\int \frac{d\omega d^2p}{\gamma|\omega|/p+p^2}\frac{1}{i\tilde{\Sigma}(\omega)-v_F p_x - N(p_y^2/2m_B)} \\ &\times \frac{1}{i\tilde{\Sigma}(\omega)-v_F q_x - v_F p_x - N(p_y^2/2m_B) - N(q_y p_y/m_B)}, \end{aligned}$$

where p_x is the projection of $\mathbf{p}$ along $\mathbf{k_F}$.

Like its $q=0$ counterpart, this vertex is characterized by poles in p_x from the fermionic propagators lying in the same half plane. The only nonzero contribution then comes from the branch cut in the bosonic propagator. At the branch cut, $p_x \sim p_y$ which allows us to neglect the quadratic curvature terms in the fermionic Green's functions.

This makes possible a direct integration over p_y. This integral can be separated from the rest of the expression, and reads

$$\begin{aligned}\int dp_y \frac{p}{\gamma|\omega|+p^3} &= \frac{1}{|p_x|}\int_{-\infty}^{+\infty} dz \frac{\sqrt{1+z^2}}{(1+z^2)^{3/2}+\gamma(|\omega|/|p_x|^3)} \\ &= \frac{2p_x^2}{\gamma|\omega|}\int_0^{+\pi/2} du \frac{1}{|p_x|^3/\gamma|\omega|+(\cos u)^3}, \end{aligned} \quad \text{(C7)}$$

where we successively defined $z=p_y/|p_x|$ and $z=\tan u$.

This last integral can be approximated by its asymptotic form, namely

$$\int \frac{dp_y p}{\gamma|\omega| + p^3} = \begin{cases} \dfrac{\pi}{|p_x|}, & \text{if } |p_x|^3 \gg \gamma\omega \\ \dfrac{4\pi}{3\sqrt{3}} \dfrac{1}{(\gamma|\omega|)^{1/3}} - \dfrac{1}{2} \dfrac{p_x^2}{\gamma|\omega|} \ln \dfrac{p_x^2}{(\gamma|\omega|)^{2/3}} \\ + \left(\ln 2 - \dfrac{1}{2} \right) \dfrac{p_x^2}{\gamma|\omega|}, & \text{if } |p_x|^3 \ll \gamma\omega. \end{cases} \tag{C8}$$

The only nonvanishing contribution once we take the integral over p_x comes from the ln term. After expanding in q_x, this contribution reads

$$\left.\frac{\Delta g}{g}\right|_{q,\Omega=0} - \left.\frac{\Delta g}{g}\right|_{q=\Omega=0} \sim \frac{\bar{g} v_F}{\gamma} q_x \times \int \frac{d\omega}{|\omega|} \int dp_x \frac{p_x^2 \ln p_x^2}{[i\tilde{\Sigma}(\omega) - v_F p_x]^3}. \tag{C9}$$

Defining the scaled momentum $z = v_F p_x / \tilde{\Sigma}(\omega)$ and performing the integration over z, one obtains two terms, the dominant one being

$$\left.\frac{\Delta g}{g}\right|_{q,\Omega=0} - \left.\frac{\Delta g}{g}\right|_{q=\Omega=0} \sim i \frac{\bar{g}}{\gamma v_F^2} q_x \int_{|v_F q_x|} \frac{d\omega}{\omega} \ln[i\tilde{\Sigma}(\omega)], \tag{C10}$$

where the frequency integral runs over $|\tilde{\Sigma}(\omega)| > |v_F q_x|$ since as we expanded in $v_F q_x$, we assumed that it was smaller than $|\tilde{\Sigma}(\omega)|$.

Performing the remaining integral, one finds

$$\left.\frac{\Delta g}{g}\right|_{q,\Omega=0} - \left.\frac{\Delta g}{g}\right|_{q=\Omega=0} \sim \frac{q_x}{k_F} \ln|q_x|. \tag{C11}$$

4. q, Ω finite

Finally, we consider the general vertex where both external bosonic momentum and frequency are nonzero. In analytic form, this writes

$$\left.\frac{\Delta g}{g}\right|_{q,\Omega} \sim g^2 \int d\omega d^2 p G(\mathbf{k_F} + \mathbf{p} + \mathbf{q}, \omega + \Omega) G(\mathbf{k_F} + \mathbf{p}, \omega) \chi(\mathbf{p}, \omega)$$

$$\sim \bar{g} \int \frac{d\omega d^2 p}{\gamma|\omega|/p + p^2} \frac{1}{i\tilde{\Sigma}(\omega) - v_F p_x - N(p_y^2/2m_B)} \times \frac{1}{i\tilde{\Sigma}(\omega + \Omega) - v_F q_x - v_F p_x - N(p_y^2/2m_B) - N(q_y p_y / m_B)},$$

where p_x is defined as $p_x = \mathbf{p} \cdot \mathbf{k_F}$.

Integrating over p_x first, there are two contributions. One comes from the branch cut in the bosonic propagator, and gives similar results to the ($q=0$, $\Omega=0$) and the (q finite, $\Omega=0$) vertices up to small correction from the finiteness of the external frequency. We neglect it here and focus on the other contribution which comes from the poles in the fermionic propagators:

$$\left.\frac{\Delta g}{g}\right|_{q,\Omega} \sim i \frac{\bar{g}}{v_F} \int_0^\Omega d\omega \int dp_y \frac{|p_y|}{\gamma|\omega| + |p_y|^3} \times \frac{1}{i\tilde{\Sigma}(\Omega - \omega) + i\tilde{\Sigma}(\omega) - v_F q_x - N(q_y p_y / m_B)}, \tag{C12}$$

where the simplification of the frequency integral comes from the poles in p_x.

This vertex correction strongly depends on the interplay between the external q_x, q_y, and Ω, and is in particular quite sensitive to the momentum anisotropy. We now analyze the various possibilities.

For the generic case where $q_x \sim q_y$ (we use the notation q to designate them), one can neglect the quadratic term in the fermionic dispersion, allowing us to perform the integration over p_y, leaving us with

$$\left.\frac{\Delta g}{g}\right|_{q,\Omega} \sim i \frac{\bar{g}}{v_F \gamma^{1/3}} \int_0^\Omega \frac{d\omega \omega^{-1/3}}{i\tilde{\Sigma}(\Omega - \omega) + i\tilde{\Sigma}(\omega) - v_F q_x}. \tag{C13}$$

Restricting ourselves to the quantum critical regime (i.e., $\Omega \leq \omega_0$) for which $\tilde{\Sigma}(\omega) = \omega_0^{1/3} \omega^{2/3}$, one has

$$\left.\frac{\Delta g}{g}\right|_{q,\Omega} = \mathcal{F}\left(\frac{v_F q_x}{\Sigma(\Omega)} \right), \tag{C14}$$

where $\mathcal{F}(x) = \int_0^1 \frac{dz}{z^{1/3}} \frac{1}{(1-z)^{2/3} + z^{2/3} + ix}$, has the following asymptotic behavior:

$$\begin{cases} \mathcal{F}(x \ll 1) = O(1) \\ \mathcal{F}(x \gg 1) = O\left(\dfrac{1}{x} \right). \end{cases} \tag{C15}$$

If the typical q is on the bosonic mass shell, then $q_x \sim q_y \sim (\gamma\Omega)^{1/3}$, and one has

$$\left.\frac{\Delta g}{g}\right|_{q,\Omega} \sim \frac{\Sigma(\Omega)}{v_F q_x} \sim \sqrt{\alpha} \left(\frac{\Omega}{\omega_{\mathrm{Max}}} \right)^{1/3}. \tag{C16}$$

However, we encountered in previous computations (e.g., self-energies) that a strong anisotropy can be observed between the components of the bosonic momentum, with $q_y \gg q_x$. In this case, the full expression of the vertex correction is a bit complicated and we choose to present here the

most relevant case for which the curvature term dominates over $v_F q_x$ in the fermionic propagator. The vertex correction then no longer depends on q_x and writes

$$\left.\frac{\Delta g}{g}\right|_{q,\Omega} \sim \frac{\bar{g}}{v_F}\int_0^{\Omega} d\omega \int_0^{\infty} dp_y \frac{p_y}{\gamma\omega + p_y^3} \times \frac{\tilde{\Sigma}(\Omega-\omega)+\tilde{\Sigma}(\omega)}{\left[\tilde{\Sigma}(\Omega-\omega)+\tilde{\Sigma}(\omega)\right]^2 + [N(q_y p_y/m_B)]^2}. \tag{C17}$$

Defining $u=p_y/(\gamma\omega)^{1/3}$ and $z=\omega/\Omega$, it is possible to rewrite the vertex correction in this regime as

$$\left.\frac{\Delta g}{g}\right|_{q,\Omega} \sim \mathcal{G}\left(\beta\frac{(\gamma\Omega)^{1/3}}{q_y}\right), \tag{C18}$$

where $\beta=\frac{m_B}{Nm}$ and $\mathcal{G}(x)$ is the following double integral:

$$\mathcal{G}(x) = \int_0^{\infty} \frac{duu}{1+u^3}\int_0^1 \frac{dzz^{-1/3}[(1-z)^{2/3}+z^{2/3}]}{[(1-z)^{2/3}+z^{2/3}]^2 + u^2 z^{2/3}/x^2} \sim x^2 \ln^2 x, \quad \text{if } x \ll 1. \tag{C19}$$

Finally, for the computations of the full dynamic polarization bubble we also need the vertex averaged over the directions of q. The generic structure of this vertex, which we define as $\langle \Delta g/g\rangle$ is the same as in Eq. (C14), i.e.,

$$\left\langle\frac{\Delta g}{g}\right\rangle\Big|_{\mathrm{q},\Omega} = \tilde{\mathcal{F}}\left(\frac{v_F q}{\tilde{\Sigma}(\Omega)}\right), \quad \tilde{\mathcal{F}}(0)=O(1),$$

$$\tilde{\mathcal{F}}(x\gg 1) = O\left(\frac{1}{x}\right). \tag{C20}$$

However, it is essential for our further analysis that the expansion of $\tilde{\mathcal{F}}(x)$ at large x holds in odd powers of $1/x$, i.e., $\tilde{\mathcal{F}}(x\gg 1)=a_1/x+a_3/x^3+\cdots$. In particular, there is no term $O(1/x^2)$, which we found in the polarization operator without vertex corrections [see Eq. (A7)].

5. FOUR-LEG VERTEX

In this paragraph, we compute the renormalized four-leg vertex $\Gamma_2(q,\Omega)$ presented in Fig. 3, which reads

$$\Gamma_2(q,\Omega) \sim g^4 \int d\omega \int d^2p \chi\left(\frac{\Omega+\omega}{2},\frac{\mathbf{p}+\mathbf{q}}{2}\right) \times \chi\left(\frac{\Omega-\omega}{2},\frac{\mathbf{q}-\mathbf{p}}{2}\right) G\left(\frac{\Omega+\omega}{2},\mathbf{k_F}+\frac{\mathbf{p}+\mathbf{q}}{2}\right) \times G\left(\frac{\Omega-\omega}{2},\mathbf{k_F}+\frac{\mathbf{q}-\mathbf{p}}{2}\right). \tag{C21}$$

Performing the integration over p_x, projection of $\mathbf{p}$ along $\mathbf{k_F}$, we obtain

$$\Gamma_2(q,\Omega) \sim \frac{\bar{g}^2}{v_F}\int_0^{\Omega} \frac{d\omega dp_y}{\gamma(\Omega-\omega)+(q^2+p_y^2-2q_y p_y)^{3/2} i\tilde{\Sigma}(\Omega+\omega/2)+i\tilde{\Sigma}(\Omega-\omega/2)-v_F q_x - N(q_y^2+p_y^2/4m_B)} \times \frac{\sqrt{(q^2+p_y^2)^2-4q_y^2p_y^2}}{\gamma(\Omega+\omega)+(q^2+p_y^2+2q_y p_y)^{3/2}}. \tag{C22}$$

It is convenient at this stage to define the reduced variables $z=\omega/\Omega$ and $y=p_y/|q_y|$:

$$\Gamma_2(q,\Omega) \sim \bar{g}\frac{(\gamma\Omega)^{1/3}}{|q_y|^3}\int_0^1 \frac{dzdy}{(\gamma\Omega/|q_y|^3)(1-z)+|1-y|^3} \frac{1}{i[(1-z)^{2/3}+(1+z)^{2/3}]-(v_F q_x/\Sigma(\Omega))-(1+y^2/\beta)(|q_y|^3/\gamma\Omega)^{2/3}} \times \frac{|1-y^2|}{(\gamma\Omega/|q_y|^3)(1+z)+|1+y|^3}, \tag{C23}$$

where we assumed that $\Omega\leq\omega_0$, and we used that in all our computations, the perpendicular component of the bosonic momentum is always either dominant or comparable to the parallel one, so that one has $q_y\sim q$.

Comparing this renormalized vertex with the bare one given by $\Gamma_1(q,\Omega)\sim\frac{\bar{g}q_y^{-2}}{1+\gamma|\Omega|/|q_y|^3}$, one has for the ratio of the two:

$$\frac{\Gamma_2}{\Gamma_1} \sim \frac{(\gamma\Omega)^{1/3}}{|q_y|}\int_0^1 \frac{dzdy}{(\gamma\Omega/|q_y|^3)(1-z)+|1-y|^3} \frac{1}{i[(1-z)^{2/3}+(1+z)^{2/3}]-v_F q_x/\Sigma(\Omega)-[(1+y^2)/\beta][|q_y|^2/(\gamma\Omega)^{2/3}]} \times \frac{|1-y^2|}{(\gamma\Omega/|q_y|^3)(1+z)+|1+y|^3}, \tag{C24}$$

which only depends on two parameters: the ratios $\frac{v_F q_x}{\Sigma(\Omega)}$ and $\frac{|q_y|^3}{\gamma\Omega}$.

In the generic case of an external bosonic momentum on the mass shell, i.e., $q_x \sim q_y \sim (\gamma\Omega)^{1/3}$ one has

$$\frac{\Gamma_2}{\Gamma_1} \sim \frac{\Sigma(\Omega)}{v_F q_x} \sim \sqrt{\alpha}\left(\frac{\Omega}{\omega_{\mathrm{Max}}}\right)^{1/3}. \tag{C25}$$

On the contrary, for a typical $q_x \sim \Sigma(\Omega)/v_F$ and $q_y \sim (\gamma\Omega)^{1/3}$:

$$\frac{\Gamma_2}{\Gamma_1} \sim \beta, \tag{C26}$$

up to logarithmic factors.

APPENDIX D: STATIC SPIN SUSCEPTIBILITY

1. Diagrams

In this appendix we present the details of our calculations of the singular terms in the static spin susceptibility. We discuss in great detail the calculation of the first two diagrams in Fig. 5 (vertex and self-energy correction diagrams). These two diagrams can be computed explicitly both away from and at the QCP. We labeled the total contribution from these two diagrams as $\Pi_A(q,0)$. The remaining two diagrams [their total contribution is $\Pi_B(q,0)$] cannot be computed explicitly at the QCP, and we compute them in an approximate scheme.

In explicit form, the first two diagrams in Fig. 5 are given by

$$\Pi_{1a}(q,0) = \Gamma_a \frac{\bar{g}^2}{(2\pi)^6} \int d^2K d\omega d^2l d\Omega G(\omega,k)^2 \times G(\omega+\Omega,k+l) G(\omega,k+q) \chi(l,\Omega), \tag{D1}$$

$$\Pi_{1b}(q,0) = \Gamma_b \frac{\bar{g}^2}{(2\pi)^6} \int d^2K d\omega d^2l d\Omega G(\omega,k) \times G(\omega+\Omega,k+l) G(\omega+\Omega,k+q+l) \times G(\omega,k+q) \chi(l,\Omega), \tag{D2}$$

where $\Gamma_{a,b}$ are numerical prefactors coming from spin summation. For symmetry reasons, one has to count the first diagram twice, so that the total contribution reads

$$\Pi_A(q,0) = 2\Pi_{1a}(q,0) + \Pi_{1b}(q,0). \tag{D3}$$

a. First diagram

To prove our point, we try to expand the products of fermionic Green's functions into a simpler form:

$$G(\omega,k)^2 G(\omega+\Omega,k+l) G(\omega,k+q) = \frac{G(\omega,k)^2 G(\omega,k+q)}{\kappa(l,\omega,\Omega)} - \frac{G(\omega,k) G(\omega,k+q)}{\kappa(l,\omega,\Omega)^2} + \frac{G(\omega+\Omega,k+l) G(\omega,k+q)}{\kappa(l,\omega,\Omega)^2}, \tag{D4}$$

where $\kappa(l,\omega,\Omega) = i[\Sigma(\omega+\Omega) - \Sigma(\omega)] - v_F l_x$.

The interest of such a splitting up is that one can reduce this drastically by performing the integration over k. In fact,

$$\int d\varepsilon_k G^a(\omega,k) G(\omega,k+q) = 0, \tag{D5}$$

for $a = 1,2$ since all the poles in ε_k are in the same half plane.

For this reason, we are left with

$$\Pi_{1a}(q,0) = \Gamma_a \frac{\bar{g}^2}{(2\pi)^6} \int d^2K d\omega d^2l d\Omega \chi(l,\Omega) \times \frac{G(\omega+\Omega,k+l) G(\omega,k+q)}{\kappa(l,\omega,\Omega)^2}. \tag{D6}$$

Let us keep this expression as it is for the moment and move on to the second diagram.

b. Second diagram

Following the same path, we can rewrite the product of fermionic Green's functions as

$$G(\omega,k) G(\omega+\Omega,k+l) G(\omega+\Omega,k+l+q) G(\omega,k+q) = \frac{G(\omega,k) G(\omega,k+q) - G(\omega,k) G(\omega+\Omega,k+l+q)}{\kappa(l,\omega,\Omega)^2} + \frac{G(\omega+\Omega,k+l) G(\omega+\Omega,k+l+q)}{\kappa(l,\omega,\Omega)^2} - \frac{G(\omega+\Omega,k+l) G(\omega,k+q)}{\kappa(l,\omega,\Omega)^2}, \tag{D7}$$

with the expression of κ defined above.

Once again, the integration over ε_k may give zero if the poles are in the same half plane, which reduces our previous expression to

$$\Pi_{1b}(q,0) = -\Gamma_b \frac{\bar{g}^2}{(2\pi)^6} \int d^2K d\omega d^2l d\Omega \chi(l,\Omega) \times \left(\frac{G(\omega+\Omega,k+l) G(\omega,k+q)}{\kappa(l,\omega,\Omega)^2} + \frac{G(\omega,k) G(\omega+\Omega,k+l+q)}{\kappa(l,\omega,\Omega)^2} \right). \tag{D8}$$

Changing k into $k-q$ in the second part of the integral, we have

$$\Pi_{1b}(q,0) = -\Gamma_b \frac{\bar{g}^2}{(2\pi)^6} \int d^2K d\omega d^2l d\Omega \chi(l,\Omega) \times \left(\frac{G(\omega+\Omega,k+l)G(\omega,k+q)}{\kappa(l,\omega,\Omega)^2} + \frac{G(\omega,k-q)G(\omega+\Omega,k+l)}{\kappa(l,\omega,\Omega)^2} \right). \quad \text{(D9)}$$

One can then notice that $\varepsilon_{k-q}=\varepsilon_k - v_F q \cos\theta$ changes to ε_{k+q} if one changes θ into $\theta-\pi$. This finally leads to

$$\Pi_{1b}(q,0) = -2\Gamma_b \frac{\bar{g}^2}{(2\pi)^6} \int d^2K d\omega d^2l d\Omega \chi(l,\Omega) \times \frac{G(\omega+\Omega,k+l)G(\omega,k+q)}{\kappa(l,\omega,\Omega)^2}. \quad \text{(D10)}$$

From what precedes, we have

$$\Pi_A(q,0) = 2\left(1 - \frac{\Gamma_b}{\Gamma_a}\right)\Pi_{1a}(q,0). \quad \text{(D11)}$$

Spin summation prefactors can be easily computed, and are given by

$$\begin{cases} \Gamma_a = \sum_{\alpha,\beta,\gamma,\delta} \sigma^Z_{\alpha\beta}\boldsymbol{\sigma}_{\beta\gamma}\cdot\boldsymbol{\sigma}_{\gamma\delta}\sigma^Z_{\delta\alpha} = 6 \\ \Gamma_b = \sum_{\alpha,\beta,\gamma,\delta} \sigma^Z_{\alpha\beta}\boldsymbol{\sigma}_{\beta\gamma}\sigma^Z_{\gamma\delta}\boldsymbol{\sigma}_{\delta\alpha} = -2. \end{cases}$$

This finally leads to

$$\Pi_A(q,0) = \frac{8}{3}\Pi_{1a}(q,0). \quad \text{(D12)}$$

2. Away from the QCP

In the Fermi-liquid regime we have

$$\Pi_A(q,0) = \frac{16N\bar{g}^2}{(2\pi)^6} \int d^2K d\omega d^2l d\Omega \frac{1}{[i(1+\lambda)\omega - \epsilon_k]^2} \times \frac{1}{i(1+\lambda)(\omega+\Omega)-\epsilon_{k+l}} \frac{1}{i(1+\lambda)\omega - \epsilon_{k+q}} \times \frac{1}{\xi^{-2}+l^2+\gamma(|\Omega|/l)}. \quad \text{(D13)}$$

where we used for the fermionic self-energy $\Sigma(\omega)=\lambda\omega$, since we are deep in the Fermi-liquid phase in this case.

Defining $\cos\theta = \frac{\mathbf{k}\cdot\mathbf{l}}{|\mathbf{k}||\mathbf{l}|}$ and $\cos\theta' = \frac{\mathbf{k}\cdot\mathbf{q}}{|\mathbf{k}||\mathbf{q}|}$, and integrating over k and ω, one has

$$\Pi_A(q,0) = i\frac{16Nm\bar{g}^2}{(2\pi)^5} \int_0^{2\pi} d\theta \int_0^{2\pi} d\theta' \int_{-\infty}^{+\infty} d\Omega \int_0^{\infty} \times \frac{dll}{\xi^{-2}+l^2+\gamma|\Omega|/l} \frac{\Omega}{[i(1+\lambda)\Omega - v_F l\cos\theta]^2} \times \frac{1}{i(1+\lambda)\Omega - v_F q\cos\theta' - v_F l\cos\theta}. \quad \text{(D14)}$$

The integral over θ' then gives

$$\Pi_A(q,0) = -\frac{4Nm\bar{g}^2}{\pi^4} \int_0^{\pi} d\theta \int_0^{\infty} d\Omega \int_0^{\infty} dl \times \frac{l}{\xi^{-2}+l^2+\gamma\Omega/l} \frac{\Omega}{[(1+\lambda)\Omega + iv_F l\cos\theta]^2} \times \frac{1}{\sqrt{(v_F q)^2 + [\Omega(1+\lambda)+iv_F l\cos\theta]^2}}. \quad \text{(D15)}$$

It is convenient to rescale the variables at this stage, introducing $\Omega' = \frac{(1+\lambda)\Omega}{v_F q}$ and $l' = \frac{l}{q}$, so that the previous expression reduces to

$$\Pi_A(q,0) = -\frac{4Nm\bar{g}^2}{\pi^4 v_F(1+\lambda)^2}|q| \int_0^{\pi} d\theta \int_0^{+\infty} d\Omega' \int_0^{\infty} dl' \times \frac{l}{\xi^{-2} + [\gamma v_F/(1+\lambda)](\Omega'/l')} \frac{\Omega'}{(\Omega' + il'\cos\theta)^2} \times \frac{1}{\sqrt{1+(\Omega'+il'\cos\theta)^2}}, \quad \text{(D16)}$$

where we kept only the leading order in q.

Defining z and ϕ as $z\cos\phi = l'$ and $z\sin\phi = \Omega'$, one is left with

$$\Pi_A(q,0) = -\frac{4Nm\bar{g}^2}{\pi^4 v_F(1+\lambda)^2}|q| \int_0^{\pi} d\theta \int_0^{\infty} dz \int_0^{\pi/2} d\phi \times \frac{\cos\phi}{\xi^{-2} + [\gamma v_F/(1+\lambda)]\tan\phi} \frac{z\sin\phi}{(\sin\phi + i\cos\phi\cos\theta)^2} \times \frac{1}{\sqrt{1+z^2(\sin\phi + i\cos\phi\cos\theta)^2}}. \quad \text{(D17)}$$

Subtracting the constant part $\Pi_A(0,0)$ (and neglecting it), and integrating over z, this leads to

$$\Pi_A(q,0) = \frac{4Nm\bar{g}^2}{\pi^4 v_F(1+\lambda)^2}|q| \int_0^{\pi/2} \frac{d\phi \cos\phi \sin\phi}{\xi^{-2} + [\gamma v_F/(1+\lambda)]\tan\phi} \times \int_0^{\pi} d\theta \frac{1}{(\sin\phi + i\cos\phi\cos\theta)^4}. \quad \text{(D18)}$$

The angular integration over θ can be done explicitly and gives

$$\int_0^{\pi} \frac{d\theta}{(\sin\phi + i\cos\phi\cos\theta)^4} = \frac{\pi}{2}\sin\phi(5\sin^2\phi - 3). \quad \text{(D19)}$$

Substituting this into the expression of Π_A, we are left with the following final result:

$$\Pi_A(q,0) = -\frac{2\bar{g}}{\pi^2 v_F(1+\lambda)}|q|\mathcal{H}\left(\frac{1+\lambda}{\gamma v_F \xi^2}\right), \quad \text{(D20)}$$

where $\mathcal{H}$ is defined as

$$\mathcal{H}(x) = \int_0^{\pi/2} d\phi \frac{\cos\phi \sin^2\phi(3 - 5\sin^2\phi)}{\tan\phi + x}, \quad \text{(D21)}$$

and satisfies, in the two limits,

$$\mathcal{H}(0) = \frac{1}{3}, \quad \mathcal{H}(x \gg 1) \approx \frac{2}{3x^2}. \quad \text{(D22)}$$

As one approaches the QCP, ξ gets bigger, and one can take the asymptotic form of $\mathcal{H}(x)$ for small x: $\mathcal{H}(0)=1/3$. Rearranging the prefactor for this limit, we are left with

$$\Pi_A(q,0) \underset{\xi\to\infty}{=} -\frac{8}{9\pi}\xi^{-1}|q|. \quad \text{(D23)}$$

3. At criticality

At the QCP, we have

$$\Pi_A(q,0) = \frac{16N\bar{g}^2}{(2\pi)^6}\int d^2K d\omega d^2l d\Omega \frac{1}{[i\Sigma(\omega) - \epsilon_k]^2} \times \frac{1}{i\Sigma(\omega+\Omega) - \epsilon_{k+l}} \frac{1}{i\Sigma(\omega) - \epsilon_{k+q}} \times \frac{1}{l^2 + \gamma(|\Omega|/l)}, \quad \text{(D24)}$$

where we considered that, close to criticality, the self-energy dominates completely the bare ω term in the fermionic propagators.

We expand both energies as $\epsilon_{k+l}=\epsilon_k+v_F l_x+\frac{l_y^2}{2m_B}$ and $\epsilon_{k+q}=\epsilon_k+v_F q\cos\theta$, and perform the integration over ϵ_k, leading to

$$\Pi_A(q,0) = i\frac{16Nm\bar{g}^2}{(2\pi)^5}\int_0^{2\pi} d\theta \int_{-\infty}^{+\infty} dl_x \int_{-\infty}^{+\infty} d\Omega \int_0^{\Omega} d\omega \int_{-\infty}^{\infty} \frac{dl_y l}{\gamma|\Omega| + l^3} \frac{1}{[i\Sigma(\Omega-\omega) + i\Sigma(\omega) - v_F l_x - N(l_y^2/2m_B)]^2} \times \frac{1}{i\Sigma(\Omega-\omega) + i\Sigma(\omega) + v_F q\cos\theta - v_F l_x - N(l_y^2/2m_B)}. \quad \text{(D25)}$$

The integration over l_x brings two contributions. One comes from the poles in the fermionic propagator, and can be neglected here since both poles are in the same half plane. The other contribution comes from the branch cut in the bosonic propagator, and since at the branch cut $l_x \sim l_y$, one can safely drop the quadratic term in the fermionic propagators. This allows us to integrate over l_y. Out of the terms arising from this integral, the only nonvanishing ones come from the nonanalyticities of the integrated bosonic propagator defined as

$$\int dl_y \chi(\mathbf{l},\Omega) = \int dl_y \frac{1}{l^2 + \gamma v_F|\Omega|/\sqrt{(v_F l)^2 + c^2\Sigma(\Omega)^2}}. \quad \text{(D26)}$$

We use here the full form of the polarization operator, Eq. (A8), as we will see that typical $v_F l_x \gtrsim \Sigma(\Omega)$ and typical l_y are only larger in a logarithmic sense.

This integral was performed in a slightly different form in Eq. (C8), but the method is the same: introducing u such that $\tan u = \frac{v_F l_y}{\sqrt{(v_F l_x)^2+\Sigma(\Omega)^2}}$, one has

$$\int dl_y \chi(\mathbf{l},\Omega) = \frac{(v_F l_x)^2 + c^2\Sigma(\Omega)^2}{\gamma v_F^2|\Omega|} \times \int_0^{\pi/2} \frac{du}{\cos^3 u - \delta\cos^2 u + \epsilon}, \quad \text{(D27)}$$

where we introduced $\delta = \frac{c^2\Sigma(\Omega)^2[(v_F l_x)^2 + c^2\Sigma(\Omega)^2]^{1/2}}{\gamma v_F^3|\Omega|}$ and $\epsilon = \frac{[(v_F l_x)^2 + c^2\Sigma(\Omega)^2]^{3/2}}{\gamma v_F^3|\Omega|}$.

In the process of integrating over l_x, two nonanalytic contributions arise from Eq. (D27). One comes from $l_x \gtrsim (\gamma\Omega)^{1/3}$ and goes like $\frac{\pi}{(\gamma|\Omega|)^{1/3}}$. Plugging this back into Π_A and subtracting (and neglecting) a constant term, we obtain for this term, which we label $\Pi_A^{(1)}(q,0)$,

$$\Pi_A^{(1)}(q,0) \sim Nm\bar{g}^2 v_F^2 q^2 \int_{-\infty}^{+\infty} dl_x \int_{-\infty}^{+\infty} d\Omega \int_0^{\Omega} d\omega \times \frac{1}{|l_x|} \frac{1}{[i\Sigma(\Omega-\omega) + i\Sigma(\omega) - v_F l_x]^5}, \quad \text{(D28)}$$

where we subtracted $\Pi_A(0,0)$ and expanded in q.

We further simplify the integrals, noticing that the fermionic propagator is dominated by $v_F l_x$ since $l_x \sim (\gamma\Omega^{1/3})$:

$$\Pi_A^{(1)}(q,0) \sim q^2 \frac{Nm\bar{g}^2}{v_F^3} \int_0^{\omega_{\text{Max}}} d\Omega \int dl_x \frac{\Omega}{l_x^6} \sim q^2 \frac{Nm\bar{g}^2}{v_F^3\gamma^{5/3}} \int_0^{\omega_{\text{Max}}} \frac{d\Omega}{\Omega^{2/3}} \sim \sqrt{\alpha} q^2, \quad \text{(D29)}$$

where we substituted $l_x \sim (\gamma\Omega)^{1/3}$ in the last steps. We see that $\Pi_A^{(1)}(q,0)$ is analytic in q and furthermore small in α. This term can therefore be safely neglected.

The other nonanalytic contribution from Eq. (D27) comes from typical $v_F l_x \sim \Sigma(\Omega)$. It can be seen from an expansion of Eq. (D27) for small values of both δ and ϵ, and goes like

$$-\frac{(v_F l_x)^2 + c^2\Sigma(\Omega)^2}{2v_F^2\gamma|\Omega|}\ln[(v_F l_x)^2 + c^2\Sigma(\Omega)^2]. \quad \text{(D30)}$$

One can explicitly verify that to get the logarithm, we only need the polarization operator $\Pi(l,\Omega)$ to order $1/l^3$. Like we argued in Appendix C, to this order, the polarization bubble can be evaluated with the full fermionic Green's functions but without vertex corrections.

Substituting Eq. (D30) into the expression for Π_A and subtracting a constant part, we obtain

$$\Pi_A^{(2)}(q,0) = i\frac{8Nm\bar{g}^2}{(2\pi)^5\gamma v_F}q\int_0^{2\pi}d\theta\int_{-\infty}^{+\infty}dl_x\int_{-\infty}^{+\infty}\frac{d\Omega}{|\Omega|}\int_0^{\Omega}d\omega \times\frac{\cos\theta[(v_F l_x)^2 + c^2\Sigma(\Omega)^2]}{[i\Sigma(\Omega-\omega)+i\Sigma(\omega)-v_F l_x]^3} \times\frac{\ln[(v_F l_x)^2 + c^2\Sigma(\Omega)^2]}{i\Sigma(\Omega-\omega)+i\Sigma(\omega)+v_F q\cos\theta - v_F l_x}. \quad \text{(D31)}$$

Using the $\theta\leftrightarrow-\theta$ symmetry, and splitting the integral over Ω into two parts, one can rearrange this expression as

$$\Pi_A^{(2)}(q,0) = i\frac{Nm\bar{g}^2}{c\pi^5\gamma v_F^2}q\int_0^{\pi}d\theta\int_{-\infty}^{+\infty}dz\int_0^{+\infty}\frac{d\Omega}{\Omega}\int_0^{\Omega}d\omega\frac{1}{\Sigma(\Omega)}\frac{\cos\theta(1+z^2)}{(i\{[\Sigma(\Omega-\omega)+\Sigma(\omega)]/c\Sigma(\Omega)\}-z)^3} \times\frac{\ln(1+z^2)}{i\{[\Sigma(\Omega-\omega)+\Sigma(\omega)]/c\Sigma(\Omega)\}+v_F q\cos\theta/c\Sigma(\Omega)-z}, \quad \text{(D32)}$$

where we defined $z=v_F l_x/[c\Sigma(\Omega)]$.

Let us now isolate the integral over z, given by

$$J=\int_{-\infty}^{+\infty}dz\frac{(1+z^2)\ln(1+z^2)}{(ia-z)^3(ia+b-z)}, \quad \text{(D33)}$$

where $a=\frac{\Sigma(\Omega-\omega)+\Sigma(\omega)}{c\Sigma(\Omega)}$ and $b=\frac{v_F q\cos\theta}{c\Sigma(\Omega)}$, and $a\geq 0$.

Performing the contour integration in the lower half plane (where lies the branch cut), one gets

$$J=-2\pi\int_1^{\infty}dy\frac{1-y^2}{(y+a)^3(y+a-ib)}=-2\pi\int_1^{\infty}dy\frac{(1-y^2)(y+a+ib)}{(y+a)^3[(y+a)^2+b^2]}. \quad \text{(D34)}$$

Once Eq. (D34) is plugged back into Eq. (D32), only the imaginary term survives due to the symmetry of the integral in θ. We are left with

$$\Pi_A^{(2)}(q,0) = \frac{4Nm\bar{g}^2}{c^2\pi^4\gamma v_F}q^2\int_0^{\pi/2}d\theta\int_1^{+\infty}dy\int_0^{+\infty}d\Omega\int_0^1 dw\frac{1}{\Sigma(\Omega)^2}\frac{\cos^2\theta}{\{c^{-1}[(1-w)^{2/3}+w^{2/3}]+y\}^3} \times\frac{1-y^2}{\{y+c^{-1}[(1-w)^{2/3}+w^{2/3}]\}^2+[v_F q\cos\theta/c\Sigma(\Omega)]^2}, \quad \text{(D35)}$$

where we changed variables, defining $w=\omega/\Omega$.

Introducing the new variable $t=\left(\frac{c\Sigma(\Omega)}{v_F q\cos\theta}\right)^{3/2}$, this rewrites as

$$\Pi_A^{(2)}(q,0) = \frac{4Nm\bar{g}^2}{c^{3/2}\pi^4\gamma v_F^{3/2}\omega_0^{1/2}}q^{3/2}\int_0^{\pi/2}d\theta(\cos\theta)^{3/2} \times\int_1^{+\infty}dy\int_0^1 dw\frac{1}{\{c^{-1}[(1-w)^{2/3}+w^{2/3}]+y\}^3} \times\int_0^{+\infty}dt\frac{1-y^2}{1+t^{4/3}\{y+c^{-1}[(1-w)^{2/3}+w^{2/3}]\}^2}. \quad \text{(D36)}$$

A final change in variables leads to

$$\Pi_A^{(2)}(q,0) = \frac{4Nm\bar{g}^2}{c^{3/2}\pi^4\gamma v_F^{3/2}\omega_0^{1/2}}q^{3/2}\int_0^{\pi/2}d\theta(\cos\theta)^{3/2} \times\int_1^{+\infty}dy\int_0^1 dw\frac{1-y^2}{\{c^{-1}[(1-w)^{2/3}+w^{2/3}]+y\}^{9/2}} \times\int_0^{+\infty}dv\frac{1}{1+v^{4/3}}, \quad \text{(D37)}$$

where $v=t\{y+c^{-1}[(1-w)^{2/3}+w^{2/3}]\}^{3/2}$.

Performing the integral over y, one is left with three independent integrals contributing to the numerical prefactor:

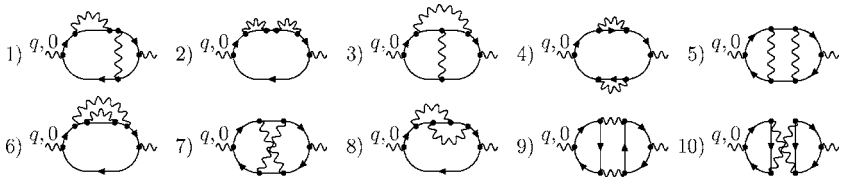

FIG. 8. The ten two-loop diagrams for the charge susceptibility.

$$\Pi_A^{(2)}(q,0) = -\frac{32Nm\bar{g}^2}{105\pi^4\gamma v_F^{3/2}\omega_0^{1/2}}q^{3/2}\int_0^{\pi/2} d\theta(\cos\theta)^{3/2} \times \int_0^1 dw \frac{5c+2[(1-w)^{2/3}+w^{2/3}]}{[c+(1-w)^{2/3}+w^{2/3}]^{5/2}} \times \int_0^{+\infty} dv \frac{1}{1+v^{4/3}}. \quad \text{(D38)}$$

These integrals can be performed separately and read

$$\int_0^{\pi/2} d\theta(\cos\theta)^{3/2} = \frac{\sqrt{2}\pi^{3/2}}{6[\Gamma(3/4)]^2} \simeq 0.8740,$$

$$\int_0^{+\infty} \frac{dv}{1+v^{4/3}} = \frac{3\pi\sqrt{2}}{4} \simeq 3.3322,$$

$$\int_0^1 dw \frac{5c+2s(w)}{[c+s(w)]^{5/2}} \simeq 0.9438, \quad \text{(D39)}$$

where we used the notation $s(w)=(1-w)^{2/3}+w^{2/3}$.

Collecting all integrals, and rearranging the prefactor, the final result for the contribution of the first two diagrams then writes

$$\Pi_A^{(2)}(q,0) = -0.1053\sqrt{k_F}q^{3/2}. \quad \text{(D40)}$$

This term is nonanalytic in q and does not contain α in the prefactor. This term is obviously much larger than $\Pi_A^{(1)} \times(q,0)$, hence $\Pi_A(q,0)\approx\Pi_A^{(2)}(q,0)$.

4. Other two diagrams

The computation of the other two diagrams in Fig. 5 proceeds along the same way. Far away from criticality, when $\gamma v_F\xi^2/(1+\lambda)$ is small, and one can just expand perturbatively in the interaction, the sum of these two "drag" diagrams, which we label here and in the main text as Π_B, was shown in Ref. 39 to be equal to $\Pi_A(q,0)$ to the leading order in $\bar{g}$ [which in our model is $\bar{g}^3$, see Eqs. (D20)–(D22)]. Near criticality such a simple relation no longer holds, but $\Pi_A(q,0)$ and $\Pi_B(q,0)$ remain of the same sign and of comparable magnitude.

At criticality, we obtained for $\Pi_B(q,0)$

$$\Pi_B(q,0) = \frac{1}{12^{3/4}\pi^4}q^{3/2}\sqrt{k_F}I, \quad \text{(D41)}$$

where in rescaled variables (e.g., momentum is in units of q)

$$I = \int d\Omega dx x \int_0^{2\pi} d\theta \frac{S^2(x,\Omega,\theta)}{S_1(x,\Omega)S_1(x+\cos\theta,\Omega)} \quad \text{(D42)}$$

and $S(x,\Omega,\theta)$ and $S_1(x,\Omega)$ are given by

$$S(x,\Omega,\theta) = \int_0^{\Omega} d\omega \int_0^{2\pi} \frac{d\theta_1}{i\Sigma^* - x\cos(\theta_1)} \times \frac{1}{i\Sigma^* - \cos(\theta+\theta_1) - x\cos\theta_1}, \quad \text{(D43)}$$

$$S_1(x,\Omega) = \int_0^{\Omega} \frac{d\omega}{x^2+(\Sigma^*)^2}, \quad \text{(D44)}$$

where we introduced $\Sigma^*=\Sigma^*(\omega,\Omega)=(\Omega-\omega)^{2/3}+\omega^{2/3}$.

We could not evaluate this integral explicitly, and we compute it under the following simplifying assumptions:

(i) We compute $S_1(x,\Omega)$ by expanding to leading order in $(\Sigma^*/x)^2$, evaluating the frequency integral and plugging the result back into the denominator. This way, we approximated $S_1(x,\Omega)$ by

$$S_1(x,\Omega) \approx \frac{\Omega}{x^2+(c\Omega^{2/3})^2}, \quad \text{(D45)}$$

where $c\approx 1.2$ [see Eq. (A6)]. This procedure is similar to the one which led to Eq. (A8), but here we cannot justify that only the $1/x$ and $1/x^3$ terms are relevant.

(ii) We replace Σ^* by the same $c\Omega^{2/3}$ in the integrand for $S(x,\Omega,\theta)$.

(iii) We assume that the internal momenta are larger than the external ones, i.e., $x\gg 1$ (x is measured in units of q), neglected terms of order $O(1)$ compared to $O(x)$ and set the lower limit of the integration over x to some number b.

(iv) We choose b by applying the same approximate computation scheme to $\Pi_A(q,\omega)$, requesting that the result coincides with the exact expression, Eq. (D40).

Carrying out this calculation for $\Pi_B(q,0)$ we obtain

$$\Pi_B(q,0) \approx -0.14\sqrt{k_F}q^{3/2}. \quad \text{(D46)}$$

This is the result that we cited in the text.

APPENDIX E: TWO-LOOP RENORMALIZATION OF THE CHARGE SUSCEPTIBILITY

In this appendix we show that the singular contributions to the static charge susceptibility from individual diagrams cancel out in the full expression of $\chi_c(q)$. The cancellation of the singularities in the charge response has been extensively studied in 1D systems.[44]

There are ten different two-loop diagrams for the charge susceptibility, presented in Fig. 8. The last two diagrams are

identical to the ones we considered in the main text. We already argued there that these two diagrams cancel out in the case of a QCP in the charge channel.

The other eight diagrams have to be considered together. We demonstrate that the total contribution from these eight diagrams vanishes once one linearizes the dispersion of the intermediate fermions. This still leaves out the contributions from nonlinear terms in the dispersion, but one can show that these contributions are regular.

To begin with, consider one of these diagrams, e.g., diagram 7 in Fig. 8. In analytic form, the contribution from this diagram is

$$\Pi_7(q) = 2\int d^2q_1 d\omega_1 d^2q_2 d\omega_2 G_k G_{k+q} G_{k+q_1} G_{k+q_2+q} \times G_{k+q_1+q_2} G_{k+q_1+q_2+q} \chi_{q_1} \chi_{q_2}, \tag{E1}$$

where we labeled $q_i=(\mathbf{q}_i,\omega_i)$, and the combinatoric factor 2 comes from the summation over spin indices.

Introduce now

$$G_k G_{k+q_i} = \frac{1}{\alpha_{q_i}}(G_k - G_{k+q_i}), \tag{E2}$$

where

$$\alpha_{q_i} = i\omega_i - q_i \cos\,\theta_i, \tag{E3}$$

and θ_i is the angle between $\mathbf{k}\approx\mathbf{k}_F$ and $\mathbf{q}_i$. Shortening the notations further as $q_1\equiv 1$ and $q_2\equiv 2$, using the symbolic notation $\int_{1,2}$ for the six-dimensional integral over q_1 and q_2, and applying Eq. (E2), we obtain

$$\Pi_7(q) = 2\int_{1,2}\chi_1\chi_2\left[\frac{G_{k+q}G_{k+1+2}}{\alpha_1^2\alpha_2^2} - \frac{G_{k+q}G_{k+1+2}}{\alpha_1\alpha_2(\alpha_1+\alpha_2)^2} - 2\frac{G_{k+q}G_{k+1}}{\alpha_2^2(\alpha_1^2-\alpha_2^2)}\right]. \tag{E4}$$

Similarly,

$$\Pi_8(q) = 2\int_{1,2}\chi_1\chi_2\left[\frac{G_{k+q}G_{k+1+2}}{\alpha_1\alpha_2(\alpha_1+\alpha_2)^2} - 2\frac{G_{k+q}G_{k+1}}{\alpha_1^2(\alpha_1^2-\alpha_2^2)}\right] \tag{E5}$$

and further

$$\Pi_5(q) = 2\int_{1,2}\chi_1\chi_2\left[\frac{G_{k+q}G_{k+1+2}}{\alpha_1\alpha_2(\alpha_1+\alpha_2)^2} + 2\frac{G_{k+q}G_{k+1}}{\alpha_1^2(\alpha_1^2-\alpha_2^2)}\right], \tag{E6}$$

$$\Pi_3(q) = 2\int_{1,2}\chi_1\chi_2\left[-\frac{G_{k+q}G_{k+1+2}}{\alpha_1^2\alpha_2^2} + 2\frac{G_{k+q}G_{k+1}}{\alpha_1^2\alpha_2^2}\left(\frac{\alpha_1^2+\alpha_2^2}{\alpha_1^2-\alpha_2^2}\right)\right], \tag{E7}$$

$$\Pi_2(q) = 4\int_{1,2}\chi_1\chi_2\frac{G_{k+q}G_{k+1}}{\alpha_1^2\alpha_2^2}\left(\frac{\alpha_2^2}{\alpha_1^2-\alpha_2^2}\right), \tag{E8}$$

$$\Pi_1(q) = 4\int_{1,2}\frac{\chi_1\chi_2}{\alpha_1^2\alpha_2^2}\left[G_{k+q}G_{k+1+2}\frac{\alpha_2^2}{\alpha_1^2-\alpha_2^2} - G_{k+q}G_{k+1}\frac{3\alpha_2^2-\alpha_1^2}{\alpha_1^2-\alpha_2^2}\right], \tag{E9}$$

$$\Pi_4(q) = \int_{1,2}\frac{\chi_1\chi_2}{\alpha_1^2\alpha_2^2}\left[G_{k+q}G_{k+1+2} - 2G_{k+q}G_{k+1}\right], \tag{E10}$$

and finally,

$$\Pi_6(q) = \int_{1,2}\frac{\chi_1\chi_2}{\alpha_1^2\alpha_2^2}\left[G_{k+q}G_{k+1+2}\frac{\alpha_1^2+\alpha_2^2}{(\alpha_1+\alpha_2)^2} - 2G_{k+q}G_{k+1}\right]. \tag{E11}$$

Collecting the prefactors for $G_{k+q}G_{k+1+2}$ and $G_{k+q}G_{k+1}$ from all of the eight contributions we find that they cancel out.

APPENDIX F: MASS-SHELL SINGULARITY

In this appendix, we analyze in more detail the form of the self-energy near the fermionic mass shell. The interest to the mass-shell behavior of the self-energy was triggered by recent studies of the self-energy near a mass shell in a 2D Fermi liquid[31] and for 2D Dirac fermions.[45] In both cases, the lowest-order self-energy diverges at the mass shell, which forces to re-sum the perturbative series.

At first glance, the same situation holds in our analysis at the QCP. Evaluating the self-energy in a two-loop expansion *around free fermions* and using the fermionic dispersion with the curvature, we obtain near the mass shell:[46]

$$\Sigma(k,\omega) \sim \frac{1}{N^2}(i\omega-\epsilon_k)\left[N\ln\frac{i\omega-\epsilon_k}{\epsilon_k}\right]^2. \tag{F1}$$

This result implies that the "effective" quasiparticle residue for the Eliashberg theory, $Z_{\text{eff}}\propto d\Sigma/d\epsilon_k$ logarithmically diverges on the mass shell of free fermions. Without the curvature of the dispersion, the divergence would be stronger than logarithm.

The issue we now have to address is whether Z still diverges on the mass shell if we expand around the Eliashberg solution, i.e., around fermions with

$$G_0(k,\omega) = \frac{1}{i\tilde{\Sigma}(\omega)-\epsilon_k}, \tag{F2}$$

where, we remind, $\tilde{\Sigma}(\omega)=\omega+\Sigma(\omega)$.

It turns out that this is not the case: the expansion around the Eliashberg solution leads to a finite residue Z. At the two-loop order, we obtain, instead of Eq. (F1)

$$\Sigma(k,\omega) \sim \frac{1}{N^2}\int_0^1 dz\int_{1-z}^1 dz'[i\Sigma(\omega)\psi_{z,z'}-\epsilon_k] \times\left[\ln\frac{N[i\Sigma(\omega)\psi_{z,z'}-\epsilon_k]}{\epsilon_k}\right]^2, \tag{F3}$$

where

$$\psi_{z,z'} = (1-z)^{2/3} + (1-z')^{2/3} + (z+z'-1)^{2/3}. \quad \text{(F4)}$$

For simplicity, we restricted ourselves to the quantum critical regime where $\tilde{\Sigma}(\omega) \approx \Sigma(\omega)$. If $\psi_{z,z'}$ were equal to a constant, as it is when the system is in the Fermi-liquid regime, and $\Sigma(\omega)=\lambda\omega$, then Z would diverge at $\omega=\epsilon/(1+\lambda)$. However, since $\Sigma(\Omega-\omega)+\Sigma(\omega)$ does not reduce to $\Sigma(\Omega)$, we have two additional integrations over z and z', and the logarithmic singularity is washed out. In particular, at $\epsilon_k = i\tilde{\Sigma}(\omega)$, i.e., at the "Matsubara mass shell," we have

$$Z_{\text{eff}} \sim \frac{1}{N^2}\left[\frac{\pi^2}{6}\ln^2 N - 4.08 \ln N + 2.88\right], \quad \text{(F5)}$$

in which case Z_{eff} is just a constant. Combining this with our earlier result that the renormalization of ϵ_k is also finite, Eq. (5.30), we obtain for the full fermionic Green's function at the smallest ω and ϵ_k

$$G(k,\omega) = \frac{Z_{\text{eff}}}{i\tilde{\Sigma}(\omega) - \epsilon_k^*}, \quad \text{(F6)}$$

where ϵ_k^* differs from ϵ_k by a constant factor.

[1] J. A. Hertz, Phys. Rev. B **14**, 1165 (1976); A. J. Millis, Phys. Rev. B **48**, 7183 (1993); T. Moriya, *Spin Fluctuations in Itinerant Electron Magnetism*, Springer Series in Solid State Physics Vol. 56 (Springer-Verlag, Berlin, 1985).

[2] B. L. Altshuler, L. B. Ioffe, and A. J. Millis, Phys. Rev. B **50**, 14048 (1994).

[3] D. V. Khveshchenko, Phys. Rev. B **49**, 16893 (1994); **52**, 4833 (1995).

[4] C. Nayak and F. Wilczek, Nucl. Phys. B **430**, 534 (1994).

[5] P. A. Lee, Phys. Rev. Lett. **63**, 680 (1989).

[6] B. Blok and H. Monien, Phys. Rev. B **47**, 3454 (1993).

[7] P. A. Lee, Phys. Rev. Lett. **63**, 680 (1989); L. B. Ioffe and A. I. Larkin, Phys. Rev. B **39**, 8988 (1989); N. Nagaosa and P. A. Lee, Phys. Rev. Lett. **64**, 2450 (1990); Phys. Rev. B **46**, 5621 (1992).

[8] B. I. Halperin, P. A. Lee, and N. Read, Phys. Rev. B **47**, 7312 (1993); M. P. Lilly, K. B. Cooper, J. P. Eisenstein, L. N. Pfeiffer, and K. W. West, Phys. Rev. Lett. **82**, 394 (1999).

[9] R. Roussev and A. J. Millis, Phys. Rev. B **63**, 140504(R) (2001); Z. Wang, W. Mao, and K. Bedell, Phys. Rev. Lett. **87**, 257001 (2001).

[10] A. V. Chubukov, A. M. Finkel'stein, R. Haslinger, and D. K. Morr, Phys. Rev. Lett. **90**, 077002 (2003).

[11] M. Dzero and L. P. Gorkov, Phys. Rev. B **69**, 092501 (2004).

[12] A. V. Chubukov, Phys. Rev. B **71**, 245123 (2005).

[13] V. Oganesyan, S. A. Kivelson, and E. Fradkin, Phys. Rev. B **64**, 195109 (2001).

[14] M. J. Lawler, D. G. Barci, V. Fernandez, E. Fradkin, and L. Oxman, Phys. Rev. B **73**, 085101 (2006).

[15] W. Metzner, D. Rohe, and S. Andergassen, Phys. Rev. Lett. **91**, 066402 (2003); L. Dell'Anna and W. Metzner, Phys. Rev. B **73**, 045127 (2006).

[16] H. Y. Kee and Y. B. Kim, J. Phys.: Condens. Matter **16**, 3139 (2004).

[17] S. Kivelson and E. Fradkin, cond-mat/0507459 (unpublished).

[18] Ar. Abanov, A. V. Chubukov, and J. Schmalian, Adv. Phys. **52**, 119 (2003); A. V. Chubukov, D. Pines, and J. Schmalian, in *The Physics of Superconductors*, edited by K. H. Bennemann and J. B. Ketterson (Springer, New York 2003), Vol. 1, p. 495.

[19] C. Castellani, C. DiCastro, and M. Grilli, Z. Phys. B: Condens. Matter **103**, 137 (1997).

[20] A. Houghton and J. B. Marston, Phys. Rev. B **48**, 7790 (1993); H.-J. Kwon, J. B. Marston, and R. Shankar, J. Phys.: Condens. Matter **6**, 4909 (1994); A. Houghton, H.-J. Kwon, and J. B. Marston, Phys. Rev. B **50**, 1351 (1994); **52**, 8002 (1995); Adv. Phys. **49**, 141 (2000).

[21] A. H. Castro Neto and E. Fradkin, Phys. Rev. Lett. **72**, 1393 (1994); Phys. Rev. B **49**, 10877 (1994); **51**, 4084 (1995).

[22] W. Metzner, C. Castellani, and C. diCastro, Adv. Phys. **47**, 317 (1998).

[23] A. Chubukov and D. V. Khveshchenko, cond-mat/0604376, Phys. Rev. Lett. (to be published).

[24] P. Kopietz, Int. J. Mod. Phys. B **12**, 1673 (1998).

[25] G. M. Eliashberg, Zh. Eksp. Teor. Fiz. **43**, 1005 (1962) [Sov. Phys. JETP **16**, 780 (1963)]; D. J. Scalapino, in *Superconductivity* edited by R. D. Parks (Dekker, New York, 1969), Vol. 1, p. 449; F. Marsiglio and J. P. Carbotte, in *The Physics of Conventional and Unconventional Superconductors*, edited by K. H. Bennemann and J. B. Ketterson (Springer-Verlag, Berlin, 2003), Vol. 1.

[26] D. Belitz, T. R. Kirkpatrick, and T. Vojta, Phys. Rev. B **55**, 9452 (1997).

[27] A. V. Chubukov and D. L. Maslov, Phys. Rev. B **68**, 155113 (2003).

[28] D. Belitz, T. R. Kirkpatrick, and T. Vojta, Rev. Mod. Phys. **77**, 579 (2005).

[29] A. V. Chubukov, C. Pépin, and J. Rech, Phys. Rev. Lett. **92**, 147003 (2004).

[30] C. Pépin, J. Rech, and R. Ramazashvili, Phys. Rev. B **69**, 172401 (2004).

[31] A. V. Chubukov, D. L. Maslov, S. Gangadharaiah, and L. I. Glazman, Phys. Rev. B **71**, 205112 (2005).

[32] E. C. Stoner, Rep. Prog. Phys. **11**, 43 (1946).

[33] Ar. Abanov and A. Chubukov, Phys. Rev. Lett. **93**, 255702 (2004).

[34] A. V. Chubukov, Phys. Rev. B **72**, 085113 (2005).

[35] G. Y. Chitov and A. J. Millis, Phys. Rev. Lett. **86**, 5337 (2001); Phys. Rev. B **64**, 054414 (2001).

[36] A. V. Chubukov, D. L. Maslov, and A. J. Millis, Phys. Rev. B **73**, 045128 (2006).

[37] V. M. Galitski, A. V. Chubukov, and S. Das Sarma, Phys. Rev. B **71**, 201302(R) (2005).

[38] J. Betouras, D. Efremov, and A. Chubukov, Phys. Rev. B **72**, 115112 (2005).

[39] D. Maslov, A. Chubukov, and R. Saha, cond-mat/0609102 (unpublished).

[40] A. J. Millis, A. J. Schofield, G. G. Lonzarich, and S. A. Grigera, Phys. Rev. Lett. **88**, 217204 (2002).
[41] S. A. Brazovskii, Zh. Eksp. Teor. Fiz. **68**, 42 (1975) [Sov. Phys. JETP **41**, 85 (1975)]; J. Schmalian and M. Turlakov, Phys. Rev. Lett. **93**, 036405 (2004).
[42] D. Belitz, T. R. Kirkpatrick, and A. Rosch, Phys. Rev. B **73**, 054431 (2006); Phys. Rev. B **74**, 024409 (2006).
[43] D. Belitz and T. R. Kirkpatrick, Phys. Rev. Lett. **89**, 247202 (2002); T. R. Kirkpatrick and D. Belitz, Phys. Rev. B **67**, 024419 (2003).
[44] A. Neumayr and W. Metzner, Phys. Rev. B **58**, 15449 (1998); J. Stat. Phys. **96**, 613 (1999); C. Kopper and J. Magnen, Ann. Henri Poincare **2**, 513 (2001).
[45] A. V. Chubukov and A. M. Tsvelik, Phys. Rev. B **73**, 220503(R) (2006).
[46] D. Maslov (private communication).